

Spring 2026 – Systems Biology of Reproduction
Discussion Outline – Epigenetics and Transgenerational Reproductive Disease
Eric Nilsson – Biol 475/575
10:35-11:50 am, Tuesday & Thursday
March 12, 2026
Week 9

Epigenetics and Transgenerational Reproductive Disease

Primary Papers:

1. Kubsad, et al. (2019) Scientific Reports 9 :6372
2. Sadler-Riggelman, et al. (2019) Environmental Epigenetics 5(3) dvz013
3. Beck, et al. (2021) Epigenetics & Chromatin 14:6

Discussion

Student 12: Reference 1 above

- What transgenerational reproductive phenotypes were observed?
- What is glyphosate and what are its effects on sperm?
- What is generational toxicology?

Student 14: Reference 2 above

- What environmental exposures were used?
- What were the Sertoli cell effects observed?
- What basic information on testis disease was obtained?

Student 15: Reference 3 above

- What technology and epigenetic analysis was used?
- What differential epigenetic regions were observed?
- What transgenerational integration of epigenetic processes was observed?

SCIENTIFIC REPORTS



OPEN

Assessment of Glyphosate Induced Epigenetic Transgenerational Inheritance of Pathologies and Sperm Epimutations: Generational Toxicology

Deepika Kubsad, Eric E. Nilsson, Stephanie E. King, Ingrid Sadler-Riggelman, Daniel Beck & Michael K. Skinner

Ancestral environmental exposures to a variety of factors and toxicants have been shown to promote the epigenetic transgenerational inheritance of adult onset disease. One of the most widely used agricultural pesticides worldwide is the herbicide glyphosate (N-(phosphonomethyl)glycine), commonly known as Roundup. There are an increasing number of conflicting reports regarding the direct exposure toxicity (risk) of glyphosate, but no rigorous investigations on the generational actions. The current study using a transient exposure of gestating F0 generation female rats found negligible impacts of glyphosate on the directly exposed F0 generation, or F1 generation offspring pathology. In contrast, dramatic increases in pathologies in the F2 generation grand-offspring, and F3 transgenerational great-grand-offspring were observed. The transgenerational pathologies observed include prostate disease, obesity, kidney disease, ovarian disease, and parturition (birth) abnormalities. Epigenetic analysis of the F1, F2 and F3 generation sperm identified differential DNA methylation regions (DMRs). A number of DMR associated genes were identified and previously shown to be involved in pathologies. Therefore, we propose glyphosate can induce the transgenerational inheritance of disease and germline (e.g. sperm) epimutations. Observations suggest the generational toxicology of glyphosate needs to be considered in the disease etiology of future generations.

Glyphosate (N-(phosphonomethyl)glycine) was discovered in 1950 and was commercialized for its herbicidal activity as Roundup in the 1970s by Monsanto, St. Louis Missouri¹. Glyphosate is the world's most commonly used herbicide accounting for nearly 72% of global pesticide usage¹. It is the primary herbicide used in the agriculture of corn, soy, and canola, with extensive use in the USA, Supplemental Figure S1. The current "safe" standard set by the Environmental Protection Agency (EPA) for daily chronic reference dose of glyphosate is 1.75 milligrams per kilogram of body weight¹. The no observable adverse effect level (NOAEL) is 50 mg/kg per day dose². The allowed industry exposure levels are 2.5–4.5 mg/kg per day². High exposure dose studies involving 50–500 mg/kg per day have been reported^{3–9}. According to the European Food Safety Authority (EFSA) there is low acute toxicity observed by oral, dermal, or inhalation routes¹⁰. Glyphosate acts by inhibiting the 5-enolpyruvylshikimate-3-phosphate synthase (EPSP) enzyme that is involved in the metabolism of aromatic amino acids in plants. This inhibition leads to a protein shortage and eventually plant death¹¹. The absence of this biochemical pathway in vertebrates, a rapid metabolism, and elimination of glyphosate in mammals (~5–10 hr half-life) has led to the assumption that low levels of toxicity are expected in humans and other mammals^{2,10,11}.

There are many conflicting reports regarding the toxicity of glyphosate^{12,13}. In March 2015 the International Agency of Research on Cancer classified glyphosate as a Grade 2a carcinogen based on prevalence of liver and kidney tumors in chronic feeding studies¹. Shortly after, this statement was retracted in 2016¹⁴. Previous reviews of the literature have discussed the opposing opinions and the scientific studies involved^{1,12,13}. Epidemiology studies have suggested direct exposure associations with diseases such as autism¹⁵, but appropriate animal or

Center for Reproductive Biology, School of Biological Sciences, Washington State University, Pullman, WA, 99164-4236, USA. Correspondence and requests for materials should be addressed to M.K.S. (email: skinner@wsu.edu)

clinical studies have not been performed. A wide variety of different organisms have been used to assess the ecotoxicological actions of glyphosate¹⁶. Direct glyphosate exposure studies in mammals (i.e. mice and rats) have suggested a variety of different pathologies. A complicating factor is Roundup contains additional compounds along with glyphosate, but the actions are presumed to be only through glyphosate. Glyphosate, or Roundup, direct exposure has been linked to reproductive toxicity, birth defects¹⁷, reduced sperm production^{18,19} in rodents, and increased risk of liver metabolic pathologies⁴. Testis pathologies develop following direct glyphosate exposure involving Leydig cell, Sertoli cell and spermatogenic cell apoptosis and damage, as well as reduced testosterone production²⁰. Additional male reproductive abnormalities include delayed onset puberty, behavioral alterations, and testis pathology^{21–24}. Glyphosate induced female pathologies involve uterine abnormalities, altered ovarian steroidogenesis, and implantation pathology^{25–27} in rodents. A review of a small number of human epidemiological studies involving direct exposure to glyphosate concluded no risk for human development and reproduction²⁸. Therefore, a mixture of studies exist showing no direct exposure effects versus induced pathologies. An increasing number of recent published studies suggest a potential risk of direct glyphosate exposure^{1,12,13}. Regulatory agencies consider the herbicide to be minimally or not toxic^{1,10}. The published literature has been focused on the direct exposure of an individual to glyphosate which is the primary current standard for toxicology risk assessment studies. No previous studies have examined the potential transgenerational impacts of glyphosate on successive generations not having continued direct glyphosate exposure.

Epigenetic transgenerational inheritance involves the germline (sperm or egg) mediated inheritance of epigenetic information between generations that leads to pathologies or phenotypic variation in the absence of continued direct exposures^{29–31}. Epigenetics is defined as “molecular factors and processes around DNA that regulate genome activity (e.g. gene expression) independent of DNA sequence, and that are mitotically stable”²⁹. The epigenetic processes include DNA methylation, histone modifications, non-coding RNA, chromatin structure, and RNA methylation. This non-genetic form of inheritance allows environmental factors to induce epigenetic alterations at critical developmental periods in the germline (sperm or egg) which can then be passed to subsequent generations^{29,30}. These critical developmental periods involve the epigenetic reprogramming that occurs in the early embryo following fertilization³², and the reprogramming in the primordial germ cells in early gonadal development³³. During adult gametogenesis, in particular spermatogenesis in the testis, epigenetic programming can also be altered³⁴. Preconception adult exposures have also been shown to promote the transgenerational inheritance of pathologies^{29,35}. Previous studies with a number of environmental toxicants have been shown to induce the transgenerational inheritance of pathologies, disease and sperm epigenetic alterations. This includes the fungicide vinclozolin^{36–38}, plastic derived compounds (bisphenol A and phthalates)³⁹, pesticides permethrin⁴⁰, dichlorodiphenyltrichloroethane (DDT) and methoxychlor^{41,42}, hydrocarbons (jet fuel JP8)⁴³, dioxin⁴⁴, and herbicide atrazine⁴⁵. In addition to environmental toxicants, nutrition and stress can also promote the transgenerational inheritance of pathologies^{29,30}. Human studies have also demonstrated epigenetic transgenerational inheritance in responses to nutrition, smoking, stress, and other environmental exposures³¹. Environmentally induced transgenerational inheritance of pathologies and phenotypic variations have been shown in plants, worms, flies, fish, birds, rodents, pigs, and humans²⁹. Therefore, the environmentally induced epigenetic transgenerational inheritance phenomenon is induced by a wide variety of toxicants and environmental factors, and appears to be a highly conserved non-genetic inheritance process. The current study examines the influence of glyphosate on the transgenerational inheritance of pathologies and sperm epimutations.

Results

Analysis of the transgenerational actions of glyphosate used outbred Sprague Dawley female rats (F0 generation) transiently exposed (25 mg/kg body weight glyphosate daily) during days 8 to 14 of gestation. This is half the NOAEL exposure of 50 mg/kg/day¹⁰, and due to rapid metabolism turnover would lead to a decreased (5–10 mg/kg) dose during the transient exposure period. The F1 generation animals (direct fetal exposure) were bred within the lineage to generate the F2 generation (direct germline exposure), which were bred to generate the F3 generation (transgenerational, no direct exposure). A control lineage used F0 generation gestating females administered vehicle control dimethyl sulfoxide (DMSO) or phosphate buffered saline (PBS). The control and glyphosate lineages were aged to 1 year and euthanized for pathology and sperm epigenetic analysis. No sibling or cousin breeding (crosses) was used in order to avoid any inbreeding artifacts in either the control or glyphosate lineages. Generally, 6–8 founder gestating females from different litters were bred, and 5 animals of each sex from each litter used to generate 25–50 individuals of each sex for each generation for analysis, as previously described⁴¹. Therefore, litter bias was negligible, and the full spectrum of pathology within the generation and lineage was assessed.

Pathology Analysis. Upon dissection at one year of age, abdominal and thoracic organs were briefly examined for obvious gross abnormalities and pathologies. No pathologies or remarkable abnormalities were observed with the exceptions of some animals showing enlarged roughened kidneys (associated with histological evidence of renal disease), and some female animals showing enlarged fluid-filled uteri. All animals that died or were euthanized for welfare reasons prior to 1 year of age were submitted for necropsy and examined for gross and histologic pathologies by the Washington Animal Disease Diagnostic Laboratory (WADDL) at Washington State University College of Veterinary Medicine. For the eleven animals so submitted there were three F3 generation glyphosate control rats that showed aspiration pneumonia, dermal necrosis, or hepatic centrilobular necrosis. There were four F2 generation glyphosate lineage rats showing metritis, dystocia, hepatic necrosis, or adrenal cortical necrosis. There were four F3 generation glyphosate lineage rats showing granulomatous furunculosis, ulcerative balanoposthitis, or seizures for which the underlying diagnosis was open.

Upon dissection at 1 year of age the testis, prostate, kidney, and ovary were collected and examined for histopathologies, Supplemental Figure S2. Stained paraffin sections of isolated tissues were examined by three different

Male pathology

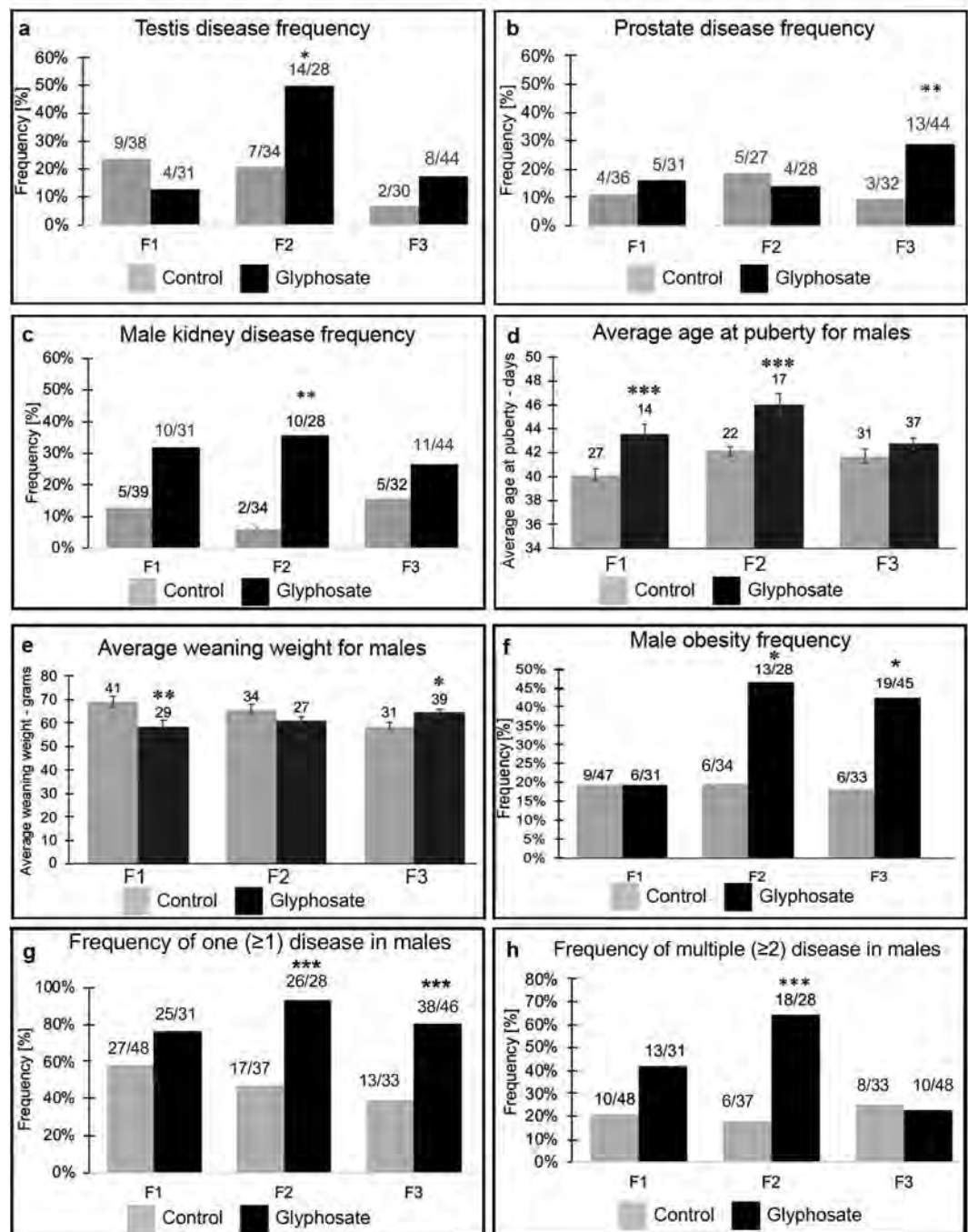


Figure 1. Male pathology analysis in F1, F2 and F3 generation control and glyphosate lineage 1 year-old rats. (a) testis disease frequency, (b) prostate disease frequency, (c) male kidney disease frequency, (d) average puberty age for males, (e) average weaning weight for males, (f) male obesity frequency, (g) frequency of one disease in males, and (h) frequency of multiple disease in males. The pathology number ratio with total animal number is listed for each bar graph (a–f), or mean \pm SEM (d,e), presented with asterisks indicating a statistical difference (* $p < 0.05$, ** $p < 0.01$, and *** $p < 0.001$ in comparison with control lineage animals.

trained pathology observers blinded to the exposure lineages to assess the presence of specific histological abnormalities as described in the Methods²⁹, (Supplemental Figure S2). The male and female pathologies are summarized in Figs 1 and 2, respectively, with the diseased individuals per total number of individuals presented for each generation and lineage, Supplemental Tables S1–S3. For the purposes of this paper an animal was considered to have a diseased tissue if the number of histological abnormalities was markedly increased (i.e. greater than two standard deviations) compared to that of the controls for that tissue, as described in Methods. Previously we have confirmed with apoptosis analysis an increase in spermatogenic cell death in testes^{36,37}. Testis disease was

Female pathology

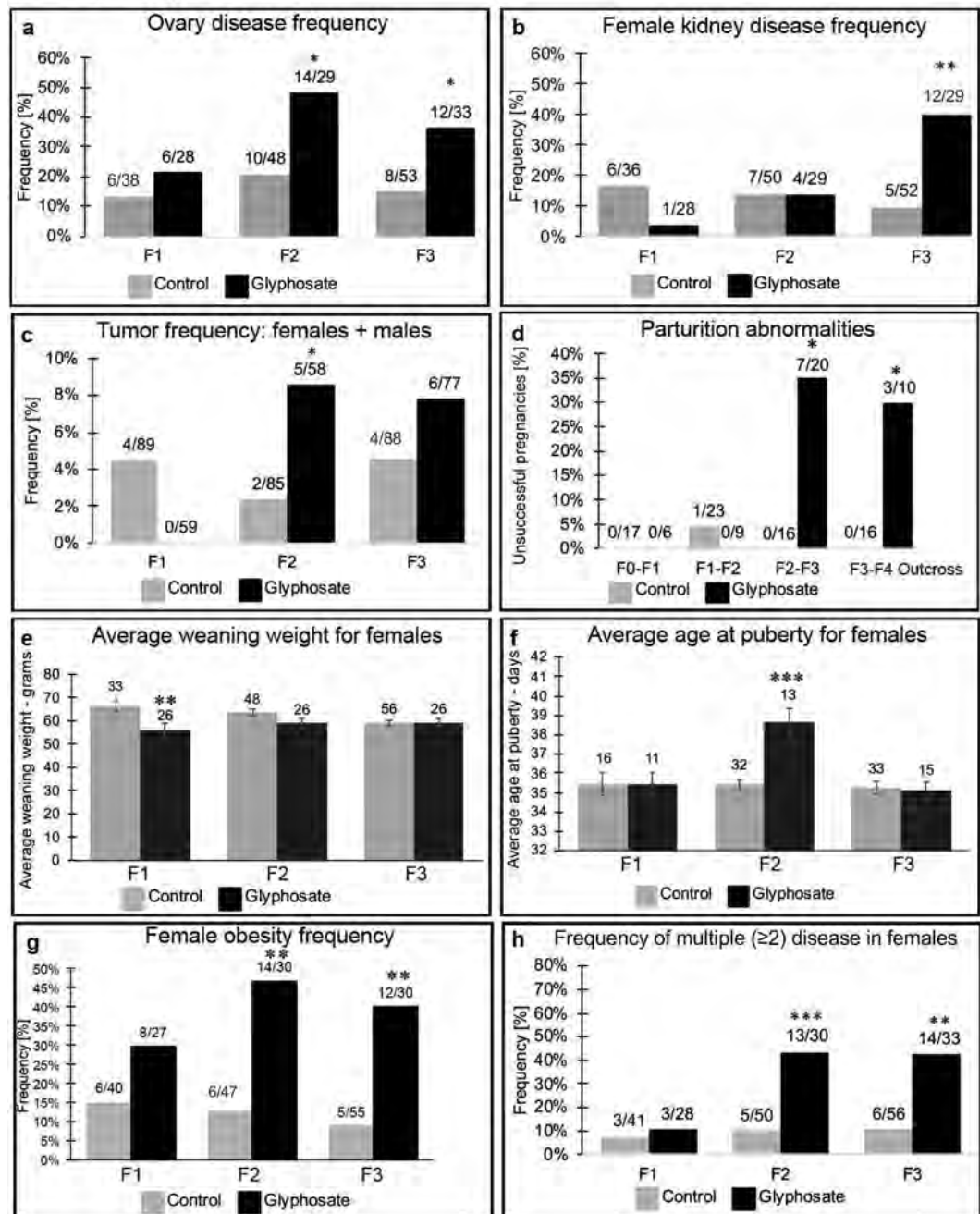


Figure 2. Female pathology analysis in F1, F2 and F3 generation control and glyphosate lineage 1-year old rats. (a) ovary disease frequency, (b) female kidney disease frequency, (c) tumor frequency (males and females), (d) parturition abnormalities, (e) average weaning weight for females, (f) average age of puberty for females, (g) female obesity frequency, and (h) frequency of multiple disease in females. The pathology number ratio with total animal number is listed for each bar graph or mean \pm SEM (e,f), presented with asterisks indicating a statistical difference (* $p < 0.05$, ** $p < 0.01$, and *** $p < 0.001$ in comparison with control lineage animals.

characterized by the presence of histopathologies including azoospermia, atretic seminiferous tubules, presence of vacuoles in basal regions of the seminiferous tubules, sloughed germ cell in the lumen of tubules, and lack of tubule lumen²⁹, (Supplemental Figure S2). The most common histology abnormalities were atrophy and vacuoles, followed by sloughed cells and debris in the tubule lumen. The frequency or incidence of testis disease was found to be significantly elevated in the F2 generation glyphosate lineage, but no effect was observed in the direct exposure F1 generation or transgenerational F3 generation at one year of age, Fig. 1a. The different mechanisms and exposures for each generation (F1 generation direct somatic exposure, F2 generation direct germline exposure and F3 generation no exposure) can generate distinct pathologies for each generation²⁹. No gross abnormalities were observed in the corresponding epididymis at the time of dissection.

Prostate disease was characterized by atrophic or hyperplastic prostate glandular epithelium, and the presence of vacuole spaces in the epithelium as previously described⁴⁶ (Supplemental Figure S2). The most common histological abnormalities were epithelial cell atrophy and vacuoles, followed by hyperplasia. The prostate atrophy and regions with the presence of vacuoles are generally distinct from the regions showing hyperplasia. The frequency or incidence of prostate disease was similar for the control and glyphosate F1 and F2 generation males at one year of age, Fig. 1b. Interestingly, there was an increased frequency of prostate disease observed in the F3 generation glyphosate lineage males ($p < 0.01$). Therefore, one of the transgenerational pathologies (F3 generation) observed was prostate disease in approximately 30% of glyphosate lineage males, a three-fold increase in disease rate over controls, Fig. 1b.

Kidney disease was characterized by the presence of an increased number of proteinaceous fluid filled cysts, reduction in size of glomeruli, and thickening of Bowman's capsules, as previously described^{37,47} (Supplemental Figure S2). The most common histological abnormalities were cysts, presumably derived from dilated tubules, and thickened Bowman capsules, followed by reduced glomerular areas. There was an increase in kidney disease frequency in the glyphosate lineage males in the F2 generation, but not F1 or F3 generations, Fig. 1c. The frequency of kidney disease was found to be similar for both the F1 and F2 generation between the control and the glyphosate lineage females. There was an increased incidence of kidney disease observed in the F3 generation glyphosate lineage females affecting nearly 40% of females (a four-fold increase in disease rate) compared to the F3 generation control females, Fig. 2b.

Ovarian disease was characterized by the development of polycystic ovaries with an increase in the number of small and large cysts showing negligible granulosa cells, as previously described⁴⁸ (Supplemental Figure S2). The most common histological abnormalities were small cysts followed by large cysts. In addition, follicle counts were performed to determine any changes in the primordial follicle pool size, as previously described^{48,49}. The frequency of ovarian disease was not significantly different between control and glyphosate lineages in the F1 generation. However, there was a significant increase in ovarian disease observed in the F2 and F3 generation glyphosate lineage females when compared to the control lineage, Fig. 2a.

Tumor development was also monitored in males and females, and found to increase in the F2 generation glyphosate female lineage, but not the F1 or F3 generation glyphosate lineages, Fig. 2c. The most predominant tumors to develop in the male and female were mammary adenomas, as previously described^{37,41}. One mammary fibrosarcoma, one lymphoma, one trichoepithelioma and one aural fibrosarcoma were also identified. Tumor histopathology analysis was performed by WADDL.

Pubertal analysis revealed delayed pubertal onset in males in the F1 and F2 generation glyphosate lineage, but no effects in the F3 generation, Fig. 1d. Female pubertal onset was delayed in the F2 generation glyphosate lineage, and no effects were observed in the F1 or F3 generations, Fig. 2f.

Analysis of potential direct fetal exposure toxicity effects of glyphosate in the F1 generation and subsequent F2 and F3 generations included evaluation of litter sizes, sex ratios and weaning body weights of pups. There was no effect on litter size or sex ratio observed for any generation, Supplemental Figure S3. There was significantly lower weaning body weight observed for the F1 generation in the glyphosate lineage for both males ($p < 0.01$), Fig. 1e, and females ($p < 0.01$), Fig. 2e. In the F3 generation, there was no statistical difference in weaning weights for females, but an increase in males between the control and glyphosate lineages (Figs 1e and 2e).

A parturition (birth) abnormality was observed, and involved either the death of the late stage gestating mother or her pups immediately after or during birth. This phenotype was not observed in the F0 generation breeding to produce the F1 generation in either the glyphosate or control lineages. In F1 breeding to produce F2 generation offspring there was one instance in the control population where a parturition abnormality was observed, and no such instance occurred in that generation in the glyphosate lineage, Fig. 2d. However, during the gestation of F2 generation mothers with the F3 generation fetuses, dramatic parturition abnormalities were observed in the glyphosate lineage. The frequency of unsuccessful parturition was 35% ($p < 0.03$). Out of the 7 cases that were classified as unsuccessful pregnancies, Fig. 2d, there were 5 maternal mortalities observed. Necropsy of these animals by WADDL diagnosed 2 cases of dystocia, 1 case of severe rhinitis, 1 case of adrenal gland necrosis, and 1 case in which the cause was unknown. To further investigate the parturition abnormalities an outcross of F3 generation glyphosate lineage males with a wildtype female was performed. There were parturition abnormalities observed with a frequency of 30% ($p < 0.04$), Fig. 2d. In the paternal outcross generation, there were 3 cases of maternal mortality. The causes of maternal death confirmed by WADDL were 2 cases in which the cause of death was identified as dystocia, and 1 case of hyperplasia-mastitis. In order to quantify the rates of initial successful pregnancies, fertility rates of the females were compared between the control and the glyphosate lineages. Fertility rate was defined as the number of pregnancies divided by the number of breedings. Results showed no significant difference in the comparison of glyphosate and control lineage fertility rates in any generation, Supplemental Figure S3a.

The weight, body mass index (BMI), abdominal adiposity, and adipocyte cell size were analyzed in order to assess the frequency of obesity in glyphosate and control lineage males and females, as described in the Methods⁴⁵ (Supplemental Figure S2). Analysis of potential obese phenotypes in the F1, F2, and F3 generation glyphosate and control lineages identified a significant increase in the obese phenotype of the F2 and F3 glyphosate lineage males and females, Figs 1f and 2g. The frequency of obesity was not found to be different between the control versus glyphosate lineage F1 generation males and females. Therefore, a transgenerational (F3 generation) obese phenotype was observed in approximately 40% of the glyphosate lineage females and 42% of the glyphosate lineage males, Figs 1f and 2g.

Direct exposure studies to glyphosate have been shown to induce behavioral abnormalities in the exposed F0 generation^{50–53}. Behavioral analysis of the glyphosate and control lineage transgenerational F3 generation at 11 months of age was done. Both a light and dark box (LDB) and elevated plus maze (EPM) were used to assess potential anxiety behavior⁵⁰. The F3 generation glyphosate lineage males and females had fewer total light side

attempts and fewer total attempts compared to the controls in the light and dark box, Supplemental Figure S4a–e. No changes in other light and dark box parameters were observed. For the elevated plus maze with an open and closed arm results indicate that there was no behavioral difference observed ($p > 0.05$) for the control or glyphosate (open arm time or closed arm time per total time ratio) lineage F3 generation females or males, Supplemental Figure S4g and i. None of the other parameters of the EPM analysis were found to be altered, Supplemental Figure S4f–j. Although there was a reduced number of light and total attempts in the LDB by the glyphosate lineage F3 generation males, none of the other LDB or EPM parameters supported a behavioral effect, Supplemental Figure S4. Therefore, no major behavioral effects were observed in the F3 generation glyphosate lineage males or females.

The incidence of disease and abnormalities in all F1, F2 and F3 generation control and glyphosate lineage males and females is presented in Figs 1 and 2 and Supplemental Tables S1–S3 (a–d). The specific diseases associated with each individual animal are shown in Tables S1 (a–d), S2 (a–d) and S3 (a–d). This information was used for the analysis of one (≥ 1) disease and multiple (≥ 2) disease incidence, Figs 1 and 2. The frequency of one (≥ 1) disease in F1, F2 or F3 generation glyphosate lineage females was not statistically different from control lineage animals. In males, the frequency rate of one (≥ 1) male disease did not differ from the controls in the F1 generation, but increased significantly in the F2 and F3 generations, Fig. 1g. The frequency of multiple diseases (≥ 2) for females was not significant for the F1 generation, but the frequency increased for glyphosate lineage females in the F2 generation ($p < 0.01$) and F3 generation ($p < 0.01$) (Fig. 2h). Over 40% of the F3 generation glyphosate lineage females (2-fold increase) developed disease and abnormalities when compared to the controls. The frequency of multiple disease in the F1 and F3 generation males was not statistically different from controls, but an increase in multiple disease frequency was observed in the F2 generation males ($p < 0.01$) (Fig. 1h). Therefore, the F3 generation glyphosate lineage females had a significant increase in multiple diseases, suggesting a transgenerational increase in disease susceptibility.

Sperm Epigenetic Analysis. Glyphosate induced transgenerational inheritance of disease and pathology requires the germline (sperm or egg) transmission of epigenetic information between generations²⁹. Therefore, sperm was collected from the control and glyphosate lineage F1, F2 and F3 generation males for epigenetic analysis. Potential differential DNA methylation regions (DMRs) in the sperm were identified using a comparison between the control and glyphosate lineage, as described in the Methods⁴⁵. The sperm DNA was isolated, fragmented and the methylated DNA immunoprecipitated (MeDIP) with a methyl-cytosine antibody. The MeDIP DNA fragments were sequenced for an MeDIP-Seq analysis as described in the Methods⁵⁴. The sperm DMR numbers are presented in Fig. 3 for a variety of p-value cutoff thresholds, and $p < 10^{-6}$ was selected as the threshold for all subsequent analyses. The total number of DMRs for the control versus glyphosate lineage F1 generation is 264 with 40 of them having multiple neighboring 100 bp windows, Fig. 3a. The F2 generation had 174 DMRs with 6 of them with two multiple windows detected, Fig. 3b. The transgenerational F3 generation sperm were found to have 378 total DMRs with 31 of these having multiple neighboring windows, Fig. 3c. Therefore, the glyphosate lineage sperm were found to have altered DNA methylation in direct exposure F1 and F2 generations, as well as the transgenerational F3 generation⁵⁵. Interestingly, there was negligible overlap of the sperm DMRs between each generation, Fig. 3d. Previous studies have observed that direct exposure and transgenerational generation DMRs are distinct, apparently due to the unique mechanisms for direct exposure toxicity and transgenerational actions of environmental exposures^{29,55}. Observations indicate glyphosate can promote germline epigenetic alterations in DNA methylation.

The chromosomal locations of the DMRs for each generation are presented in Fig. 4. Nearly all chromosomes had DMRs for the F1, F2 and F3 generations, indicated by arrowhead, along with clusters of DMRs indicated by black boxes, Fig. 4. Therefore, the DMR identified were genome-wide on all chromosomes. The genomic features of the DMRs were investigated and shown to have a low CpG density “CpG deserts”⁵⁶, and be predominantly 1 kb in length, Supplemental Figure S5. Similar DMR genomic factors were observed for the F1, F2 and F3 generations. The F3 generation DMR data was used in a permutation analysis to show the number of DMRs identified (red line) is not due to random variation in the control and glyphosate data, Fig. 5a, and correlated with the false discovery rate (FDR) analysis performed. In addition, a principle component analysis (PCA), with the DMRs not whole genome, of the F3 generation DMRs showed efficient separation of the control versus glyphosate DMR data and clustering of control DMR data, Fig. 5b. Similar observations were made with the F1 and F2 generation DMR PCA analysis, Supplemental Figure S6. These data demonstrate that statistically significant DMRs are observed for the F1, F2 and F3 generations sperm.

The DMR associated genes were identified for DMRs within 10 kb of a gene to include gene promoters and listed in Supplemental Figures S4, S5 and S6 for the F1, F2 and F3 generation DMR lists, respectively. The majority of DMRs were not associated with genes. The genes and associated gene categories for each DMR and associated genes are provided. A summary of the DMR associated gene categories indicates transcription, signaling, metabolism, receptors, and cytokines are predominant, Fig. 6a. A summary of DMR associated gene categories are presented for the F1, F2 and F3 generation gene categories. The DMR associated gene pathways are presented in Fig. 6b. The top five KEGG (Kyoto Encyclopedia of Genes and Genomes) gene pathways for the F1, F2 and F3 generations are listed with number of DMR associated genes involved in the pathway shown in brackets. The only pathway that overlaps in all three generations is the metabolic pathway, but this pathway involves hundreds of genes and sub-pathways so is anticipated. Other common pathways between the F1 and F2 generations and F2 and F3 generations are present. Various signaling pathways are the most common pathways identified.

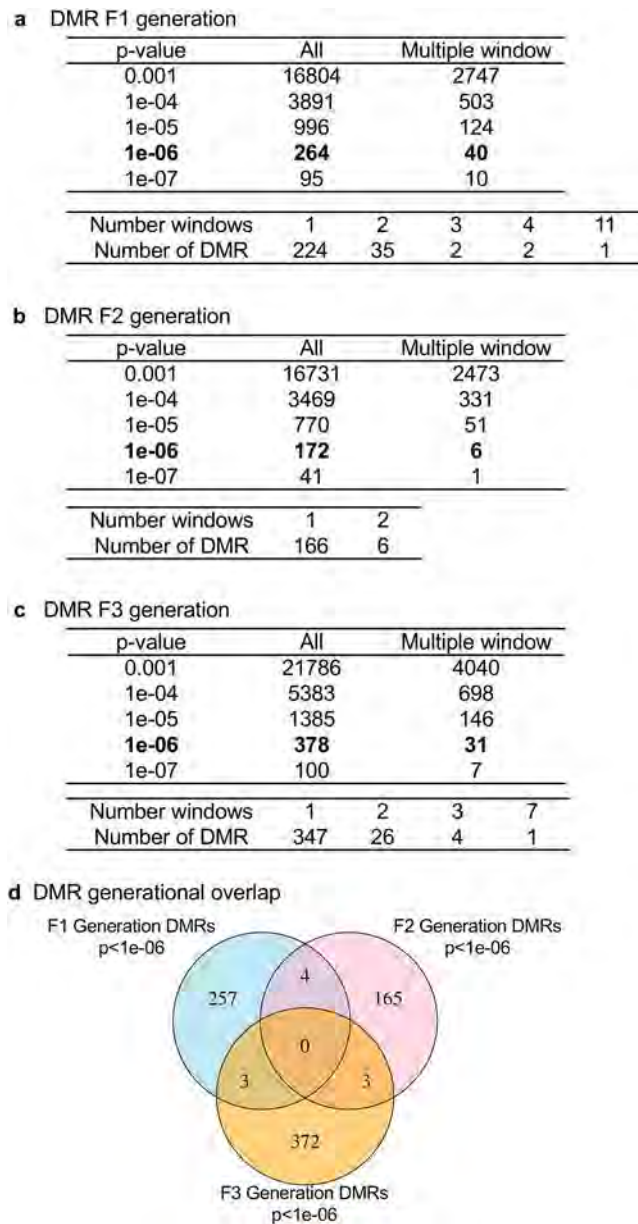


Figure 3. Epigenetic analysis and DMR identification. The number of DMRs found using different p-value cutoff thresholds. The All column shows all DMRs. The Multiple Window column shows the number of DMRs containing at least two significant windows. The number of DMR with each specific number of significant windows at a p-value threshold of 1e-06 is shown below each table. **(a)** DMR F1 Generation. **(b)** DMR F2 Generation. **(c)** DMR F3 Generation. **(d)** DMR overlap Venn diagram.

Discussion

Glyphosate is the most commonly used pesticide worldwide with predominant use in corn, soy and canola crops, Supplemental Figure S1. Although there have been many reports regarding the potential toxicity of glyphosate^{1,12,13}, direct exposure has been suggested by regulatory agencies to have minimal or no toxicity^{10,11}. A recent study suggested glyphosate induced female reproduction abnormalities in the offspring of exposed rats²⁷. The current study provides the first analysis of potential transgenerational impacts of glyphosate in mammals. The exposure of a gestating female directly exposes the F0 generation female, the F1 generation offspring, and the germline within the F1 generation offspring that will generate the F2 generation grand-offspring⁴⁵. Therefore, the first transgenerational generation is the F3 generation great-grand-offspring not having any direct exposure⁵⁵, Fig. 7. The direct exposure mechanisms of action in the F0, F1 and F2 generations are distinct from the transgenerational germline mediated actions. Although the F2 generations grand-offspring can have a mixture of direct exposure and generational actions²⁹, the lack of any direct exposure is first observed in the transgenerational F3 generation, Fig. 7. The impacts of transient glyphosate exposure on a F0 generation gestating female and subsequent generations not receiving any further exposure were assessed. Preconception adult exposures

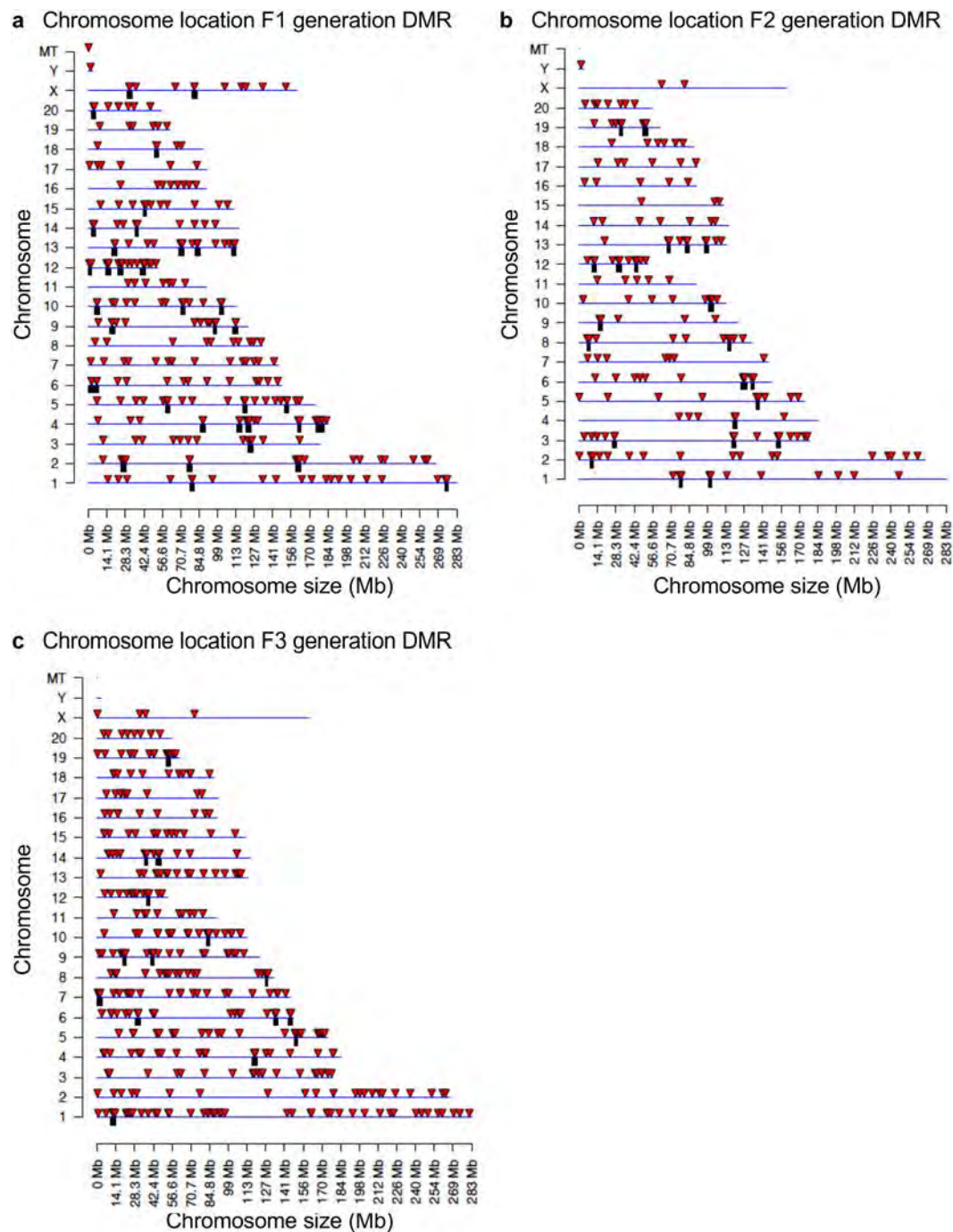


Figure 4. Chromosomal location of DMRs at a p-value threshold of 1e-06. **(a)** Chromosome locations of F1 generation DMRs. **(b)** Chromosome location F2 generation DMRs. **(c)** Chromosome location F3 generation DMRs. Triangles indicate DMRs. Rectangles indicate clusters of DMRs.

(e.g. abnormal diet and mercury) of males and females have also been shown to promote transgenerational impacts^{57,58}. The current study focused on gestating female exposure actions.

The impacts of environmental exposures on subsequent generations can be referred to as “Generational Toxicology”, and suggests ancestral exposures can promote the onset of disease and pathology in subsequent generations. The mechanism involved is epigenetic transgenerational inheritance through epigenetic alterations of the germline²⁹. Although many exposures can influence both the directly exposed individuals and transgenerational individuals, recent observations suggest some toxicants or exposures have negligible impacts on the direct exposed individuals, but can influence subsequent generations never having direct exposure. For example, a recent study with the herbicide atrazine was found to have negligible impacts on the direct exposed F0, F1 or F2 generations, but increased pathologies in the transgenerational F3 generation⁴⁵. Therefore, classic toxicology analysis with atrazine demonstrates negligible or low risk of direct exposure, so relative safety for the compound,

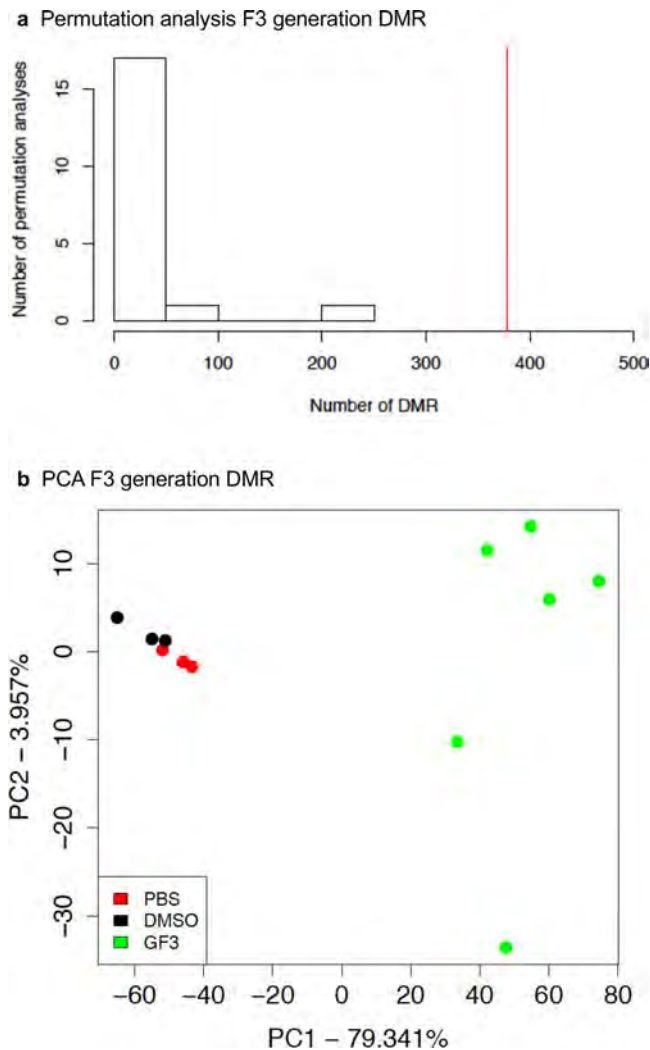


Figure 5. Permutation and principle component DMR analysis (PCA). **(a)** The number of F3 generation DMR for all permutation analyses. The vertical red line shows the number of DMR found in the original analysis. All DMRs are defined using an edgeR p-value threshold of $1e-06$. **(b)** DMR PCA using DMRs and not whole genome for F3 generation control and glyphosate DMR analysis with legend insert. The control (PBS), control (DMSO) and glyphosate F3 generation lineage (GF3) indicated.

since “Generational Toxicology” is not considered. The possibility glyphosate may have similar transgenerational actions was investigated.

Analysis of the direct actions of glyphosate demonstrated no overt toxicity on the F0, F1, F2 or F3 generations considering the lack of impacts on litter size, sex ratios or fertility, Figure S3. The F1 generation offspring had negligible pathologies in any of the tissues analyzed. The only effects observed were on weaning weights in both males and females, and a delay in puberty in males. Therefore, classic toxicology analysis of the F0 and F1 generations demonstrated negligible toxicity or pathology from direct glyphosate exposure. In contrast, the F2 generation grand-offspring, derived from a direct exposure F1 generation germline²⁹, had significant increases in testis disease, kidney disease, obesity, and multiple diseases in males, Fig. 1. The F2 generation females had significant increases in ovary disease, obesity, mammary gland tumors, parturition abnormalities, and multiple disease susceptibility, Fig. 2. The transgenerational F3 generation great-grand-offspring males had increased prostate disease, obesity, and single disease frequencies, while females had increased ovarian disease, kidney disease, parturition abnormalities, and multiple disease susceptibility, Figs 1 and 2. A unique pathology observed with glyphosate exposure, and seldom seen in previous transgenerational studies⁵⁹, was the parturition abnormalities. Over 30% of the F2 generation female rats in the later stages of gestation died of dystocia and/or had litter mortality. This was also seen in the paternal outcross F3 generation gestating female rats, Fig. 2. Although dystocia and parturition mortalities are not a common occurrence in humans today due to improved obstetric care, the underlying pathology observed may reflect parturition abnormalities such as premature birth rates and infant abnormalities seen today^{60,61}. In addition, the significantly higher obesity rates observed in the F2 and F3 generation male and female rats appear to correlate with the dramatic increase in obesity in the human population observed over the past several generations⁶². Many of the pathology frequencies observed to be induced by glyphosate

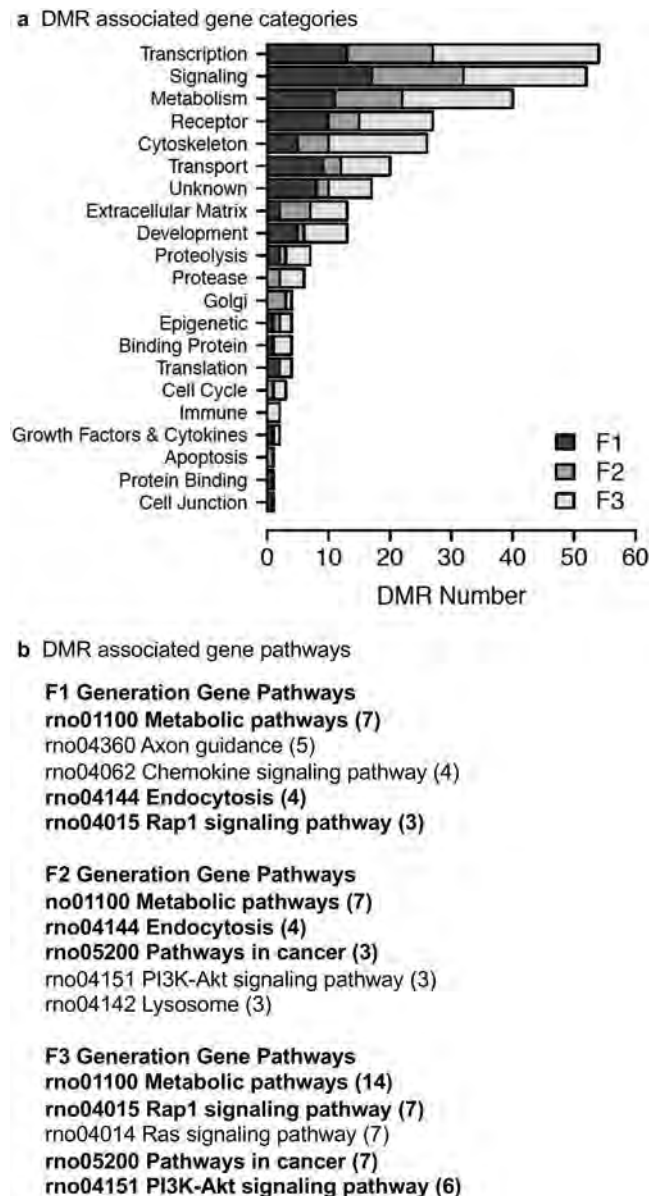


Figure 6. DMR gene associations. (a) DMR associated gene functional categories (genes within 10 kb DMR). (b) KEGG pathways containing DMR associated genes. Number DMR associated genes in pathway in brackets. Pathways in bold are common to at least two generations.

transgenerationally are similar to the frequency of pathology in the human population today, for example the 40% obesity frequency identified. In contrast to the negligible pathology and disease observed in the F0 and F1 generations, significant pathology was observed in the F2 generation and transgenerational F3 generation males and females. Therefore, based on the associations of glyphosate exposure, the transgenerational disease and sperm epigenetic alterations, we propose glyphosate promotes the epigenetic transgenerational inheritance of disease.

Interpretation of the data needs to take into consideration the experimental design and technical limitation of the study. The current study used a mode of administration to control the exposure dose that does not allow a classic risk assessment. The experimental dose used does provide an environmentally relevant exposure of twice the allowed industry exposure (2.8–5 mg/kg/day) following metabolism of the glyphosate and half the NOAEL. Therefore, the current study was performed to simply determine the potential that glyphosate may promote the epigenetic transgenerational inheritance of pathology and sperm epimutations. Observations suggest future glyphosate risk assessment will need to consider generational toxicology and transgenerational impacts. Classic and current toxicology studies only involve direct exposure of the individual, while impacts on future generations are not assessed. In addition, a technical limitation of the study to consider was the observation that a founder effect derived from one control lineage female and one control lineage male from the F0 generation, whose offspring when bred to the F2 generation resulted in nearly all offspring having obesity. This level of disease (100% in females) suggests an abnormality and founder effect. This was calculated and confirmed as outlined in

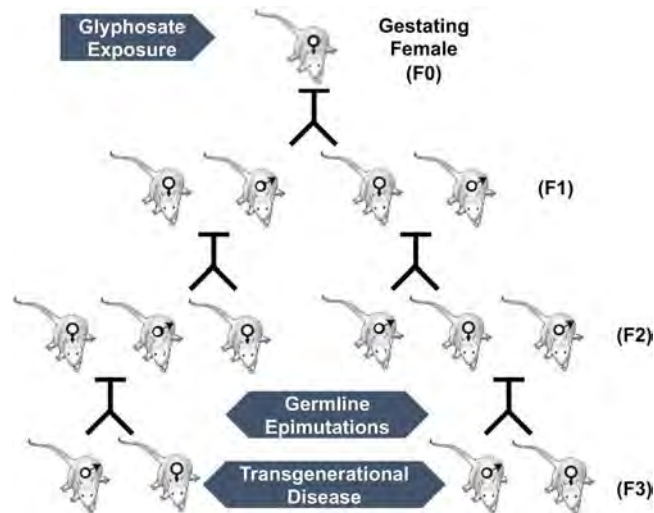


Figure 7. Schematic of generational (F0, F1, F2 and F3) transmission through male and female lineage to the transgenerational F3 generation.

Supplemental Figure S7, and resulted in the removal of all individuals from these control founders lineages. A replacement was made with a concurrently generated control population using PBS (phosphate buffered saline) versus DMSO (dimethyl sulfoxide) as vehicle control exposure. A principle component analysis (PCA) with the DMRs was performed on the PBS and DMSO controls in the epigenetic analysis (Fig. 5b and Supplemental Figure S6), and they clustered together with the F3 generation and to a lesser extent in the F1 and F2 generations. Separately, a histopathology analysis comparison of the PBS and DMSO controls did not find any statistical difference pathologies between the controls. In addition, analysis of the pathologies with the affected founders lineages present still identified similar generational pathologies with the exception of the frequency of kidney disease and obesity being reduced. Therefore, a founder effect was identified, and the replacement controls were shown to correlate well. Although potential founder effects for other pathologies were considered in the F1 generation controls and glyphosate lineages, no other founder effects were identified. Finally, rodent models have long been used as model organisms to study human related phenomena. Rodent animal studies should be considered relevant to humans due to the extensive evolutionary conservation of the vast majority of physiological systems among mammals. Although the specific physiological impact and pathologies may vary, the current study indicates transgenerational impacts need to be considered.

The molecular mechanisms involved in epigenetic transgenerational inheritance requires germline (sperm and egg) epigenetic alterations, termed “epimutations”²⁹. A recent study identified the concurrent transgenerational alterations in DNA methylation, ncRNAs and histone retention have been observed in sperm⁵⁴. Although the focus of the current study is to identify the presence of epimutations only involved DNA methylation analysis, other epigenetic processes are also anticipated to be involved. A comparison of control versus glyphosate lineage F1, F2 and F3 generation male sperm DNA identified DMRs at each generation. As previously demonstrated⁵⁴, negligible overlap of DMRs were observed between the generations (Fig. 3d) which appears to reflect the very different mechanisms of action between direct exposure in the F1 and F2 generation versus the transgenerational F3 generation mechanisms (germline induced embryonic stem cell alteration)²⁹. The genomic features of the DMRs were similar to those previously described involving CpG deserts²⁹. DMR gene associations were determined and found to have common gene functional categories and some overlap in gene pathways between generations, but specific genes did not overlap.

Approximately ~43% of the F3 generation DMR are associated with genes, while the majority (57%) are intergenic. These intergenic regions have been proposed to influence associated disease functions⁶³ in the regulation of ncRNA that can act distally across megabases^{64,65}. The DNA methylation can also stabilize copy number variation and suppress transposons, and alter chromatin structure^{66,67}. Therefore, the DMRs are proposed to be functional with some impacting gene expression⁶³. The, sperm epimutations identified (i.e. DMRs) are proposed to in part mediate the transgenerational pathology phenotype observed.

Although the DNA methylation is correlated with the transgenerational pathology, and previous studies shown to have regulatory roles in germline inheritance mechanisms²⁹, a functional role for DNA methylation remains to be elucidated. Interestingly, alterations in germline ncRNAs has been shown to be functionally linked and determined by injection of altered sperm ncRNA into eggs and observing the induced transgenerational phenotypes³⁰. Further research is needed, but the current literature suggests a functional role for the altered germline epigenome in mediating transgenerational epigenetic inheritance. For example, a DNA methylation epigenetic alteration in a plant flowering phenotype has been shown to be epigenetically inherited for over a 100 generations^{29,68}. Similar alterations in drosophila and *C. elegans* have also been reported^{29,69–71}, but the epigenetic process is distinct and appears to involve histone alterations. Observations suggest the phenomenon does not appear easily reversible. Previous studies have shown that environmentally induced epigenetic transgenerational

inheritance does not impact genetics of the F1 generation sperm, as shown by analysis of copy number variations (CNVs) or point mutations^{72,73}, but genetic mutations start to appear in the F3 generation sperm^{72,73}. Therefore, the integrated actions of epigenetics and genetics may contribute to the transgenerational phenotypes, but this remains to be elucidated.

The F1 generation offspring epigenetic alterations are due to direct exposure of specific somatic cell types⁵⁵ and negligible pathology or disease was observed. The transgenerational F3 generation great-grand-offspring developed pathology and appears to involve the presence of germline (i.e. sperm) epimutations. The proposal is following fertilization the epigenetic alterations potentially alter the early developing stem cells in the embryo. This may result in epigenetic and transcription alterations in all somatic cell types and lineages derived from these embryonic stem cells²⁹. We have observed this in the Sertoli cells in the testis⁷⁴, in prostate epithelial cells⁴⁶, and in granulosa cells in the ovary⁷⁵. Therefore, the pathology and disease observed in the F3 generation appear to be in part the result of cell type specific epigenetic and transgenerational alterations for potentially all cells and tissues²⁹. Glyphosate exposure of the F0 and F1 generation had negligible toxicity and pathology, which supports direct exposure having low risk, however, the transgenerational germline mediated inheritance promotes significant pathology and disease.

Conclusions

In summary, glyphosate was found to promote the epigenetic transgenerational inheritance of disease and pathology through germline (i.e. sperm) epimutations. Negligible pathology was observed in the F0 and F1 generations, while a significant increase in pathology and disease was observed in the F2 generation grand-offspring and F3 generation great-grand-offspring. Therefore, glyphosate appears to have a low or negligible toxic risk for direct exposure, but promotes generational toxicology in future generations. Observations suggest generational toxicology needs to be incorporated into the risk assessment of glyphosate and all other potential toxicants, as previously described⁴⁵. The ability of glyphosate and other environmental toxicants to impact our future generations needs to be considered, and is potentially as important as the direct exposure toxicology done today for risk assessment.

Methods

Animal studies and breeding. As previously described⁷⁶, female and male rats of an outbred strain Hsd:Sprague Dawley[®]SD[®]TM (Harlan) at 70 to 100 days of age were fed ad lib with a standard rat diet and ad lib tap water. Timed-pregnant females on days 8 through 14 of gestation⁵⁹ were administered daily intraperitoneal injections of glyphosate (25 mg/kg BW/day dissolved in PBS) (Chem Service, Westchester PA) or dimethyl sulfoxide (DMSO) or Phosphate Buffered Saline (PBS), as previously described⁴⁷. Twenty-five mg/kg for glyphosate is 0.4% of rat oral LD50 and 50% of the NOAEL and considering glyphosate rapid metabolism approximately twice the occupational exposure 3–5 mg/kg per daily exposure^{10,77}. There was a founder effect observed in the offspring of a specific male from the control population treated with PBS, manifesting as abnormally high rates (80–100%) of obesity in descendants, Supplemental Figure S7. Therefore, a portion of original control colony was excluded from the study due to the obesity founder effects identified. These animals were replaced with offspring from DMSO-treated controls from a concurrent study. Disease phenotypes were compared from both DMSO lineage and PBS lineage controls, with no significant differences observed with histopathology evaluations between the two populations, Fig. 5 and Supplemental Figure S6.

As previously described⁷⁶, the gestating female rats treated were designated as the F0 generation. F1–F3 generation control and glyphosate lineages were housed in the same room and racks with lighting, food and water as previously described^{37,47,78}. All experimental protocols for the procedures with rats were pre-approved by the Washington State University Animal Care and Use Committee (protocol IACUC # 6252). All methods were performed in accordance with the relevant guidelines and regulations.

Tissue harvest and histology processing. Rats were euthanized at 12 months of age by CO₂ inhalation and cervical dislocation for tissue harvest. Testis, prostate, ovary, kidney, and gonadal fat pads were fixed in Bouin's solution (Sigma) followed by 70% ethanol, then processed for paraffin embedding and hematoxylin, and eosin (H & E) staining by standard procedures for histopathological examination. Paraffin five micron sections were processed, stained, and provided by Nationwide Histology, Spokane WA, USA.

Histopathology examination and disease classification. The oversight of the pathology analysis involved the co-author, Dr. Eric Nilsson, DVM/PhD, with over 20 years of pathology analysis in rats^{45,46}. The Washington Animal Disease Diagnostic Laboratory (WADDL) at the Washington State University College of Veterinary Medicine has board certified veterinary pathologists and assisted in initially establishing the criteria for the pathology analyses and identifying parameters to assess³⁷. WADDL performed full necropsies as required on animals that died prior to the time of scheduled sacrifice at one year, and performed tumor classifications in the current study.

Upon dissection a brief examination of abdominal and thoracic organs was performed to look for obvious abnormalities. The current study found no significant gross pathology of heart, lung, liver, gastro-intestinal track, or spleen. The tissues evaluated histologically were selected from previous literature showing them to have pathology in transgenerational models^{36–45}, with an emphasis on reproductive organs. Histopathology readers were trained to recognize the specific abnormalities evaluated for this study in rat testis, ventral prostate, ovary and kidney (see below). The different pathology readers were used for each tissue and were blinded to the treatment groups. A set of quality control (QC) slides was generated for each tissue and was read by each reader prior to evaluating any set of experimental slides. These QC slide results are monitored for reader accuracy and concordance. WADDL was consulted when any questions developed. Previous studies by the laboratory help confirm and validate the pathology analysis^{36–45}.

As previously described²⁹, testis histopathology criteria included the presence of vacuoles in the seminiferous tubules, azoospermic atretic seminiferous tubules, and ‘other’ abnormalities including sloughed spermatogenic cells in center of the tubule and a lack of a tubule lumen (Supplemental Figure S2). As previously described^{46,79}, prostate histopathology criteria included the presence of vacuoles in the glandular epithelium, atrophic glandular epithelium and hyperplasia of prostatic gland epithelium (Supplemental Figure S2). Kidney histopathology criteria included reduced size of glomerulus, thickened Bowman’s capsule, and the presence of proteinaceous fluid-filled cysts >50 µm in diameter (Supplemental Figure S2). Ovary sections were assessed for the two pathologies of primordial follicle loss and ovarian cysts, as previously described⁴⁸ (Supplemental Figure S2). Ovarian cysts have little or no granulosa cell layer, a smooth border, and are 50–250 µm (small cysts) or >250 µm (large cysts) in diameter. A cut-off was established to declare a tissue ‘diseased’ based on the mean number of histopathological abnormalities plus two standard deviations from the mean of control group tissues, as assessed by each of the three individual observers blinded to the treatment groups. This number (i.e. greater than two standard deviations) was used to classify rats into those with and without testis, ovary, prostate, or kidney disease in each lineage. A rat tissue section was finally declared ‘diseased’ only when at least two of the three observers marked the same tissue section ‘diseased’.

Obesity was assessed with an increase in adipocyte size (area), body mass index (BMI) and abdominal adiposity, as previously described^{40,41,80–82}. BMI was calculated with weight (g)/length (cm)² with the length of the animal measured from the nose to the base of the tail. Gonadal fat pad slides were imaged using a Nikon Eclipse E800 microscope (10×) with an AVT Prosilica GE1050C Color GigE camera. Five field of view image captures were taken per slide in varying parts of the fat pad. Adipocyte size was measured converting pixels into microns using Adiposoft⁸³. Measurements of the 20 largest cells from each image for a total of 100 were averaged as hypertrophic cells are the most metabolically relevant and susceptible to cell death⁸⁴. Obesity and lean phenotypes were determined utilizing the mean of the control population males and females, and a cut off of 1.5 standard deviations above and below the mean (Supplemental Figure S2).

Behavior analysis. As previously described⁴⁵, behavior analysis was performed to evaluate general anxiety⁸⁵ with both an elevated plus maze and Light and Dark, box as previously described^{86,87}. F3 generation male and female rats from control and glyphosate lineages were used for the behavioral studies at 11 months of age. The elevated plus-maze consisted of a “plus”-shaped platform made of black opaque Plexiglas, with each platform 10 cm in width and 50 cm in length, creating a 10 × 10 cm neutral zone in the center. Two of the arms were enclosed with black Plexiglas walls 40 cm high, with no ceiling. For this task, rats were placed individually into the center (neutral) zone of the maze, facing an open arm. Rats were allowed to explore for a 5 min period, and the number of open and closed arm entries and time spent on the open and closed arms were recorded. The Light and Dark box consists of a small dark compartment that made up one third of the apparatus with the other two thirds being an illuminated compartment. The rats were placed individually in the light zone, facing the dark zone, as previously recommended^{88,89}. Similarly, the number light and dark compartment entries and time spent on the light and dark compartments were recorded.

Statistical analyses for pathology. As previously described⁷⁶, for results that yielded continuous data (age at puberty, weight at euthanization, sex ratio, litter size, fertility rate, parturition abnormality behavioral parameters), treatment groups were analyzed using Student’s t-test. For results expressed as the proportion of affected animals that exceeded a pre-determined threshold (testis, prostate, kidney or ovary disease frequency, tumor frequency, lean/obese frequency), groups were analyzed using Fisher’s exact test.

Sperm Epigenetic Analysis. Epididymal sperm collection and DNA isolation. The protocol is described in detail in reference⁷⁶. Briefly, the epididymis was dissected free of fat and connective tissue, then, after cutting open the cauda, placed into 6 ml of phosphate buffer saline (PBS) for 20 minutes at room temperature. Further incubation at 4 °C will immobilize the sperm. The tissue was then minced, the released sperm pelleted at 4 °C 3,000 × g for 10 min, then resuspended in NIM buffer and stored at –80 °C for further processing.

An appropriate amount of rat sperm suspension was used for DNA extraction. Previous studies have shown mammalian sperm heads are resistant to sonication unlike somatic cells^{90,91}. Somatic cells and debris were therefore removed by brief sonication (Fisher Sonic Dismembrator, model 300, power 25), then centrifugation and washing 1–2 times in 1xPBS. The resulting pellet was resuspended in 820 µL DNA extraction buffer and 80 µL 0.1 M DTT added, then incubated at 65 °C for 15 minutes. 80 µL proteinase K (20 mg/ml) was added and the sample was incubated at 55 °C for 2–4 hours under constant rotation. Protein was removed by addition of protein precipitation solution (300 µL, Promega A795A), incubation for 15 min on ice, then centrifugation at 13,500 rpm for 30 minutes at 4 °C. One ml of the supernatant was precipitated with 2 µL of glycoblue (Invitrogen, AM9516) and 1 ml of cold 100% isopropanol. After incubation, the sample was spun at 13,500 × g for 30 min at 4 °C, then washed with 70% cold ethanol. The pellet was air-dried for about 5 minutes then resuspended in 100 µL of nuclease free water. For all generations, equal amounts of DNA from each individual’s sample was used to produce 6 different DNA pools per lineage and the pooled DNA used for methylated DNA immunoprecipitation (MeDIP).

Methylated DNA Immunoprecipitation (MeDIP). The protocol is described in detail in reference⁷⁶. Genomic DNA was sonicated and run on 1.5% agarose gel for fragment size verification. The sonicated DNA was then diluted with TE buffer to 400 µL, then heat-denatured for 10 min at 95 °C, and immediately cooled on ice for 10 min to create single-stranded DNA fragments. Then 100 µL of 5X IP buffer and 5 µg of antibody (monoclonal mouse anti 5-methyl cytidine; Diagenode #C15200006) were added, and the mixture was incubated overnight on a rotator at 4 °C. The following day magnetic beads (Dynabeads M-280 Sheep anti-Mouse IgG; Life Technologies 11201D) were pre-washed per manufacturer’s instructions, and 50 µL of beads were added to the

500 µl of DNA-antibody mixture from the overnight incubation, then incubated for 2 h on a rotator at 4 °C. After this incubation, the samples were washed three times with 1X IP buffer using a magnetic rack. The washed samples were then resuspended in 250 µl digestion buffer (5 mM Tris PH 8, 10 mM EDTA, 0.5% SDS) with 3.5 µl Proteinase K (20 mg/ml), and incubated for 2–3 hours on a rotator at 55°. DNA clean-up was performed using a Phenol-Chloroform-Isoamylalcohol extraction, and the supernatant precipitated with 2 µl of glycoblue (20 mg/ml), 20 µl of 5 M NaCl and 500 µl ethanol in –20 °C freezer for one to several hours. The DNA precipitate was pelleted, washed with 70% ethanol, then dried and resuspended in 20 µl H₂O or TE. DNA concentration was measured in Qubit (Life Technologies) with the ssDNA kit (Molecular Probes Q10212).

MeDIP-Seq Analysis. MeDIP DNA was used to create libraries for next generation sequencing (NGS) using the NEBNext® Ultra™ RNA Library Prep Kit for Illumina® (San Diego, CA) starting at step 1.4 of the manufacturer's protocol to generate double stranded DNA from the single-stranded DNA resulting from MeDIP. After this step, the manufacturer's protocol was followed indexing each sample individually with NEBNext Multiplex Oligos for Illumina. The WSU Spokane Genomics Core sequenced the samples on the Illumina HiSeq 2500 at PE50, with a read size of approximately 50 bp and approximately 20 million reads per pool. Twelve libraries were run in one lane.

Statistics and Bioinformatics. The DMR identification and annotation methods follow those presented in previous published papers^{45,54}. Data quality was assessed using the FastQC program (<https://www.bioinformatics.babraham.ac.uk/projects/fastqc/>), and reads were cleaned and filtered to remove adapters and low quality bases using Trimmomatic⁹². The basic read quality was verified using summaries produced by the FastQC program. The new data was cleaned and filtered to remove adapters and low quality bases using Trimmomatic⁹². The reads for each MeDIP sample were mapped to the Rnor 6.0 rat genome using Bowtie2⁹³ with default parameter options. The mapped read files were then converted to sorted BAM files using SAMtools⁸³. The MEDIPS R package⁸⁴ was used to calculate differential coverage between control and exposure sample groups. The edgeR p-value⁹⁴ was used to determine the relative difference between the two groups for each genomic window. Windows with an edgeR p-value less than an arbitrarily selected threshold were considered DMRs. The DMR edges were extended until no genomic window with an edgeR p-value less than 0.1 remained within 1000 bp of the DMR. The false discovery rate (FDR) p-value was <0.05 for all DMRs identified at an edgeR p-value < 1e-06.

DMRs were annotated using the biomaRt R package⁹⁵ to access the Ensembl database⁹⁶. The genes that associated with DMR were then input into the KEGG pathway search^{97,98} to identify associated pathways. The DMR associated genes were then automatically sorted into functional groups using information provided by the DAVID⁹⁹ and Panther¹⁰⁰ databases incorporated into an internal curated database (www.skinner.wsu.edu under genomic data). All molecular data has been deposited into the public database at NCBI (GEO # GSE118557) and R code computational tools available at GitHub (<https://github.com/skinnerlab/MeDIP-seq>) and www.skinner.wsu.edu.

Data Availability

All molecular data has been deposited into the public database at NCBI (GEO # GSE118557) and R code computational tools available at GitHub (<https://github.com/skinnerlab/MeDIP-seq>) and www.skinner.wsu.edu.

References

1. Benbrook, C. M. Trends in glyphosate herbicide use in the United States and globally. *Environ Sci Eur* **28**, 3, <https://doi.org/10.1186/s12302-016-0070-0> (2016).
2. Connolly, A. *et al.* Exploring the half-life of glyphosate in human urine samples. *Int J Hyg Environ Health*. <https://doi.org/10.1016/j.ijheh.2018.09.004> (2018).
3. Gay, M. *et al.* A phenotypic approach to the discovery of compounds that promote non-amyloidogenic processing of the amyloid precursor protein: Toward a new profile of indirect beta-secretase inhibitors. *Eur J Med Chem* **159**, 104–125, <https://doi.org/10.1016/j.ejmech.2018.08.092> (2018).
4. Jasper, R., Locatelli, G. O., Pilati, C. & Locatelli, C. Evaluation of biochemical, hematological and oxidative parameters in mice exposed to the herbicide glyphosate-Roundup(R). *Interdiscip Toxicol* **5**, 133–140, <https://doi.org/10.2478/v10102-012-0022-5> (2012).
5. Kimmel, G. L., Kimmel, C. A., Williams, A. L. & DeSesso, J. M. Evaluation of developmental toxicity studies of glyphosate with attention to cardiovascular development. *Crit Rev Toxicol* **43**, 79–95, <https://doi.org/10.3109/10408444.2012.749834> (2013).
6. Prasad, S., Srivastava, S., Singh, M. & Shukla, Y. Clastogenic effects of glyphosate in bone marrow cells of swiss albino mice. *Journal of toxicology* **2009**, 308985, <https://doi.org/10.1155/2009/308985> (2009).
7. Romano, R. M., Romano, M. A., Bernardi, M. M., Furtado, P. V. & Oliveira, C. A. Prepubertal exposure to commercial formulation of the herbicide glyphosate alters testosterone levels and testicular morphology. *Arch Toxicol* **84**, 309–317, <https://doi.org/10.1007/s00204-009-0494-z> (2010).
8. Dallegre, E. *et al.* Pre- and postnatal toxicity of the commercial glyphosate formulation in Wistar rats. *Arch Toxicol* **81**, 665–673, <https://doi.org/10.1007/s00204-006-0170-5> (2007).
9. Benedetti, A. L., Vituri Cde, L., Trentin, A. G., Domingues, M. A. & Alvarez-Silva, M. The effects of sub-chronic exposure of Wistar rats to the herbicide Glyphosate-Biocarb. *Toxicol Lett* **153**, 227–232, <https://doi.org/10.1016/j.toxlet.2004.04.008> (2004).
10. (EFSA), E. F. S. A. Conclusion on the peer review of the pesticide risk assessment of the active substance glyphosate. *EFSA Journal* **13**, 4302, <https://doi.org/10.2903/j.efsa.2015.4302> (2015).
11. Mesnage, R., Defarge, N., Spiroux de Vendomois, J. & Seralini, G. E. Potential toxic effects of glyphosate and its commercial formulations below regulatory limits. *Food Chem Toxicol* **84**, 133–153, <https://doi.org/10.1016/j.fct.2015.08.012> (2015).
12. Mesnage, R. & Antoniou, M. N. Facts and Fallacies in the Debate on Glyphosate Toxicity. *Front Public Health* **5**, 316, <https://doi.org/10.3389/fpubh.2017.00316> (2017).
13. Bai, S. H. & Ogbourne, S. M. Glyphosate: environmental contamination, toxicity and potential risks to human health via food contamination. *Environ Sci Pollut Res Int* **23**, 18988–19001, <https://doi.org/10.1007/s11356-016-7425-3> (2016).
14. Brusick, D., Aardema, M., Kier, L., Kirkland, D. & Williams, G. Genotoxicity Expert Panel review: weight of evidence evaluation of the genotoxicity of glyphosate, glyphosate-based formulations, and aminomethylphosphonic acid. *Crit Rev Toxicol* **46**, 56–74, <https://doi.org/10.1080/10408444.2016.1214680> (2016).

15. Nevison, C. D. A comparison of temporal trends in United States autism prevalence to trends in suspected environmental factors. *Environmental health: a global access science source* **13**, 73, <https://doi.org/10.1186/1476-069X-13-73> (2014).
16. de Brito Rodrigues, L. *et al.* Ecotoxicological assessment of glyphosate-based herbicides: Effects on different organisms. *Environmental toxicology and chemistry/SETAC* **36**, 1755–1763, <https://doi.org/10.1002/etc.3580> (2017).
17. Garry, V. F. *et al.* Birth defects, season of conception, and sex of children born to pesticide applicators living in the Red River Valley of Minnesota, USA. *Environmental health perspectives* **110**(Suppl 3), 441–449 (2002).
18. Yousef, M. I. *et al.* Toxic effects of carbofuran and glyphosate on semen characteristics in rabbits. *J Environ Sci Health B* **30**, 513–534, <https://doi.org/10.1080/03601239509372951> (1995).
19. Cai, W. *et al.* Effects of glyphosate exposure on sperm concentration in rodents: A systematic review and meta-analysis. *Environ Toxicol Pharmacol* **55**, 148–155, <https://doi.org/10.1016/j.etap.2017.07.015> (2017).
20. Clair, E., Mesnage, R., Travert, C. & Seralini, G. E. A glyphosate-based herbicide induces necrosis and apoptosis in mature rat testicular cells *in vitro*, and testosterone decrease at lower levels. *Toxicol In Vitro* **26**, 269–279, <https://doi.org/10.1016/j.tiv.2011.12.009> (2012).
21. Romano, M. A. *et al.* Glyphosate impairs male offspring reproductive development by disrupting gonadotropin expression. *Arch Toxicol* **86**, 663–673, <https://doi.org/10.1007/s00204-011-0788-9> (2012).
22. Hernandez-Plata, I., Giordano, M., Diaz-Munoz, M. & Rodriguez, V. M. The herbicide glyphosate causes behavioral changes and alterations in dopaminergic markers in male Sprague–Dawley rat. *Neurotoxicology* **46**, 79–91, <https://doi.org/10.1016/j.neuro.2014.12.001> (2015).
23. Cattani, D. *et al.* Developmental exposure to glyphosate-based herbicide and depressive-like behavior in adult offspring: Implication of glutamate excitotoxicity and oxidative stress. *Toxicology* **387**, 67–80, <https://doi.org/10.1016/j.tox.2017.06.001> (2017).
24. Owagboriaye, F. O. *et al.* Reproductive toxicity of Roundup herbicide exposure in male albino rat. *Exp Toxicol Pathol* **69**, 461–468, <https://doi.org/10.1016/j.etp.2017.04.007> (2017).
25. Ingaramo, P. I. *et al.* Effects of neonatal exposure to a glyphosate-based herbicide on female rat reproduction. *Reproduction* **152**, 403–415, <https://doi.org/10.1530/REP-16-0171> (2016).
26. Perego, M. C. *et al.* Influence of a Roundup formulation on glyphosate effects on steroidogenesis and proliferation of bovine granulosa cells *in vitro*. *Chemosphere* **188**, 274–279, <https://doi.org/10.1016/j.chemosphere.2017.09.007> (2017).
27. Milesi, M. M. *et al.* Perinatal exposure to a glyphosate-based herbicide impairs female reproductive outcomes and induces second-generation adverse effects in Wistar rats. *Arch Toxicol* **92**, 2629–2643, <https://doi.org/10.1007/s00204-018-2236-6> (2018).
28. de Araujo, J. S., Delgado, I. F. & Paumgarten, F. J. Glyphosate and adverse pregnancy outcomes, a systematic review of observational studies. *BMC Public Health* **16**, 472, <https://doi.org/10.1186/s12889-016-3153-3> (2016).
29. Nilsson, E., Sadler-Riggelman, I. & Skinner, M. K. Environmentally Induced Epigenetic Transgenerational Inheritance of Disease. *Environmental Epigenetics* **4**, 1–13, <https://doi.org/10.1093/eep/dvy016> (2018).
30. Gapp, K., von Ziegler, L., Tweedie-Cullen, R. Y. & Mansuy, I. M. Early life epigenetic programming and transmission of stress-induced traits in mammals: how and when can environmental factors influence traits and their transgenerational inheritance? *BioEssays: news and reviews in molecular, cellular and developmental biology* **36**, 491–502, <https://doi.org/10.1002/bies.201300116> (2014).
31. Pembrey, M., Saffery, R. & Bygren, L. O. Human transgenerational responses to early-life experience: potential impact on development, health and biomedical research. *J Med Genet* **51**, 563–572, [doi:10.1093/medgenet-2014-102577](https://doi.org/10.1093/medgenet/2014-102577) (2014).
32. Hackett, J. A. & Surani, M. A. DNA methylation dynamics during the mammalian life cycle. *Philosophical transactions of the Royal Society of London. Series B, Biological sciences* **368**, 20110328, <https://doi.org/10.1098/rstb.2011.0328> (2013).
33. von Meyenn, F. *et al.* Comparative Principles of DNA Methylation Reprogramming during Human and Mouse *In Vitro* Primordial Germ Cell Specification. *Developmental cell* **39**, 104–115, <https://doi.org/10.1016/j.devcel.2016.09.015> (2016).
34. Ben Maamar, M. *et al.* Developmental origins of transgenerational sperm DNA methylation epimutations following ancestral DDT exposure. *Developmental biology* **445**, 280–293, <https://doi.org/10.1016/j.ydbio.2018.11.016> (2018).
35. Bruner-Tran, K. L. *et al.* Developmental exposure of mice to dioxin promotes transgenerational testicular inflammation and an increased risk of preterm birth in unexposed mating partners. *PLoS one* **9**, e105084, <https://doi.org/10.1371/journal.pone.0105084> (2014).
36. Anway, M. D., Cupp, A. S., Uzumcu, M. & Skinner, M. K. Epigenetic transgenerational actions of endocrine disruptors and male fertility. *Science* **308**, 1466–1469, [doi:10.1126/science.1120183](https://doi.org/10.1126/science.1120183) (2005).
37. Anway, M. D., Leathers, C. & Skinner, M. K. Endocrine disruptor vinclozolin induced epigenetic transgenerational adult-onset disease. *Endocrinology* **147**, 5515–5523, [doi:10.1210/en.2006-0640](https://doi.org/10.1210/en.2006-0640) (2006).
38. Guerrero-Bosagna, C., Settles, M., Lucker, B. & Skinner, M. Epigenetic transgenerational actions of vinclozolin on promoter regions of the sperm epigenome. *PLoS one* **5**(1–17), e13100, <https://doi.org/10.1371/journal.pone.0013100> (2010).
39. Manikkam, M., Tracey, R., Guerrero-Bosagna, C. & Skinner, M. Plastics Derived Endocrine Disruptors (BPA, DEHP and DBP) Induce Epigenetic Transgenerational Inheritance of Obesity, Reproductive Disease and Sperm Epimutations. *PLoS one* **8**(1–18), e55387 (2013).
40. Manikkam, M., Tracey, R., Guerrero-Bosagna, C. & Skinner, M. Pesticide and Insect Repellent Mixture (Permethrin and DEET) Induces Epigenetic Transgenerational Inheritance of Disease and Sperm Epimutations. *Reproductive toxicology* **34**, 708–719 (2012).
41. Skinner, M. K. *et al.* Ancestral dichlorodiphenyltrichloroethane (DDT) exposure promotes epigenetic transgenerational inheritance of obesity. *BMC medicine* **11**(228), 221–216 (2013).
42. Manikkam, M., Haque, M. M., Guerrero-Bosagna, C., Nilsson, E. & Skinner, M. K. Pesticide methoxychlor promotes the epigenetic transgenerational inheritance of adult onset disease through the female germline. *PLoS one* **9**(1–19), e102091 (2014).
43. Tracey, R., Manikkam, M., Guerrero-Bosagna, C. & Skinner, M. Hydrocarbons (jet fuel JP-8) induce epigenetic transgenerational inheritance of obesity, reproductive disease and sperm epimutations. *Reproductive toxicology* **36**, 104–116, <https://doi.org/10.1016/j.reprotox.2012.11.011> (2013).
44. Manikkam, M., Tracey, R., Guerrero-Bosagna, C. & Skinner, M. K. Dioxin (TCDD) induces epigenetic transgenerational inheritance of adult onset disease and sperm epimutations. *PLoS one* **7**(1–15), e46249, <https://doi.org/10.1371/journal.pone.0046249> (2012).
45. McBirney, M. *et al.* Atrazine Induced Epigenetic Transgenerational Inheritance of Disease, Lean Phenotype and Sperm Epimutation Pathology Biomarkers. *PLoS one* **12**(1–37), e0184306 (2017).
46. Anway, M. D. & Skinner, M. K. Transgenerational effects of the endocrine disruptor vinclozolin on the prostate transcriptome and adult onset disease. *Prostate* **68**, 517–529, <https://doi.org/10.1002/pros.20724> (2008).
47. Manikkam, M., Guerrero-Bosagna, C., Tracey, R., Haque, M. M. & Skinner, M. K. Transgenerational actions of environmental compounds on reproductive disease and identification of epigenetic biomarkers of ancestral exposures. *PLoS one* **7**(1–12), e31901, <https://doi.org/10.1371/journal.pone.0031901> (2012).
48. Nilsson, E. *et al.* Environmentally Induced Epigenetic Transgenerational Inheritance of Ovarian Disease. *PLoS one* **7**(1–18), e36129 (2012).
49. Nilsson, E. E., Schindler, R., Savenkova, M. I. & Skinner, M. K. Inhibitory actions of Anti-Mullerian Hormone (AMH) on ovarian primordial follicle assembly. *PLoS one* **6**(1–10), e20087, <https://doi.org/10.1371/journal.pone.0020087> (2011).

50. Crews, D. *et al.* Transgenerational epigenetic imprints on mate preference. *Proceedings of the National Academy of Sciences of the United States of America* **104**, 5942–5946, doi:0610410104 (2007).
51. Skinner, M. K. Endocrine disruptor induction of epigenetic transgenerational inheritance of disease. *Molecular and cellular endocrinology* **398**, 4–12, doi:S0303-7207(14)00223-8 (2014).
52. Walters, J. L., Lansdell, T. A., Lookingland, K. J. & Baker, L. E. The effects of gestational and chronic atrazine exposure on motor behaviors and striatal dopamine in male Sprague-Dawley rats. *Toxicology and applied pharmacology* **289**, 185–192, <https://doi.org/10.1016/j.taap.2015.09.026> (2015).
53. Lin, Z., Dodd, C. A. & Filipov, N. M. Short-term atrazine exposure causes behavioral deficits and disrupts monoaminergic systems in male C57BL/6 mice. *Neurotoxicology and Teratology* **39**, 26–35, <https://doi.org/10.1016/j.ntt.2013.06.002> (2013).
54. Ben Maamar, M. *et al.* Alterations in sperm DNA methylation, non-coding RNA expression, and histone retention mediate vinclozolin-induced epigenetic transgenerational inheritance of disease. *Environmental Epigenetics* **4**(1–19), dvy010, <https://doi.org/10.1093/eepdvy010> (2018).
55. Skinner, M. K. What is an epigenetic transgenerational phenotype? F3 or F2. *Reproductive toxicology* **25**, 2–6, doi:S0890-6238(07)00278-X (2008).
56. Skinner, M. K. & Guerrero-Bosagna, C. Role of CpG Deserts in the Epigenetic Transgenerational Inheritance of Differential DNA Methylation Regions. *BMC Genomics* **15**, 692 (2014).
57. Lane, M., Zander-Fox, D. L., Robker, R. L. & McPherson, N. O. Peri-conception parental obesity, reproductive health, and transgenerational impacts. *Trends Endocrinol Metab* **26**, 84–90, <https://doi.org/10.1016/j.tem.2014.11.005> (2015).
58. Carvan, M. J. R. *et al.* Mercury-induced epigenetic transgenerational inheritance of abnormal neurobehavior is correlated with sperm epimutations in zebrafish. *PLoS one* **12**(1–26), e0176155, <https://doi.org/10.1371/journal.pone.0176155> (2017).
59. Nilsson, E. E., Anway, M. D., Stanfield, J. & Skinner, M. K. Transgenerational epigenetic effects of the endocrine disruptor vinclozolin on pregnancies and female adult onset disease. *Reproduction* **135**, 713–721, doi:REP-07-0542 (2008).
60. Blencowe, H. *et al.* National, regional, and worldwide estimates of preterm birth rates in the year 2010 with time trends since 1990 for selected countries: a systematic analysis and implications. *Lancet* **379**, 2162–2172, [https://doi.org/10.1016/S0140-6736\(12\)60820-4](https://doi.org/10.1016/S0140-6736(12)60820-4) (2012).
61. Cheong, J. L. & Doyle, L. W. Increasing rates of prematurity and epidemiology of late preterm birth. *J Paediatr Child Health* **48**, 784–788, <https://doi.org/10.1111/j.1440-1754.2012.02536.x> (2012).
62. Huo, L., Lyons, J. & Magliano, D. J. Infectious and Environmental Influences on the Obesity Epidemic. *Curr Obes Rep* **5**, 375–382, <https://doi.org/10.1007/s13679-016-0224-9> (2016).
63. Haque, M. M., Nilsson, E. E., Holder, L. B. & Skinner, M. K. Genomic Clustering of differential DNA methylated regions (epimutations) associated with the epigenetic transgenerational inheritance of disease and phenotypic variation. *BMC Genomics* **17**, 418, 411–413, <https://doi.org/10.1186/s12864-016-2748-5> (2016).
64. Vance, K. W. & Ponting, C. P. Transcriptional regulatory functions of nuclear long noncoding RNAs. *Trends in genetics: TIG* **30**, 348–355, <https://doi.org/10.1016/j.tig.2014.06.001> (2014).
65. Orom, U. A. & Shiekhattar, R. Noncoding RNAs and enhancers: complications of a long-distance relationship. *Trends in genetics: TIG* **27**, 433–439, <https://doi.org/10.1016/j.tig.2011.06.009> (2011).
66. Pathak, R. & Feil, R. Environmental effects on chromatin repression at imprinted genes and endogenous retroviruses. *Curr Opin Chem Biol* **45**, 139–147, <https://doi.org/10.1016/j.cbpa.2018.04.015> (2018).
67. Lim, C. Y., Knowles, B. B., Solter, D. & Messerschmidt, D. M. Epigenetic Control of Early Mouse Development. *Curr Top Dev Biol* **120**, 311–360, <https://doi.org/10.1016/bs.ctdb.2016.05.002> (2016).
68. Cubas, P., Vincent, C. & Coen, E. An epigenetic mutation responsible for natural variation in floral symmetry. *Nature* **401**, 157–161, <https://doi.org/10.1038/43657> (1999).
69. Kelly, W. G. Multigenerational chromatin marks: no enzymes need apply. *Developmental cell* **31**, 142–144, <https://doi.org/10.1016/j.devcel.2014.10.008> (2014).
70. Xia, B., Gerstin, E., Schones, D. E., Huang, W. & Steven de Belle, J. Transgenerational programming of longevity through E(z)-mediated histone H3K27 trimethylation in Drosophila. *Aging (Albany NY)* **8**, 2988–3008, <https://doi.org/10.18632/aging.101107> (2016).
71. Klosin, A., Casas, E., Hidalgo-Carcedo, C., Vavouri, T. & Lehner, B. Transgenerational transmission of environmental information in *C. elegans*. *Science* **356**, 320–323, <https://doi.org/10.1126/science.aah6412> (2017).
72. Skinner, M. K., Guerrero-Bosagna, C. & Haque, M. M. Environmentally Induced Epigenetic Transgenerational Inheritance of Sperm Epimutations Promote Genetic Mutations. *Epigenetics: official journal of the DNA Methylation Society* **10**, 762–771 (2015).
73. McCarrey, J. R. *et al.* Tertiary Epimutations - A Novel Aspect of Epigenetic Transgenerational Inheritance Promoting Genome Instability. *PLoS one* **11**(1–15), e0168038, <https://doi.org/10.1371/journal.pone.0168038> (2016).
74. Guerrero-Bosagna, C., Savenkova, M., Haque, M. M., Nilsson, E. & Skinner, M. K. Environmentally Induced Epigenetic Transgenerational Inheritance of Altered Sertoli Cell Transcriptome and Epigenome: Molecular Etiology of Male Infertility. *PLoS one* **8**(1–12), e59922 (2013).
75. Nilsson, E. *et al.* Environmental toxicant induced epigenetic transgenerational inheritance of ovarian pathology and granulosa cell epigenome and transcriptome alterations: ancestral origins of polycystic ovarian syndrome and primary ovarian insufficiency. *Epigenetics* **13**, 875–895, <https://doi.org/10.1080/15592294.2018.1521223> (2018).
76. Nilsson, E. *et al.* Vinclozolin induced epigenetic transgenerational inheritance of pathologies and sperm epimutation biomarkers for specific diseases. *PLoS one* **13**(1–29), e0202662 (2018).
77. Menkes, D. B., Temple, W. A. & Edwards, I. R. Intentional self-poisoning with glyphosate-containing herbicides. *Hum Exp Toxicol* **10**, 103–107, <https://doi.org/10.1177/096032719101000202> (1991).
78. Skinner, M. K., Manikkam, M. & Guerrero-Bosagna, C. Epigenetic transgenerational actions of environmental factors in disease etiology. *Trends Endocrinol Metab* **21**, 214–222, doi:S1043-2760(09)00218-5 (2010).
79. Taylor, J. A., Richter, C. A., Ruhlen, R. L. & vom Saal, F. S. Estrogenic environmental chemicals and drugs: mechanisms for effects on the developing male urogenital system. *J Steroid Biochem Mol Biol* **127**, 83–95, doi:S0960-0760(11)00151-8 (2011).
80. McAllister, E. J. *et al.* Ten putative contributors to the obesity epidemic. *Critical Reviews in Food Science and Nutrition* **49**, 868–913, doi:917375057 (2009).
81. Xie, F. *et al.* Long-term neuropeptide Y administration in the periphery induces abnormal baroreflex sensitivity and obesity in rats. *Cell Physiol Biochem* **29**, 111–120, doi:000337592 (2012).
82. Phillips, L. K. & Prins, J. B. The link between abdominal obesity and the metabolic syndrome. *Curr Hypertens Rep* **10**, 156–164 (2008).
83. Li, H. *et al.* The Sequence Alignment/Map format and SAMtools. *Bioinformatics* **25**, 2078–2079, <https://doi.org/10.1093/bioinformatics/btp352> (2009).
84. Lienhard, M., Grimm, C., Morkel, M., Herwig, R. & Chavez, L. MEDIPS: genome-wide differential coverage analysis of sequencing data derived from DNA enrichment experiments. *Bioinformatics* **30**, 284–286, <https://doi.org/10.1093/bioinformatics/bt650> (2014).
85. Schneider, P., Ho, Y. J., Spanagel, R. & Pawlak, C. R. A novel elevated plus-maze procedure to avoid the one-trial tolerance problem. *Front Behav Neurosci* **5**, 43, <https://doi.org/10.3389/fnbeh.2011.00043> (2011).

86. Crews, D. *et al.* Epigenetic transgenerational inheritance of altered stress responses. *Proceedings of the National Academy of Sciences of the United States of America* **109**, 9143–9148, doi:1118514109 (2012).
87. Skinner, M. K., Anway, Savenkova, M. I., Gore, A. C. & Crews, D. Transgenerational epigenetic programming of the brain transcriptome and anxiety behavior. *PLoS one* **3**(1–11), e3745, <https://doi.org/10.1371/journal.pone.0003745> (2008).
88. Ladron de Guevara-Miranda, D. *et al.* Long-lasting memory deficits in mice withdrawn from cocaine are concomitant with neuroadaptations in hippocampal basal activity, GABAergic interneurons and adult neurogenesis. *Dis Model Mech* **10**, 323–336, <https://doi.org/10.1242/dmm.026682> (2017).
89. Colorado, R. A., Shumake, J., Conejo, N. M., Gonzalez-Pardo, H. & Gonzalez-Lima, F. Effects of maternal separation, early handling, and standard facility rearing on orienting and impulsive behavior of adolescent rats. *Behav Processes* **71**, 51–58, <https://doi.org/10.1016/j.beproc.2005.09.007> (2006).
90. Calvin, H. I. Isolation of subfractionation of mammalian sperm heads and tails. *Methods Cell Biol* **13**, 85–104 (1976).
91. Huang, T. T. Jr. & Yanagimachi, R. Inner acrosomal membrane of mammalian spermatozoa: its properties and possible functions in fertilization. *Am J Anat* **174**, 249–268, <https://doi.org/10.1002/aja.1001740307> (1985).
92. Bolger, A. M., Lohse, M. & Usadel, B. Trimmomatic: a flexible trimmer for Illumina sequence data. *Bioinformatics* **30**, 2114–2120, <https://doi.org/10.1093/bioinformatics/btu170> (2014).
93. Langmead, B. & Salzberg, S. L. Fast gapped-read alignment with Bowtie 2. *Nature methods* **9**, 357–359, <https://doi.org/10.1038/nmeth.1923> (2012).
94. Robinson, M. D., McCarthy, D. J. & Smyth, G. K. edgeR: a Bioconductor package for differential expression analysis of digital gene expression data. *Bioinformatics* **26**, 139–140, <https://doi.org/10.1093/bioinformatics/btp616> (2010).
95. Durinck, S., Spellman, P. T., Birney, E. & Huber, W. Mapping identifiers for the integration of genomic datasets with the R/Bioconductor package biomaRt. *Nature protocols* **4**, 1184–1191, <https://doi.org/10.1038/nprot.2009.97> (2009).
96. Cunningham, F. *et al.* Ensembl 2015. *Nucleic acids research* **43**, D662–669, <https://doi.org/10.1093/nar/gku1010> (2015).
97. Kanehisa, M. & Goto, S. KEGG: kyoto encyclopedia of genes and genomes. *Nucleic acids research* **28**, 27–30, doi:gkd027 (2000).
98. Kanehisa, M. *et al.* Data, information, knowledge and principle: back to metabolism in KEGG. *Nucleic acids research* **42**, D199–205, <https://doi.org/10.1093/nar/gkt1076> (2014).
99. Huang da, W., Sherman, B. T. & Lempicki, R. A. Systematic and integrative analysis of large gene lists using DAVID bioinformatics resources. *Nature protocols* **4**, 44–57, <https://doi.org/10.1038/nprot.2008.211> (2009).
100. Mi, H., Muruganujan, A., Casagrande, J. T. & Thomas, P. D. Large-scale gene function analysis with the PANTHER classification system. *Nature protocols* **8**, 1551–1566, <https://doi.org/10.1038/nprot.2013.092> (2013).

Acknowledgements

We would like to thank Ms. Margaux McBirney, Ms. Michelle Pappalardo, Ms. Hannah Kimbel and Mr. Ryan Thompson for technical assistance, Dr. Millissia Ben Maamar and Dr. Kevin Arnold for critically reviewing the manuscript. We also acknowledge Ms. Amanda Quilty for assistance in editing the manuscript and Ms. Heather Johnson for assistance in preparation of the manuscript. We thank the WSU Spokane Genomic Core laboratory. The research was supported by a grant from the John Templeton Foundation (# 61174) to MKS.

Author Contributions

M.K.S. conceived and designed the study; D.K., E.N., S.E.K., I.S.R. and D.B. performed the majority of the experiments and analyses; M.K.S. and D.K. wrote the first draft and all authors participated in editing the manuscript; D.K., E.N. and S.E.K. performed the animal studies and pathology experiments; I.S.R. performed the molecular studies; and D.B. performed the bioinformatics and statistical analysis; M.K.S. supervised the experiments and obtained the funding.

Additional Information

Supplementary information accompanies this paper at <https://doi.org/10.1038/s41598-019-42860-0>.

Competing Interests: The authors declare no competing interests.

Publisher's note: Springer Nature remains neutral with regard to jurisdictional claims in published maps and institutional affiliations.



Open Access This article is licensed under a Creative Commons Attribution 4.0 International License, which permits use, sharing, adaptation, distribution and reproduction in any medium or format, as long as you give appropriate credit to the original author(s) and the source, provide a link to the Creative Commons license, and indicate if changes were made. The images or other third party material in this article are included in the article's Creative Commons license, unless indicated otherwise in a credit line to the material. If material is not included in the article's Creative Commons license and your intended use is not permitted by statutory regulation or exceeds the permitted use, you will need to obtain permission directly from the copyright holder. To view a copy of this license, visit <http://creativecommons.org/licenses/by/4.0/>.

© The Author(s) 2019

RESEARCH ARTICLE

Epigenetic transgenerational inheritance of testis pathology and Sertoli cell epimutations: generational origins of male infertility

Ingrid Sadler-Riggelman^{1,†}, Rachel Klukovich ^{2,†}, Eric Nilsson¹, Daniel Beck¹, Yeming Xie², Wei Yan^{2,‡} and Michael K. Skinner ^{1,*,‡}

¹Center for Reproductive Biology, School of Biological Sciences, Washington State University, Pullman, WA 99164-4236, USA; ²Department of Physiology and Cell Biology, University of Nevada, Reno School of Medicine, Reno, NV 89557, USA

*Correspondence address: Center for Reproductive Biology, School of Biological Sciences, Washington State University, Pullman, WA 99164-4236, USA. Tel: +1-509-335-1524; Fax: +1-509-335-2176; E-mail: skinner@wsu.edu

†Co-first authors.

‡Co-senior authors.

Managing editor: Dana Dolinoy

Abstract

Male reproductive health has been in decline for decades with dropping sperm counts and increasing infertility, which has created a significant societal and economic burden. Between the 1970s and now, a general decline of over 50% in sperm concentration has been observed in the population. Environmental toxicant-induced epigenetic transgenerational inheritance has been shown to affect testis pathology and sperm count. Sertoli cells have an essential role in spermatogenesis by providing physical and nutritional support for developing germ cells. The current study was designed to further investigate the transgenerational epigenetic changes in the rat Sertoli cell epigenome and transcriptome that are associated with the onset of testis disease. Gestating female F0 generation rats were transiently exposed during the period of fetal gonadal sex determination to the environmental toxicants, such as dichlorodiphenyltrichloroethane (DDT) or vinclozolin. The F1 generation offspring were bred (i.e. intercross within the lineage) to produce the F2 generation grand-offspring that were then bred to produce the transgenerational F3 generation (i.e. great-grand-offspring) with no sibling or cousin breeding used. The focus of the current study was to investigate the transgenerational testis disease etiology, so F3 generation rats were utilized. The DNA and RNA were obtained from purified Sertoli cells isolated from postnatal 20-day-old male testis of F3 generation rats. Transgenerational alterations in DNA methylation, noncoding RNA, and gene expression were observed in the Sertoli cells from vinclozolin and DDT lineages when compared to the control (vehicle exposed) lineage. Genes associated with abnormal Sertoli cell function and testis pathology were identified, and the transgenerational impacts of vinclozolin and DDT were determined. Alterations in critical gene pathways, such as the pyruvate metabolism pathway, were identified. Observations suggest that ancestral exposures to environmental toxicants promote the epigenetic transgenerational inheritance of Sertoli cell epigenetic and transcriptome alterations that associate with testis abnormalities. These epigenetic

Received 11 January 2019; revised 28 August 2019; accepted 19 July 2019

© The Author(s) 2019. Published by Oxford University Press.

This is an Open Access article distributed under the terms of the Creative Commons Attribution Non-Commercial License (<http://creativecommons.org/licenses/by-nc/4.0/>), which permits non-commercial re-use, distribution, and reproduction in any medium, provided the original work is properly cited. For commercial re-use, please contact journals.permissions@oup.com

alterations appear to be critical factors in the developmental and generational origins of testis pathologies and male infertility.

Key words: Sertoli cell; male infertility; testis pathology; transgenerational; vinclozolin; DDT

Introduction

Epimutations were originally defined as ‘heritable epigenetic changes in chromosomes which do not involve changes in the DNA sequence itself’ [1, 2]. A more updated definition of epigenetics is ‘molecular factors and processes that regulate genome activity independent of DNA sequence and are mitotically stable’ and for epimutations is ‘environmentally induced differential presence of epigenetic alterations that can influence genome activity compared to organisms not having the exposure’ [3]. A number of environmental factors can alter epigenetic processes such as DNA methylation, histone modifications (e.g. methylation and acetylation), chromosome structure, noncoding RNA (ncRNA), and RNA methylation to influence gene expression and genome activity. Epigenetic transgenerational inheritance describes a germline transmission of epimutations through generations without continued exposure to or presence of the original exposure beyond the F0 generation [3]. In cases where the germline is exposed during fetal gonadal sex determination, the epigenome in the germline can be modified. These epimutations appear to become ‘imprinted-like’, and potentially escape post-fertilization methylation erasure to allow transmission to the subsequent generations [4, 5]. The hypothesis is that this promotes stem cells in the embryo to develop an altered epigenome and transcriptome. Somatic cells and tissues derived from these epigenetically altered germline and stem cells will potentially develop alterations in cell type-specific epigenomes and transcriptomes [6]. These cell specific altered epigenomes will impact the fate of organs and tissues, and may be early indicators and initiators of the development of disease susceptibility later in life [7–9]. Previous examples of this phenomenon have been observed in prostate epithelial cells for prostate disease [10, 11], and granulosa cells for ovarian disease [12].

Numerous studies have shown epigenetic transgenerational inheritance to occur in different species involving a wide variety of different environmental exposures. Epigenetic transgenerational inheritance has been shown in plants [13], flies [14], worms [15], fish [16], birds [17, 18], rodents [5, 19], pigs [20], and humans [21]. Environmentally induced transgenerational diseases and abnormalities in mammals have been observed such as testis disease [8, 22, 23], prostate disease [9, 24], kidney disease [9, 24, 25], obesity [26], ovarian and uterine disease [22, 25, 27–30], tumor development [9], and behavioral changes [31–36]. A large number of environmental toxicants have been shown to be involved in triggering these transgenerational diseases and abnormalities that include the agricultural fungicide vinclozolin [5, 37–39], the herbicide atrazine [31, 40], plasticizers such as bisphenol A [22, 41] and phthalates [22], insect repellent diethyltoluamide (DEET) with the insecticide permethrin [27], pesticide methoxychlor [25], hydrocarbons (jet fuel) [28], and industrial compounds such as benzo[a]pyrene [42], the biocide tributyltin [43], mercury [16], dioxins [24, 29, 44], and the herbicide glyphosate [45].

The current study was designed to examine the ability of vinclozolin and dichlorodiphenyltrichloroethane (DDT) to induce transgenerationally affected Sertoli cell epigenome and

transcriptome alterations that associate with testis pathology. Sertoli cells play a critical role in spermatogenesis providing structural and nutritional support for the developing germ cells and are involved in the formation of the blood–testis barrier which creates a serum and pathogen free environment for the spermatogenic cells within the seminiferous tubules [46]. Therefore, Sertoli cells synthesize a number of transport binding proteins [47, 48] and provide the primary energy metabolites (i.e. pyruvate and lactate) for the developing germ cells, which are sequestered within the blood–testis barrier and unable to acquire glucose themselves [49]. A disruption in normal Sertoli cell development and function can affect spermatogenesis and promote testis pathology. Abnormal spermatogenesis and low sperm count are often linked to infertility, which can involve testis diseases like cryptorchidism, hypospadias, and testicular cancer [50–52]. Sperm counts have been declining significantly between 1973 and 2011, as shown in a 2017 meta-regression analysis [53]. Environmental factors such as endocrine disrupting chemicals, pesticides, heat, diet, stress, and smoking have been shown to be associated with this sperm count drop, and general testis health problems [53]. The molecular basis for these testis pathologies and generational impacts are investigated in the current study.

Exposure of gestating rats to the environmental toxicants such as DDT and vinclozolin leads to the epigenetic transgenerational inheritance of adult onset diseases, including testis disease and a decrease in sperm count and/or motility [26, 54]. Originally, vinclozolin’s involvement in epigenetic transgenerational inheritance of disease was observed in 2005 by Anway *et al.* [5] who found that vinclozolin exposure of gestating rats leads to epigenetic transgenerational inheritance of unique DNA methylation changes (epimutations) in sperm. Subsequent studies involving vinclozolin and DDT among other environmental toxicants confirmed these findings [26, 39, 55, 56]. Vinclozolin is an agricultural fungicide used in fruit and vegetable production and is an anti-androgenic compound that acts as a competitive antagonist of the androgen receptor [57]. DDT is a pesticide, which was widely used through the 1950s and 1960s in the USA until banned in 1972. It continues to be used in many parts of the world for insect and malaria control. DDT accumulates in the environment and in fatty tissue, and is an estrogen receptor agonist that has estrogenic effects in animals [58].

The epigenetic transgenerational inheritance phenomenon requires the germline transmission of altered epigenetic information between generations [59]. A variety of different environmental factors promoting epigenetic transgenerational inheritance were found to induce exposure specific alterations in sperm DNA methylation [5, 59]. Subsequently, vinclozolin was found to promote alterations in sperm ncRNA transgenerationally [60]. This supported previous studies indicating ncRNA germline alterations are important factors in epigenetic transgenerational inheritance [61, 62]. Recently, we observed that both vinclozolin and DDT cause concurrent alterations in cauda epididymal rat sperm DNA methylation, ncRNA, and histone retention [55, 56]. Therefore, several different epigenetic processes are likely integrated in epigenetic transgenerational inheritance. A 2013 study using vinclozolin determined that

vinclozolin impacts the epigenetic transgenerational inheritance of Sertoli cell DNA methylation and gene expression alterations [8]. This current study extends these findings with genome-wide analyses of DNA methylation and ncRNA alterations, and associated gene expression changes. These transgenerational alterations in Sertoli cell epigenetics correlate to corresponding alterations in testis pathology.

Results

Experimental Design and Testis Pathology

The F0 generation gestating female rats were exposed at approximately 90 days of age to DDT or vinclozolin during gestational days E8–E14, which corresponds to fetal gonadal sex determination and the germline differentiation period of development. The toxicants were dissolved in dimethylsulfoxide (DMSO) and administered by daily intraperitoneal injection during the transient exposure time frame. A separate group of control females was injected on the same schedule with only DMSO as a vehicle control. Each exposure lineage involved six different F0 generation females and was referred to as DDT, vinclozolin, and control lineages, respectively. This study and experimental approach were not designed for risk assessment, but to investigate the transgenerational phenomenon. The F1 generation animals were raised to 90 days of age and then bred within each lineage to obtain the F2 generation animals. The F2 generation animals were bred in the same manner to obtain the F3 generation animals. The only animals directly exposed were the F0 generation females. No sibling or cousin breeding was performed to avoid inbreeding artifacts. The male F3 generation pups were raised to 1 year of age for testis pathology analysis or to 18–22 days of age for isolation of Sertoli cells. The 20-day-old male pups were randomly divided into 3 different groups from different litters for each lineage with each group comprising 6–11 animals depending on litter sizes obtained. Within each group, the testis tissues were combined into one pool for isolation of Sertoli cells. The total Sertoli cell pools from each group were divided into two aliquots and stored as cell pellets at -80°C for DNA and RNA preparations.

The F3 generation Sertoli cells were isolated at 18–22 days of age to obtain optimally purified populations of cells. The purity of the cell preparations is routinely monitored, and has previously been shown to be $>98\%$ Sertoli cells by histology and subsequent culture purity determined with immunocytochemistry for fibronectin containing cells such as peritubular cells, as previously described [8, 63–65]. A cell fraction at this stage of 18–22 days of development allows for efficient analysis, and reduces the impact of testis pathology on the analysis since the majority of pathologies develop between 6 and 12 months of age. Therefore, at this early stage of development, the study is not confounded by the presence of disease. Another group of F3 generation animals was aged to 1 year and used to assess testis pathology. Testes were evaluated by microscopic examination of testis sections. Testis pathology was determined by the presence of atrophy of seminiferous tubules, vacuoles in the seminiferous epithelium, and sloughed spermatogenic cells in the tubule lumens, as described in Methods. Representative histopathologies are presented in [Supplementary Fig. S1](#). In the current study, DDT was found to promote testis disease in 46% of the males compared to 8% in the control lineage animals ([Fig. 1a](#)). Vinclozolin promoted a 44% frequency of testis pathology in the males ([Fig. 1a](#)). Therefore, both vinclozolin and DDT promoted the epigenetic transgenerational inheritance of testis

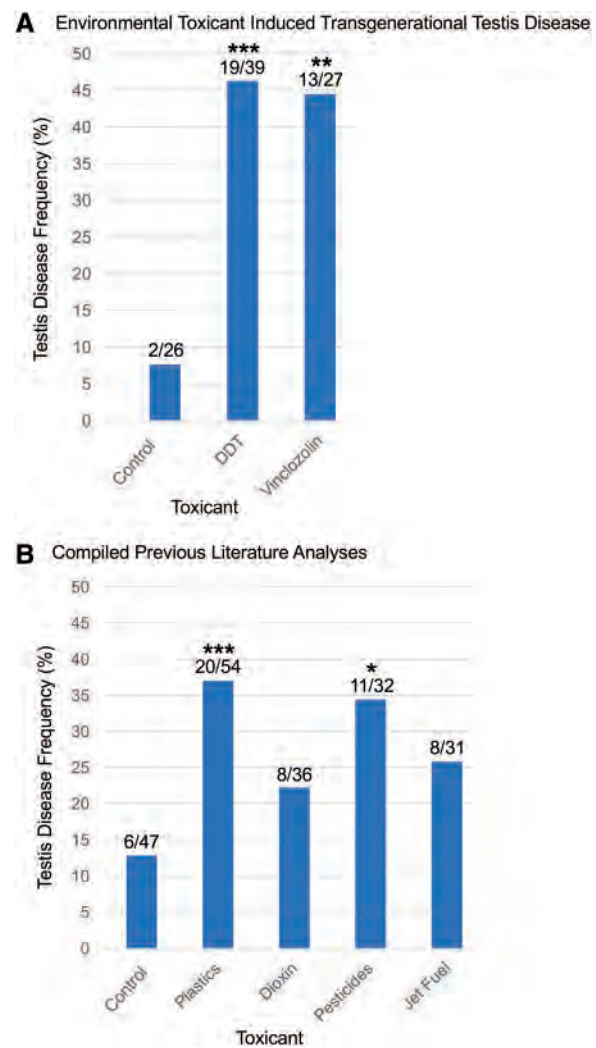


Figure 1: transgenerational induced testis disease frequency. Environmentally induced transgenerational testis disease occurrence in several separate experiments. (a) Current study vinclozolin and DDT-induced transgenerational testis disease with associated control [66, 67]. (b) Previous reports of transgenerational pathology for plastics [22, 41], dioxin [24], pesticides [27], and jet fuel hydrocarbons [28] with associated control frequency. * $P < 0.05$, ** $P < 0.01$, *** $P < 0.001$

pathology, as previously described [66, 67]. The group of animals sacrificed at 18–22 days of age for Sertoli cell preparations were used to investigate the molecular mechanisms in part involved in this transgenerational testis pathology.

Genomic DNA and RNA were isolated separately from the Sertoli cell pool aliquots from each group, and then used for methylated DNA immunoprecipitation (MeDIP) sequencing or RNA sequencing, as described in the Methods. Each of the pools contained 6–11 different animals per pool from different litters. The 9 MeDIP samples (3 control lineage pools, 3 DDT lineage pools, and 3 vinclozolin lineage pools) were enriched for methylated DNA using an MeDIP procedure employing a 5-methylcytosine specific antibody and antibody specific magnetic beads, or were processed to isolate the different RNA categories (total RNA for mRNA and long ncRNA or small ncRNA). Sequencing libraries were created for each MeDIP or RNA pool for next-generation sequencing (NGS) and run on the Illumina 2500 sequencer for MeDIP-Seq or RNA-Seq by the WSU Genomics Core

Laboratory. The procedures and bioinformatics details are described in the Methods section.

Sertoli Cell DNA Methylation Analysis

The MeDIP-Seq information was used to identify differential DNA methylated regions (DMRs) based on comparisons between control and DDT or vinclozolin lineage sequencing data. Read depth comparisons of the NGS reads identified DMRs for each of the analyses with a range of threshold P-values (Fig. 2). The DDT lineage Sertoli cell DMRs were abundant, and a $P < 1e-06$ was selected for further analysis. At $P < 1e-06$ 5359 DMRs were found with the majority of them having a single 100 bp statistically significant window, however, 533 DMRs had ≥ 2 significant windows (Fig. 2a). The corresponding false discovery rate (FDR) analysis of 0.001 correlated to the edgeR value of $P < 1e-06$ identified. The vinclozolin lineage Sertoli cell DMRs were less abundant and a $P < 1e-06$ was selected for further analysis. At this P-value 122 DMRs were found with the majority of 108 having a single 100 bp significant window DMR (Fig. 2b). All the DMR had an FDR adjusted P-value of less than 0.05. The DDT and vinclozolin lineage Sertoli cell DMRs were primarily distinct from each other with only 29 DMRs in common (Fig. 2c). This is notable, since one-fourth of the small number of DMRs in the vinclozolin lineage overlapped with the DDT lineage DMRs. The lists of DDT Sertoli cell DMRs are presented in Supplementary Table S1 and the vinclozolin Sertoli cell DMRs in Supplementary Table S2. The 29 overlapping DMRs are presented in Supplementary Table S3. The increase or decrease in DNA methylation is presented for each DMR in Supplementary Tables S1 and S2 with a log fold change indicated (exposure/control). A positive fold change is an increase in DNA methylation and negative value a decrease in DNA methylation. For the DDT lineage Sertoli cell DMRs, 70% had an increased log fold change in methylation, while 30% had a decrease in methylation. For the vinclozolin lineage Sertoli cell DMRs, 41% increased and 59% decreased in methylation. The MeDIP procedure does not identify individual CpG site DNA methylation changes, but the mean change for the DMR regions. The majority of the DMRs had 1–3 CpGs per 100 bp and were 1 kb in length so the analysis provides a mean change across the CpGs within the DMR.

The chromosomal locations of the DDT and vinclozolin transgenerational affected Sertoli cell DMRs are presented in Fig. 3. The DDT Sertoli cell DMRs are presented with the ≥ 2 windows number in Fig. 3a due to the inability to present the very large all window number of DMRs. The vinclozolin Sertoli cell DMRs for all windows are presented in Fig. 3b. All chromosomes contain DMRs, except the Y chromosome in the vinclozolin Sertoli cell lineage. Further analysis of the DMRs identified the percentage of intergenic, gene-associated, and repeat element-associated DMRs in regard to chromosomal locations. For DDT DMRs, 49% were apparently intergenic, 51% were associated with genes, and 84% were associated with a short <100 bp repeat element within the full DMR length. For vinclozolin DMRs 50% were intergenic, 50% associated with genes, and 80% associated with a short <100 bp repeat elements within the DMR region.

The numbers of DMRs at different CpG densities (CpG per 100 bp) covering all DMRs at a P-value of $P < 1e-06$ for DDT (Supplementary Fig. S2A) and vinclozolin (Supplementary Fig. S2C) demonstrate a density of 1–4 CpG per 100 bp over the entire DMR length (e.g. 1–2 kb). The predominant density is 1 CpG per 100 bp, which is a low density CpG region across the DMR total length, and has previously been termed a CpG desert [68].

A DDT Induced F3 Generation Sertoli Cell DMRs

P-value	All Window	Multiple Window
0.001	80128	16038
1e-04	31313	4456
1e-05	12798	1425
1e-06	5359	533
1e-07	2250	247

Number of windows	1	2	3	4	5	6	>7
Number of DMR	4826	454	47	12	4	3	13

B Vinclozolin Induced F3 Generation Sertoli Cell DMRs

P-value	All Window	Multiple Window
0.001	13863	1390
1e-04	2817	211
1e-05	602	45
1e-06	122	14
1e-07	36	9

Number of windows	1	2	3	4	7
Number of DMR	108	10	2	1	1

C Overlap DDT and Vinclozolin DMRs

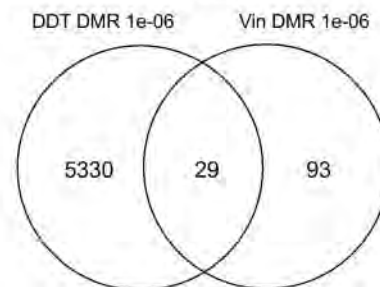


Figure 2: transgenerationally affected Sertoli cell DMRs. The number of DMRs found using different P-value cutoff thresholds. The All Window column shows all DMRs. The Multiple Window column shows the number of DMRs containing at least two significant windows. The number of DMRs with different P-value thresholds presented and the P-value threshold of $1e-06$ highlighted. (a) DDT lineage F3 generation Sertoli cells. (b) Vinclozolin lineage F3 generation Sertoli cells. (c) Venn diagram of the DDT and vinclozolin lineage DMRs at P-value $1e-06$

The length of the DMRs are presented for DDT lineage DMRs in Supplementary Fig. S2B and vinclozolin lineage DMRs in Supplementary Fig. S2D. The DMR length is assessed by extending the 100 bp window at $P < 1e-06$ out at 100 bp intervals until the $P < 0.05$ stringency is lost, as described in the Methods. The predominant DMR length is 1 kb, and all of them cover a range of 1–5 kb. The numbers of DMRs beyond 5 kb DMR length are few, but some DDT lineage DMRs appear at 10 kb DMR length. Similar observations have been made in previous studies using DDT and vinclozolin lineage sperm DMRs [55, 56].

Sertoli Cell Coding and Noncoding RNA Analysis

Expression profiles of Sertoli cell noncoding RNAs, both long and small, were determined using RNA-Seq and the differential expression was analysed between the control and vinclozolin or DDT exposure lineages. A variety of P-values were used to determine a significance threshold, and $P < 1e-04$ was used for

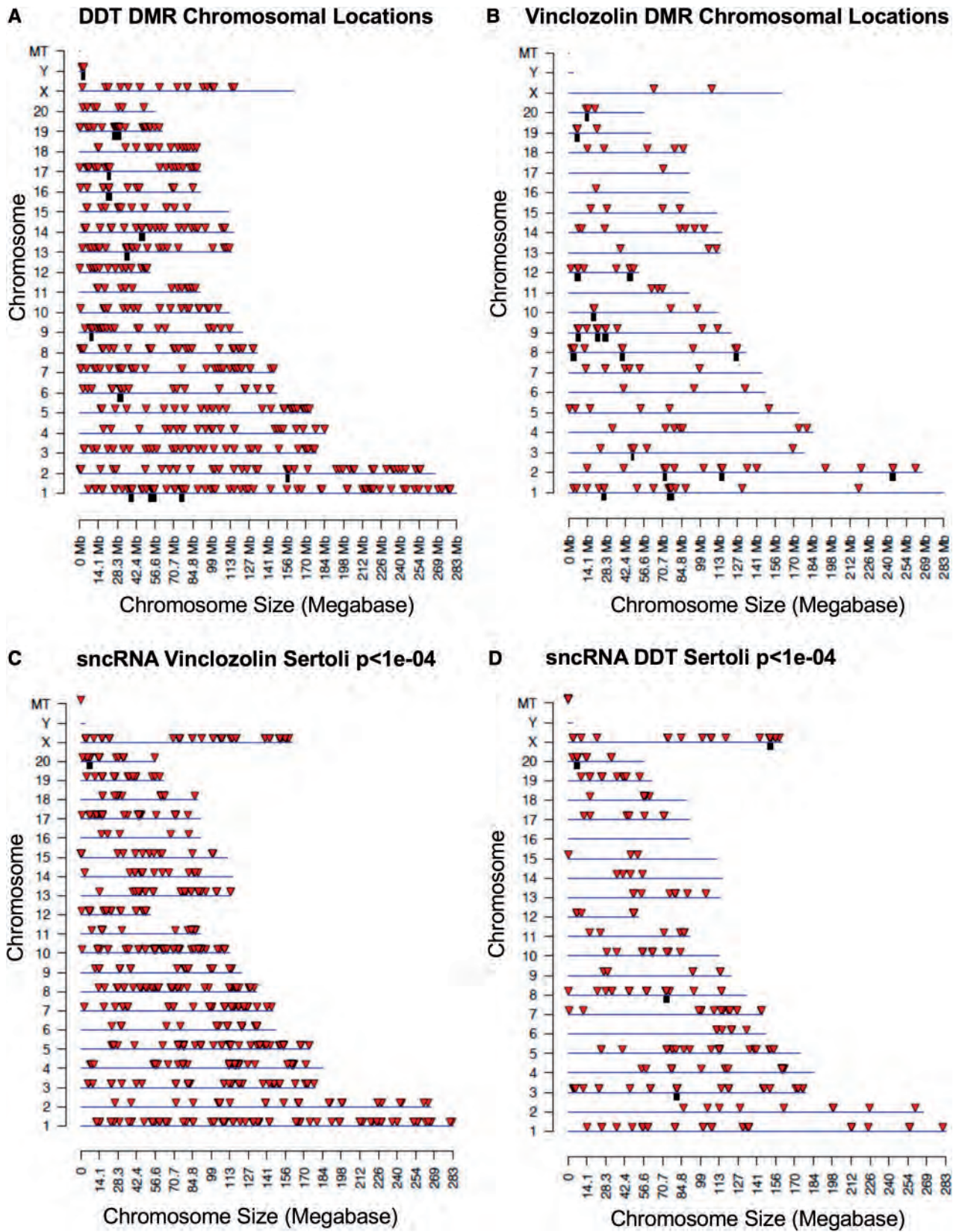


Figure 3: Sertoli cell DMR and snRNA chromosomal locations. (a) The DMR locations on the individual chromosomes. Multiple window DDT lineage DMRs at a P-value threshold of $1e-06$ are shown here. (b) The DMR locations on the individual chromosomes. All vinclozolin lineage DMRs at a P-value threshold of $1e-06$ are shown here. The red arrowheads identify the DMR sites and the black boxes the clusters of DMRs. Chromosomal locations of differentially expressed small noncoding RNAs (snRNAs). (c) Vinclozolin lineage differentially expressed snRNAs, while 220 snRNAs have an unknown location and are not shown. (d) DDT lineage differentially expressed snRNAs, while 31 snRNAs have an unknown location and are not shown. Black boxes represent clusters, while red arrowheads represent individual snRNAs, $P < 1 \times 10^{-4}$

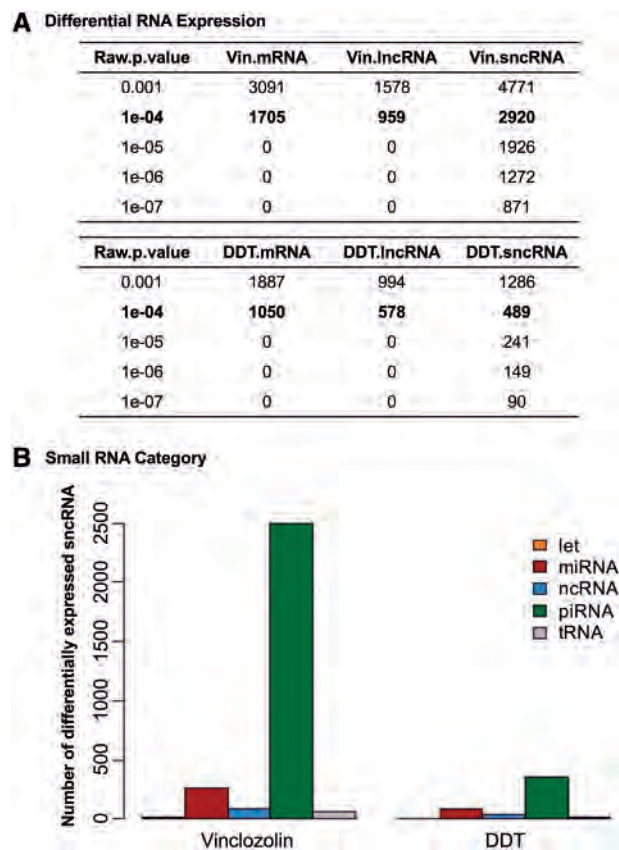


Figure 4: differentially expressed RNAs. (a) The number of differentially expressed mRNAs, long noncoding RNAs (lncRNAs) and small noncoding RNAs (sncRNAs) at different P-value thresholds for vinclozolin (Vin) and DDT lineage F3 generation Sertoli cells. (b) Differentially expressed sncRNA gene categories at $P < 1 \times 10^{-4}$

subsequent analyses (Fig. 4). The vinclozolin lineage contained the highest number of differentially expressed mRNAs compared to the DDT lineage at 1705 and 1050 mRNAs, respectively (Fig. 4a). The differentially expressed long noncoding RNAs (lncRNAs) were almost half that number, while the sncRNAs displayed extensive differential expression. The vinclozolin lineage contained 2920 differentially expressed sncRNAs, while the DDT lineage had 489. These sncRNAs were separated into sncRNA categories by type and both lineages had piRNAs as the most affected small noncoding RNA class (Fig. 4b). The increase or decrease in RNA expression is presented in Supplementary Tables S4–S12 with a log fold change indicated for each differentially expressed RNA. The DDT differential expressed RNA had for mRNA a 49% increase and 51% decrease, for lncRNA a 16% increase and 84% decrease, and for sncRNA 62% increase and 38% decrease expression. The vinclozolin differential expressed RNA had for mRNA a 57% increase and 43% decrease, for lncRNA a 13% increase and 87% decrease, and for sncRNA a 69% increase and 31% decrease in expression.

The differentially expressed RNAs were mapped to their chromosomal locations, and the differentially expressed lncRNAs and mRNAs were found on all chromosomes except for the mitochondrial genome (Fig. 5a–d). In addition, only the DDT lineage showed a differentially expressed mRNA on the Y chromosome (Fig. 5d). The sncRNAs were found on the majority of chromosomes in both lineages. The vinclozolin lineage had differential expression on all chromosomes except for the Y

chromosome, while the DDT lineage had differential expression on all chromosomes except for the Y chromosome and chromosome 16 (Fig. 3c and d). The widespread chromosomal locations of these altered RNAs indicate that ancestral exposure to an environmental toxicant can have genome-wide effects. Finally, an overlap between DMRs and differentially expressed RNAs is shown as a Venn diagram (Fig. 6). In the vinclozolin lineage, only three mRNAs are linked to the DMRs, while the differentially expressed mRNAs only overlapped with two differentially expressed lncRNAs. These weak links suggest a lack of associations among DMRs and altered RNA expression profiles (Fig. 6a). The sncRNAs displayed a sizeable overlap with both the mRNAs and lncRNAs, with two sncRNAs being common to both mRNA and lncRNA, suggesting a potential causative relationship among lncRNAs, sncRNAs, and mRNAs. This is in contrast to the DDT lineage, which had the most overlap between the DMRs and mRNAs, as well as lncRNAs. In addition, there was also some overlap between the sncRNAs and the mRNAs or lncRNAs (Fig. 6b). These observations support the proposal that the exposure-induced epigenetic transgenerational inheritance involves both DMRs and ncRNAs.

Sertoli Cell Gene Association Analysis

DMRs for both DDT and vinclozolin F3 generation lineage Sertoli cells were associated with genes that were within 10 kb distance (i.e. include promoter regions). These DMR-associated genes are presented in Supplementary Tables S1 and S2 and sorted into gene categories in Fig. 7a and b. The overlapping DMR-associated genes between the DDT and vinclozolin F3 generation lineage Sertoli cells are presented in Supplementary Table S3. The main categories for the DDT Sertoli DMR-associated genes are signaling, transcription, metabolism, and receptor, while for the vinclozolin lineage they are signaling, metabolism, and transcription. The differential expressed RNAs for both DDT and vinclozolin F3 generation lineage Sertoli cells are presented in Supplementary Tables S4–S11, and are sorted by gene categories in Fig. 7c and d. The main gene categories for both DDT and vinclozolin altered mRNAs are metabolism, signaling, transcription, cytoskeleton, and receptor. The DMR- and mRNA-associated genes (Supplementary Tables S1, S2, S10, S11) were analysed with a KEGG pathway analysis, and the top gene pathways are presented in Supplementary Fig. S3. Six gene pathways were in common between the vinclozolin DMR-associated gene pathways (Supplementary Fig. S3A) and DDT DMR-associated gene pathways (Supplementary Fig. S3B). They are the cAMP signaling pathway, endocytosis, viral carcinogenesis, pathways in cancer, MAPK signaling pathway, and Ras signaling pathway. Fourteen pathways were in common between the vinclozolin and DDT mRNA-associated gene pathways (Supplementary Fig. S3C and D).

Sertoli Cell, Testis, and Infertility Pathology Associations

Pyruvate and lactate, produced by Sertoli cells, are essential energy metabolites for spermatogenic cells sequestered within the blood–testis barrier. A previous study identified the pyruvate pathway [69, 70] to be associated with vinclozolin-induced Sertoli cell transgenerational DMRs [8]. In the current study, the pyruvate pathway was also found to be affected by both the DDT and vinclozolin Sertoli cell DMR-associated genes and mRNA, as shown in Fig. 8. As shown, the potentially altered DMR-associated genes and RNA may influence pyruvate

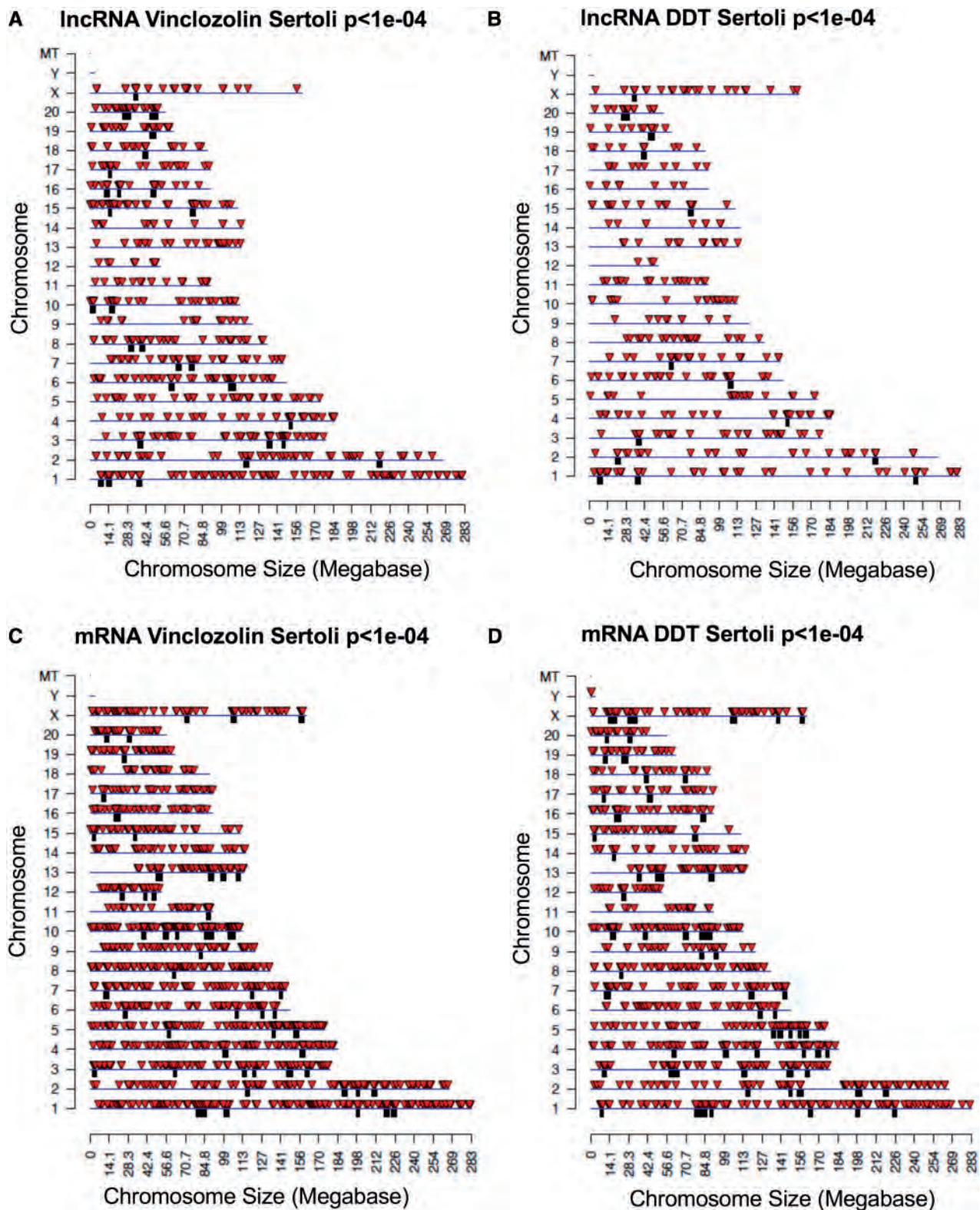


Figure 5: chromosomal locations of differentially expressed lncRNAs and mRNAs. (a) Vinclozolin lncRNA locations and (c) mRNA locations. (b) DDT lncRNAs and (d) mRNA locations. Black boxes represent clusters, while red arrowheads represent individual RNAs, $P < 1 \times 10^{-4}$

production, which would directly impact spermatogenesis in the testis.

The Sertoli cell DMRs and altered mRNAs were examined for potential overlap with previously identified genes shown to be

involved with Sertoli cell, testis, and infertility pathology. The genes previously identified to be associated with abnormal testis pathology were obtained from several exhaustive reviews [71–74]. A list of all 362 genes is presented in [Supplementary](#)

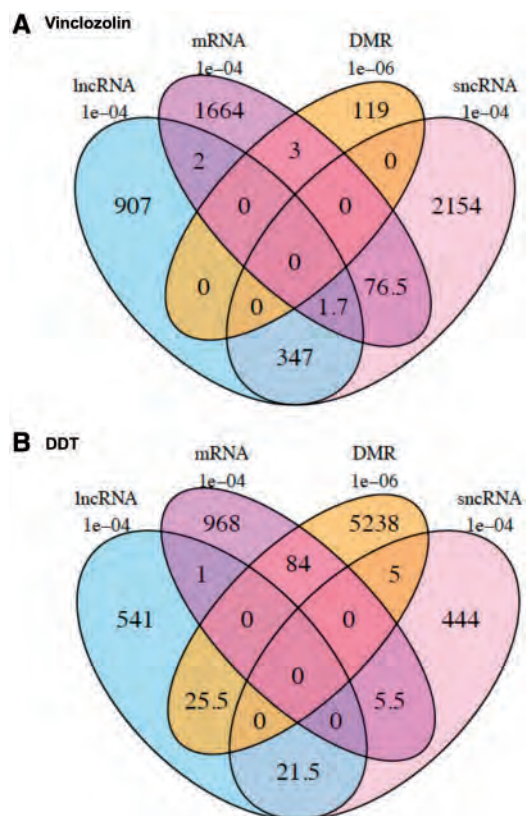


Figure 6: Venn diagram of differentially expressed epigenetic modifications. (a) Vinclozolin lineage. (b) DDT lineage

Table S13. The transgenerationally altered ncRNA had limited gene associations and no overlap observed. The Sertoli cell DMR-associated genes and mRNAs were compared, and the lists of overlapping pathology associated genes presented in [Supplementary Fig. S4](#). These associated genes were categorized as Sertoli cell, testis or male infertility linked pathology genes in [Fig. 9c](#). The vinclozolin DMR-associated genes were not found to overlap with the known pathology genes, but the altered mRNA did contain overlap with the pathology genes ([Fig. 9a and b](#)). In contrast, the DDT DMR-associated genes had 40 overlaps ([Fig. 9a and Supplementary Fig. S4C](#)) and mRNAs had 28 overlaps ([Supplementary Fig. S4B](#)). Interestingly, a large percentage of the DDT and vinclozolin pathology genes were in common, ([Supplementary Fig. S4D](#)). The DDT mRNA overlaps were distinct from the DMR overlaps. The DDT and vinclozolin mRNAs had Sertoli cell genes such as *Daz1*, *Stra8*, *Crem*, *Sox8*, and *DMRT* genes involved. The DDT DMR overlaps had *Adam2*, *Tex14*, *Acur1*, and *Csf1* genes involved. Therefore, the DDT lineage Sertoli cell DMR-associated genes and altered mRNA involved a number of genes previously shown to be involved in Sertoli cell, testis and infertility pathology ([Fig. 9c](#)).

Discussion

The experimental design used the IP injection of a gestating female rat to high environmentally relevant dose exposures for DDT and vinclozolin [25, 26]. Generally, an oral exposure to a lower dose would be used for risk assessment analysis. The current study was not designed for risk assessment, but to further investigate the transgenerational phenomenon. The observations demonstrate an environmental exposure can promote the

epigenetic transgenerational inheritance of disease susceptibility in the testis through molecular alterations in the Sertoli cells. This should not be considered a direct exposure risk assessment study, but further elucidates the epigenetic transgenerational impacts of ancestral environmental exposures.

Environmental toxicants such as DDT and vinclozolin have been shown to promote the epigenetic transgenerational inheritance of adult onset disease [59]. Epigenetic transgenerational inheritance starts with epigenetic modifications in the germline through exposure to environmental factors, which can be transmitted through the sperm and egg to subsequent generations. This germline transmission potentially leads to an altered epigenome in the stem cell of the embryo and subsequently all somatic cells and tissues [6]. The altered epigenomes appear to influence the susceptibility to disease later in life [12]. This study investigates the transgenerational effects of DDT and vinclozolin on the Sertoli cell epigenome and transcriptome. These and a number of other environmental toxicants have been shown previously to affect testis health and spermatogenesis [5, 59]. In the current study, DDT and vinclozolin were both found to promote a transgenerational testis pathology frequency of approximately 45% of the male populations examined compared to 8% in the control population ([Fig. 1a](#)). This compares with the 25–35% testis pathology frequency induced by several other toxicants as observed in previous studies ([Fig. 1b](#)). These studies showed the impacts of plastics (bisphenol A and phthalates) [22, 41], dioxin [24], pesticides (permethrin and DEET) [27], and hydrocarbons (jet fuel) [28] on the induction of transgenerational testis pathology ([Fig. 1b](#)). The testis disease frequency in these previous studies ranged between 20 and 35% compared to 13% in the independent control. The dramatic decline in human sperm concentrations of 50% over the past 50 years and corresponding increase in male infertility [53] suggest an environmental and generational aspect to male testis pathology should be considered. The current study was designed to examine a molecular mechanism for this potential environmental and generational origin of male infertility.

Sertoli cells are an essential somatic cell population in the testis, supporting spermatogenesis nutritionally and structurally. Although other testis somatic cell types such as Leydig cells and peritubular cells have critical functions, the Sertoli cell is the most integrated with spermatogenesis. Abnormal Sertoli cell function can affect testis health and fertility, as has been shown in previous studies [75]. Sertoli cells from prepubertal rats (18–22 days old) can be isolated as a highly purified population of cells. In addition, at this age, there is in general negligible disease present in the animals which would be a confounder in the study. Since the altered Sertoli cell epigenome has already been programmed earlier in development, analysis of the 18–22 days old Sertoli cell will provide insights into the molecular aspects of testis disease susceptibility later in life. Therefore, the late pubertal Sertoli cell is a good model to study the effects of environmental toxicant exposure on epigenetics and transgenerational inheritance of testis pathology. The F0 generation gestating female rats were exposed to DDT or vinclozolin during fetal days E8–14 of development which is the time of gonadal sex determination. The offspring from each generation are bred through the third generation without any further exposure to the toxicants. The F3 generation is the first true transgenerational group since during toxicant exposure of the F0 pregnant female the fetus (F1 generation), as well as the fetus's germline (F2 generation) are exposed [76]. Since the F1 and F2 generation phenotypes and molecular actions can be due to direct exposure, the current study focused only on transgenerational

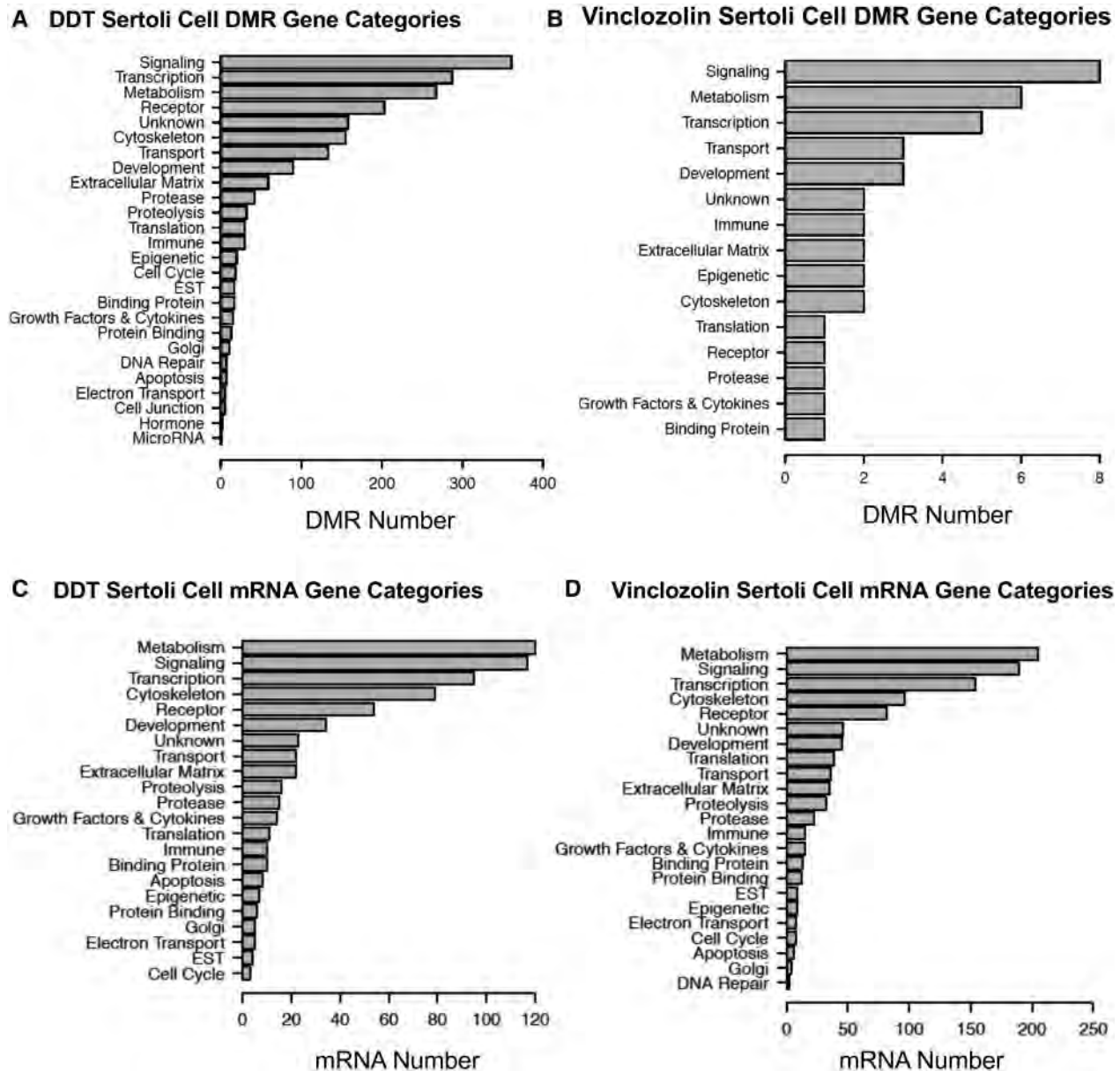


Figure 7: gene category frequency plots. (a) DDT Sertoli cell DMR and (b) vinclozolin Sertoli cell DMR gene categories. (c) DDT Sertoli cell mRNA and (d) vinclozolin Sertoli cell mRNA gene categories. The categories and numbers of DMRs or mRNAs are presented

aspects of the F3 generation. The 18–22 days old F3 generation males were sacrificed, and Sertoli cells were isolated for preparation of DNA and RNA for further study by MeDIP-Seq and RNA-Seq.

The experimental design used an intercross within the lineage to allow both maternal and paternal allelic contributions for pathology and epigenetics to be considered in the transgenerational animals. Since epigenetics involves a parent of origin allelic transmission, an outcross to wild type animals can eliminate the paternal or maternal contribution. Previous studies have demonstrated the outcross of the F3 generation to the F4 generation will promote the loss or reduction of a specific pathology [25, 26]. For example, pesticides induced pathology in an outcrossed F4 generation demonstrated that the paternal allelic outcross promoted female obesity, while the maternal outcross promoted male obesity [25, 26]. Since biological

populations are generally an intercross within a specific exposed population and not a true outcross, the intercross also is considered a more normal biology. Therefore, the current study focused on the F3 generation from an intercross. However, future studies need to investigate the impacts of an outcross to assess sex specific allelic transmission.

Transgenerationally Affected Sertoli Cell DMR Analysis

DMRs were found for both the F3 generation DDT and vinclozolin lineages through read depth comparisons between control and DDT or vinclozolin sequencing data. Although a potential limitation is the use of three pools of 6–11 animals each versus individual animal analysis, the statistical analysis with an edgeR P-value $<1e-06$ and FDR <0.05 suggests there is a low variability in the data and that analysis of pooled samples yields

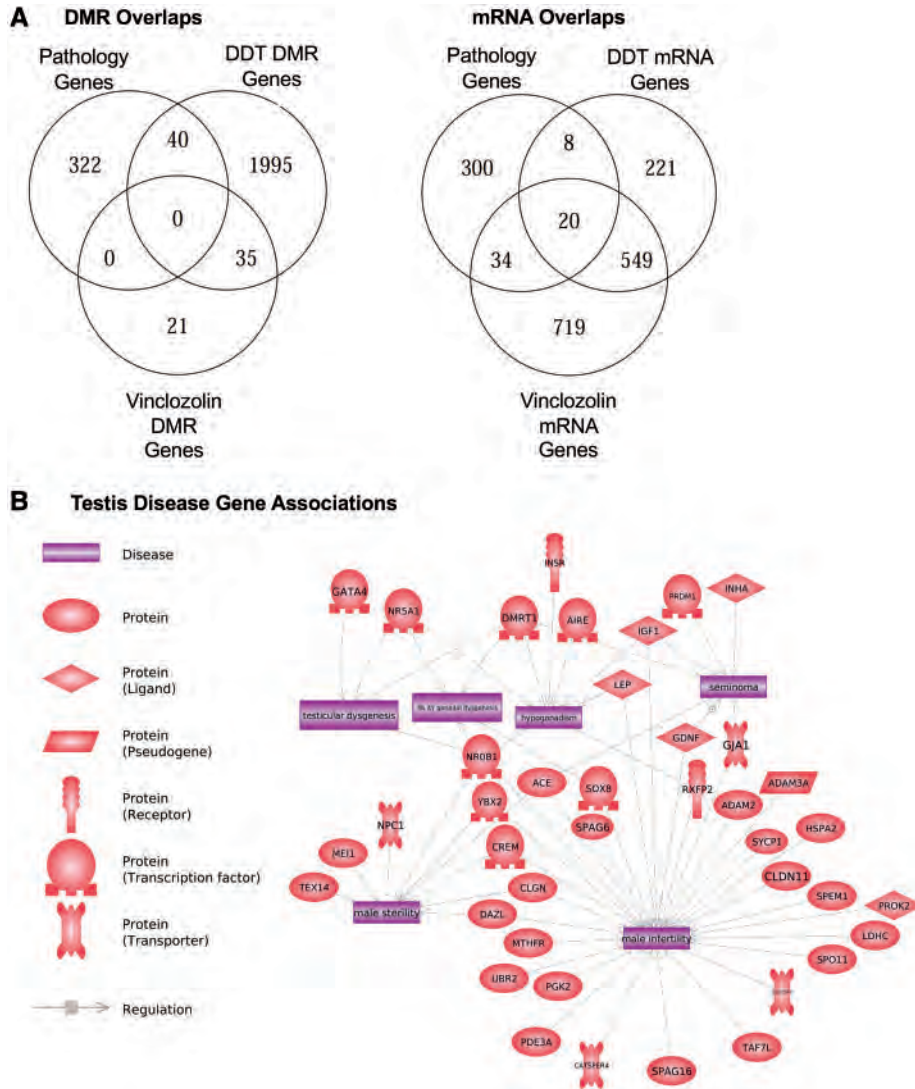


Figure 9: Sertoli cell testis and infertility-associated genes. The previously identified pathology-associated genes [71–74] in [Supplementary Table S13](#) were compared to the Sertoli cell DMR and mRNA-associated genes. (a) DMR-associated gene overlap with pathology genes. (b) mRNA overlap with pathology genes. (c) Testis disease associated genes within the gene lists in [Supplementary Fig. S4](#) in the overlapping associated genes, $P < 1e-05$. The various testis disease parameters have the associated genes linked

Transgenerationally Affected Sertoli Cell ncRNA Analysis

Being derived from the noncoding portion of the genome, non-coding RNAs were once considered to be “junk RNA.” These RNAs are transcribed, but are not protein coding, and can be divided into two categories of long (>200 nt) and small (<200 nt) ncRNA. It has since been observed that long noncoding RNAs are differentially expressed in certain diseases such as cancer [77], and after ancestral exposure to the environmental toxicant DDT [55]. This led to the proposal that ncRNAs may actually be functional, and may maintain epigenetic memory using post-transcriptional mechanisms. In addition, lncRNAs can regulate DNA methylation, remodel chromatin, and regulate histone modifications [61]. Small noncoding RNAs have been shown to be differentially expressed throughout spermatogenesis [78], such that their expression is regulated. At estimates of over 20 000 long and small ncRNAs in a single spermatozoon [79, 80], the impact of these noncoding RNAs on any offspring is potentially very significant. Observations indicate differential

expression of ncRNA is a component of transgenerationally affected Sertoli cell functions.

Transgenerationally Affected Sertoli Cell Transcriptome Analysis

The vinclozolin and DDT lineages both displayed differential coding and noncoding RNA expression profiles. Interestingly, the vinclozolin lineage had more differentially expressed RNAs in all categories, including sncRNAs, lncRNAs, and mRNAs. The most significant difference was found in the sncRNAs category with the vinclozolin lineage having 2920 altered sncRNAs, and DDT having only 489 sncRNAs. When the sncRNAs were separated by small ncRNA categories, the pattern between the vinclozolin and DDT lineages was surprisingly similar. Both overwhelmingly had piRNAs as the most differentially altered class, followed by miRNAs. Chromosomal locations of the differentially expressed RNAs indicated that although the majority of the genome was affected by differential expression, some of

the clusters were in similar chromosomal locations by type of differentially expressed large RNAs between the different lineages. The ncRNAs are anticipated to play a critical role in the epigenetic transgenerational inheritance of testis pathologies. The similarities of the DDT and vinclozolin transgenerational differentially expressed ncRNAs and mRNAs were dramatic, and future studies should further investigate the similarities of the exposure lineage transgenerational effects on the Sertoli cells.

An analysis of overlapping differential epigenetic modifications between the vinclozolin and DDT lineages revealed similarities in some RNA expression. For the vinclozolin lineage, the small noncoding RNAs had a substantial overlap with both the mRNAs with 77 and the lncRNAs with 347. In addition, out of the 122 DMRs in the vinclozolin Sertoli cells, only 3 overlapped with any RNAs, specifically the mRNA. In contrast, the DDT lineage Sertoli cells had a greater overlap of 84 of the DMRs with the mRNAs. In addition, the DMRs had a significant overlap with the lncRNAs with 26. The sncRNAs also overlapped with the lncRNAs and the mRNAs, indicating that although the DMRs may be an effector of altered RNA expression, the sncRNAs may also play a part. Observations suggest all differentially expressed epimutations may affect gene expression in an integrated manner.

Analysis of the vinclozolin and DDT actions on the transgenerational mRNA expression demonstrates a significant overlap of the altered gene expression, and nearly all the major gene pathways identified for both were the same (Supplementary Fig. S3). Interestingly, similar KEGG pathways were identified in all the epimutation data sets with metabolism, pathways in cancer, cAMP signaling pathway, P13K-Act signaling pathway, and MAPK pathway in common. The pyruvate metabolism pathway that is essential for spermatogenesis through the production of pyruvate and lactate by Sertoli cells also appears to be transgenerationally impacted (Fig. 8) as previously described [8].

Transgenerational Epimutation Associations with Sertoli Cell, Testis and Infertility Pathology

As previously described for vinclozolin lineage animals [8], the pyruvate metabolism pathway (Fig. 8) was affected in the DDT and vinclozolin lineage animals with both the DMR and mRNA-associated genes. This suggests a deficiency in an energy source for the developing germ cells, and correlates with the spermatogenic cell apoptosis and testis pathology observed (Fig. 1) [8]. Since the primary energy source (metabolite) for developing spermatogenic cells is pyruvate or lactate produced by Sertoli cells, alterations would directly impact germ cell survival.

Previous studies have identified a large number of genes associated with Sertoli cell, testis and male pathology, and infertility (Supplementary Table S13). This list of genes was obtained from several exhaustive reviews [71–74]. The previously identified pathology-associated genes were compared to the current study epimutation-associated genes for DMR and differentially expressed mRNA. A number of interesting overlaps were observed for the DDT- and vinclozolin-associated genes (Fig. 9 and Supplementary Fig. S4). Interestingly, 20 of the genes that overlapped with the pathology genes were the same between the DDT and vinclozolin altered mRNA. These included *Gata4*, *Sox8*, *Crem*, *Dmrt1*, and *Inha*. This supports the conclusion that the transgenerational epigenetic impacts on the Sertoli cells may be a component of the testis pathology observed.

Conclusions

A number of environmental toxicants have been shown to promote the epigenetic transgenerational inheritance of testis disease and male infertility [5, 8, 37, 81]. This involves epigenetic alterations in the germline (e.g. sperm) to impact the early embryonic stem cells epigenome and transcriptome. Subsequently, all cell types and tissues will have altered epigenomes and transcriptomes. The current study demonstrates that the transgenerationally affected Sertoli cells following ancestral vinclozolin or DDT exposure have alterations in DMRs, ncRNA, and mRNA. The correlations in the DMR, ncRNA, and mRNA support abnormal Sertoli cell functions that can impact spermatogenic cell development and subsequent male infertility. Since the current human male population has a dramatic increase in infertility and a decrease in sperm numbers [44, 50–53], observations suggest ancestral exposures promoting the epigenetic transgenerational inheritance of testis disease may be an important component of the etiology of male infertility. Therefore, ancestral exposures and generational impacts on male infertility need to be seriously considered in testis disease etiology.

Methods

Animal Studies and Breeding

Female and male rats of an outbred strain Hsd: Sprague Dawley SD[®]TM (Harlan) at about 70 and 100 days of age were fed ad lib with a standard rat diet and received ad lib tap water for drinking. To obtain time-pregnant females, the female rats in proestrus were pair-mated with male rats. The sperm-positive (day 0) rats were monitored for diestrus and body weight. On days 8 through 14 of gestation [82], the females received daily intraperitoneal injections of vinclozolin (100 mg/kg BW/day), DDT (25 mg/kg BW/day), or DMSO. The doses of DDT and vinclozolin used are anticipated environmental exposure [83, 84]. The vinclozolin and DDT were obtained from Chem Service Inc. (West Chester, PA) and were injected in a 20 µl DMSO vehicle, as previously described [24, 81]. Treatment lineages are designated “control,” “DDT,” or “vinclozolin” lineages. The treated gestating female rats were designated as the F0 generation. The offspring of the F0 generation rats were the F1 generation. Non-littermate females and males aged 70–90 days from the F1 generation of control, DDT or vinclozolin lineages were bred to obtain F2 generation offspring. The F2 generation rats were bred to obtain F3 generation offspring. F3 generation males were euthanized at 18–22 days for testis collection and Sertoli cell isolation, or at 1 year of age for testis pathology analysis. The F1–F3 generation offspring were not themselves treated directly with vinclozolin or DDT. The control, DDT, and vinclozolin lineages were housed in the same room and racks with lighting, food and water as previously described [24, 59, 81]. The diet consisted of free choice Teklad 2020X rodent chow (Envigo Inc.). All experimental protocols for the procedures with rats were pre-approved by the Washington State University Animal Care and Use Committee (IACUC approval # 6252).

Testis Pathology Analysis

The Washington Animal Disease Diagnostic Laboratory (WADDL) at the Washington State University College of Veterinary Medicine has board certified veterinary pathologists that assisted in initially establishing the criteria for the pathology analyses and identifying testis parameters to assess [9].

WADDL performed full necropsies as required on animals that died prior to the time of scheduled sacrifice at one year, and performed tumor classifications in the current study.

Testis were evaluated for pathologies, as previously described [24]. Testis histopathology criteria included the presence of: (i) Atrophic seminiferous tubules showing reduced Sertoli and germ cells. (ii) Round, smooth-edged, basally located vacuoles in the seminiferous epithelium. (iii) Sloughed spermatogenic cells in the tubule lumen. Representative pathologies are presented in [Supplementary Fig. S1](#). Testis sections were also examined by Terminal deoxynucleotidyl transferase-mediated dUTP nick end labeling (TUNEL) assay (In situ cell death detection kit, Fluorescein, Sigma, St. Louis, MO). A cut-off was established to declare a tissue “diseased” based on the mean number of histopathological abnormalities of each type (atrophy, vacuoles, sloughed cells in lumen, or TUNEL positive) plus two standard deviations from the mean of control tissues by each of the three individual evaluators blinded to the treatment groups. This number was used to classify rats into those with and without testis disease in each lineage. Two of three evaluators would have to score an animal’s testes as having an above-cutoff quantity of a specific histopathological abnormality (atrophy, vacuoles, or sloughed cells in lumen) in order for a rat tissue section to finally be declared “diseased”.

Testis Tissue Collection and Isolation of Sertoli Cells

The 20-day-old rats were sacrificed and the testes were dissected. Sertoli cells were prepared as described in [Tung et al. \[85\]](#). Briefly, testes were washed two times with HBSS. The tunica albuginea was removed from each testis and discarded. The tissue was then chopped with a razor blade until it appeared homogeneous, and then underwent sequential enzymatic digestion and wash steps to isolate the purified Sertoli cells. The first step uses trypsin (0.25%) and DNase (0.3 mg/ml) followed by a trypsin inhibitor (0.3 mg/ml) incubation and washes. The next digestion step involves collagenase (0.5 mg/ml) and DNase followed by the final digestion with hyaluronidase (1 mg/ml) and DNase. The final pellet will contain the purified Sertoli cells, which can be used for isolation of DNA and RNA. Enzymes used were DNase I (Sigma DN-25), Collagenase (Sigma C1639), Hyaluronidase (Sigma #H3757), and Trypsin Inhibitor Type I-S (Sigma T-6522). The purity of the Sertoli cell populations are routinely monitored with microscopy and has been previously established with fibronectin immunocytochemistry to be >98% pure, as described [8, 63–65].

DNA and RNA Isolation

Sertoli cell pellets were resuspended in 100 μ l 1 \times PBS, then combined with 820 μ l DNA extraction buffer (50 mM Tris HCl, 10 mM EDTA, pH 8.0, 0.5% SDS) and 80 μ l proteinase K (20 mg/ml). The sample was incubated at 55°C for at least 2 hours under constant rotation. Then 300 μ l of protein precipitation solution (Promega, A7953) was added, the sample mixed thoroughly and incubated for 15 minutes on ice. The sample was centrifuged at 14 000 rpm for 30 minutes at 4°C. One ml of the supernatant was transferred to a 2 ml tube and 2 μ l of glycoblue and 1 ml of cold 100% isopropanol were added. The sample was mixed well by inverting the tube several times then left in –20°C freezer for at least one hour. After precipitation the sample was centrifuged at 14 000 rpm for 20 minutes at 4°C. The supernatant was taken off and discarded without disturbing the (blue) pellet. The pellet was washed with 70% cold ethanol and centrifuged for

10 minutes at 4°C at 14 000 rpm and the supernatant was discarded. The tube was spun again briefly to collect residual ethanol to bottom of tube, and then as much liquid as possible was removed with gel loading tip. Pellet was air-dried at RT until it looked dry (about 5 minutes). Pellet was then resuspended in 100 μ l of nuclease free water.

Total RNA Isolation

Trizol reagent (Thermo Fisher) or mirVana miRNA isolation kit (Life Technologies) was used to extract total RNA from purified Sertoli cells with some modifications to the manufacturer’s protocol. The mirVana kit was used to extract control lineage Sertoli cells stored as pellets at –80°C until use. Lysis buffer was added to the cell pellets, which were heated to 65°C for 10 minutes and manually homogenized. The default protocol was used for the remainder of the extraction. The vinclozolin and DDT lineage cells were stored in 1.2 ml Trizol at –80°C until use. To recover small RNA at the RNA precipitation step, the amount of isopropanol was increased to 1 ml, then the default protocol was resumed. All RNA was eluted in 50 μ l of water with 0.5 μ l murine RNase inhibitor (NEB). RNA concentration was determined using the Qubit RNA HS Assay Kit (Thermo Fisher). An RNA 6000 Pico chip was run on the Agilent 2100 Bioanalyzer for quality control analysis.

Methylated DNA Immunoprecipitation (MeDIP)

MeDIP with genomic DNA was performed as follows: DNA isolated from Sertoli cell pools (three pools each of control, DDT, and vinclozolin lineage animals) was sonicated using the Covaris M220 the following way: the genomic DNA was diluted to 130 μ l with TE buffer into the appropriate Covaris tube. Covaris was set to 300 bp program, and the program was run for each tube in the experiment. About 10 μ l of each sonicated DNA was run on 1.5% agarose gel to verify fragment size. The sonicated DNA was transferred from the Covaris tube to a 1.7 ml microfuge tube and the volume was measured. The sonicated DNA was then diluted with TE buffer (10 mM Tris HCl, pH 7.5; 1 mM EDTA) to 400 μ l, heat-denatured for 10 minutes at 95°C, then immediately cooled on ice for 10 minutes. Then 100 μ l of 5 \times IP buffer and 5 μ g of antibody (monoclonal mouse anti 5-methyl cytidine; Diagenode #C15200006) were added to the denatured sonicated DNA. The DNA-antibody mixture was incubated overnight on a rotator at 4°C. The following day, magnetic beads (Dynabeads M-280 Sheep anti-Mouse IgG; 11201 D) were pre-washed as follows: The beads were resuspended in the vial, then the appropriate volume (50 μ l per sample) was transferred to a microfuge tube. The same volume of Washing Buffer (at least 1 ml 1 \times PBS with 0.1% BSA and 2 mM EDTA) was added and the bead sample was resuspended. Tube was then placed into a magnetic rack for 1–2 minutes and the supernatant was discarded. The tube was removed from the magnetic rack and the beads were washed once. The washed beads were resuspended in the same volume of 1 \times IP buffer (50 mM sodium phosphate pH 7.0, 700 mM NaCl, 0.25% TritonX-100) as the initial volume of beads. 50 μ l of beads were added to the 500 μ l of DNA-antibody mixture from the overnight incubation, then incubated for 2 hours on a rotator at 4°C. After the incubation the bead-antibody-DNA complex was washed three times with 1 \times IP buffer as follows: The tube was placed into magnetic rack for 1–2 minutes and the supernatant discarded, then washed with 1 \times IP buffer three times. The washed bead-DNA solution is then resuspended in 250 μ l digestion buffer with 3.5 μ l Proteinase K

(20 mg/ml). The sample was then incubated for 2–3 hours on a rotator at 55°C and then 250 µl of buffered phenol–chloroform–isoamylalcohol solution was added to the supe and the tube was vortexed for 30 seconds then centrifuged at 14 000 rpm for 5 minutes at room temperature. The aqueous supernatant was carefully removed and transferred to a fresh microfuge tube. Then 250 µl chloroform were added to the supernatant from the previous step, vortexed for 30 seconds, and centrifuged at 14 000 rpm for 5 minutes at room temperature. The aqueous supernatant was removed and transferred to a fresh microfuge tube. To the supernatant 2 µl of glycoBlue (20 mg/ml), 20 µl of 5 M NaCl and 500 µl ethanol were added and mixed well, then precipitated in –20°C freezer for 1 hour to overnight. The precipitate was centrifuged at 14 000 rpm for 20 minutes at 4°C and the supernatant was removed, while not disturbing the pellet. The pellet was washed with 500 µl cold 70% ethanol in –20°C freezer for 15 minutes, then centrifuged again at 14 000 rpm for 5 minutes at 4°C and the supernatant was discarded. The tube was spun again briefly to collect residual ethanol to bottom of tube and as much liquid as possible was removed with gel loading tip. Pellet was air-dried at RT until it looked dry (about 5 minutes) then resuspended in 20 µl H₂O or TE. DNA concentration was measured in Qubit (Life Technologies) with ssDNA kit (Molecular Probes Q10212).

MeDIP-Seq Analysis

The MeDIP DNA samples were used to create libraries for NGS using the NEBNext[®] Ultra[™] RNA Library Prep Kit for Illumina[®] (NEB, San Diego, CA) starting at step 1.4 of the manufacturer's protocol to generate double stranded DNA. After this step the manufacturer's protocol was followed. Each pool received a separate index primer. NGS was performed at WSU Spokane Genomics Core using the Illumina HiSeq 2500 with a PE50 application, with a read size of approximately 50 bp and approximately 100 million reads per pool. Five to six libraries were run in one lane. MeDIP analysis data validation has previously been shown with mass-spectrometry sequencing and bisulfite sequencing [84, 86].

Statistics and Bioinformatics

The basic read quality was verified using summaries produced by the FastQC [Simon Andrews, <http://www.bioinformatics.babraham.ac.uk/projects/fastqc/>] program. The new data was cleaned and filtered to remove adapters and low quality bases using Trimmomatic [87]. The reads for each MeDIP sample were mapped to the Rnor 6.0 rat genome using Bowtie2 [88] with default parameter options. The mapped read files were then converted to sorted BAM files using SAMtools [89]. To identify DMRs, the reference genome was broken into 100 bp windows. The MEDIPS R package [90] was used to calculate differential coverage between control and exposure sample groups. The edgeR *P*-value [91] was used to determine the relative difference between the two groups for each genomic window. Windows with an edgeR *P*-value less than an arbitrarily selected threshold were considered DMRs. The DMR edges were extended until no genomic window with an edgeR *P*-value less than 0.1 remained within 1000 bp of the DMR. CpG density and other information was then calculated for the DMR based on the reference genome. Since sequencing reads overlap for the entire DMR length some DMR with CpGs outside the DMR length are listed as 0 CpG, but when flanking regions are considered contain CpG.

This allowed the DMR to be precipitated with the antibody in the MeDIP procedure.

DMRs were annotated using the biomaRt R package [92] to access the Ensembl database [93]. The genes that overlapped with DMR were then input into the KEGG pathway search [69, 70] to identify associated pathways. The DMR-associated genes were manually then sorted into functional groups by consulting information provided by the DAVID [94], Panther [95], and Uniprot databases incorporated into an internal curated database (www.skinner.wsu.edu “under genomic data”). DMR containing repeat elements were identified using the RepeatMasker output file provided by NCBI for the Rnor 6.0 reference genome. All molecular data have been deposited into the public database at NCBI (GEO # GSE118306; SRA PRJNA480508) and R code computational tools available at GitHub (<https://github.com/skinnerlab/MeDIP-seq>) and www.skinner.wsu.edu.

mRNA and ncRNA Analysis

KAPA RNA HyperPrep Kit with RiboErase was used to construct mRNA and lncRNA libraries following the manufacturer's protocol with the following modifications: the adaptor and barcodes used were from NEBNext Multiplex Oligos for Illumina. Before the final amplifications, libraries were incubated with the USER enzyme (NEB) for 15 minutes at 37°C. PCR cycle number was determined using qPCR with the KAPA RealTime Library Amplification Kit. KAPA Pure beads were used for size selection (200–700 bp). Agilent DNA High Sensitivity chips were used for quality control analysis and the Qubit dsDNA high sensitivity assay (Thermo Fisher) was used to determine concentration. Libraries were pooled and sequenced with the Illumina HiSeq 4000 sequencer (PE100 sequencing).

The NEBNext Multiplex Small RNA Library Prep Set for Illumina was used to construct small RNA libraries with the NEBNext Multiplex Oligos for Illumina as barcodes. KAPA Pure beads were used at 1.3× and 3.7× ratios for purification and size selection, followed by the Pippin Prep 3% gel with marker P (Sage Science) for final size selection (115–160 bp). Qubit dsDNA high sensitivity assay (Thermo Fisher) was used to determine concentration and the Agilent DNA High Sensitivity Chips were used for quality control analysis. Following pooling and concentration with 2.2× KAPA Pure beads, libraries were sequenced with the Illumina HiSeq 4000 sequencer (single-end 50 bp) with a customized sequencing primer: 5'-ACA CGT TCA GAG TTC TAG AGT CCG A-3'.

ncRNA Bioinformatics and Statistics

The small ncRNA data were annotated as follows: low-quality reads and reads shorter than 15 nt were discarded by Trimmomatic (v0.33). The remaining reads were matched to known rat sncRNA, consisting of mature miRNA (miR-Base, release 21), precursor miRNA (miRBase, release 21), tRNA (Genomic tRNA Database, rn5), piRNA (piRBase), rRNA (Ensembl, release 76), and mitochondrial RNA (Ensembl, release 76) using AASRA pipeline with default parameters. Read counts generated by AASRA were statistically normalized by DESeq2.

The long ncRNA and mRNA data were annotated as follows: trimmomatic (v0.33) was used to remove adaptor sequences and the low-quality reads from the RNA sequencing data of the large RNA libraries. To identify all the transcripts, we used HiSAT2 (v2.1.0) and StringTie (v1.3.4d) to assemble the sequencing reads based on the Ensembl_Rnor_6.0. The differential expression analyses were performed by Cuffdiff. The coding and

the noncoding genes were primarily annotated through rat CDS data ensembl_Rnor_6.0. The non-annotated genes were extracted through our in-house script and then analysed by CPAT, indicating the true noncoding RNAs.

Ethics Statement

All experimental protocols for the procedures with rats were pre-approved by the Washington State University Animal Care and Use Committee (IACUC approval # 6252).

Authors Roles

MKS conceived the study and obtained funding. MKS & WY supervised the study. ISR, RK, EN, DB, YX performed technical analysis and obtained the data. DB & YX performed bioinformatics and statistical analysis. ISR and RK wrote the first draft of the manuscript. All authors edited and revised the manuscript.

Acknowledgements

We acknowledge Ms. Jayleana Barton, Ms. Hannah Kimbel and Mr. Hayden McSwiggin for technical assistance, Ms. Amanda Quilty for editorial assistance, and Ms. Heather Johnson for assistance in preparation of the manuscript. We thank the Genomics Core laboratory at WSU Spokane. This work was supported by the NIH NIEHS under Grant ES012974. The funders had no role in the conceptualization, preparation, or decision to publish this manuscript. This work was supported by the NIH NIEHS under Grant ES012974 to MKS and John Templeton Foundation grant 61174 to MKS. The funders had no role in the conceptualization, preparation, or decision to publish this manuscript.

Data Availability

All molecular data has been deposited into the public database at NCBI (GEO # GSE118306; SRA PRJNA480508) and R code computational tools available at GitHub (<https://github.com/skinnerlab/MeDIP-seq>) and www.skinner.wsu.edu.

Supplementary Data

Supplementary data are available at *EnvEpig* online.

Conflict of interest statement. None declared.

References

- Holliday R. The inheritance of epigenetic defects. *Science* 1987; **238**:163–70.
- Berger SI, Kouzarides T, Shiekhattar R, Shilatifard A. An operational definition of epigenetics. *Genes Dev* 2009; **23**:781–3.
- Nilsson E, Sadler-Riggelman I, Skinner MK. Environmentally induced epigenetic transgenerational inheritance of disease. *Environ Epigenet* 2018; **4**:1–13.
- Jirtle RL, Skinner MK. Environmental epigenomics and disease susceptibility. *Nat Rev Genet* 2007; **8**:253–62.
- Anway MD, Cupp AS, Uzumcu M, Skinner MK. Epigenetic transgenerational actions of endocrine disruptors and male fertility. *Science* 2005; **308**:1466–9.
- Skinner MK. Environmental epigenetic transgenerational inheritance and somatic epigenetic mitotic stability. *Epigenetics* 2011; **6**:838–42.
- Nilsson E, Larsen G, Manikkam M, Guerrero-Bosagna C, Savenkova M, Skinner M. Environmentally induced epigenetic transgenerational inheritance of ovarian disease. *PLoS One* 2012; **7**:e36129.
- Guerrero-Bosagna C, Savenkova M, Haque MM, Nilsson E, Skinner MK. Environmentally induced epigenetic transgenerational inheritance of altered Sertoli cell transcriptome and epigenome: molecular etiology of male infertility. *PLoS One* 2013; **8**:e59922.
- Anway MD, Leathers C, Skinner MK. Endocrine disruptor vinclozolin induced epigenetic transgenerational adult-onset disease. *Endocrinology* 2006; **147**:5515–23.
- Anway MD, Skinner MK. Transgenerational effects of the endocrine disruptor vinclozolin on the prostate transcriptome and adult onset disease. *Prostate* 2008; **68**:517–29.
- Klukovich R, Nilsson E, Sadler-Riggelman I, Beck D, Xie Y, Yan W, Skinner MK. Environmental toxicant induced epigenetic transgenerational inheritance of prostate pathology and stromal-epithelial cell epigenome and transcriptome alterations: ancestral origins of prostate disease. *Sci Rep* 2019; **9**:1–17.
- Nilsson E, Klukovich R, Sadler-Riggelman I, Beck D, Xie Y, Yan W, Skinner MK. Environmental toxicant induced epigenetic transgenerational inheritance of ovarian pathology and granulosa cell epigenome and transcriptome alterations: ancestral origins of polycystic ovarian syndrome and primary ovarian insufficiency. *Epigenetics* 2018; **13**:875–95.
- Quadrana L, Colot V. Plant transgenerational epigenetics. *Annu Rev Genet* 2016; **50**:467–91.
- Brookheart RT, Duncan JG. *Drosophila melanogaster*: an emerging model of transgenerational effects of maternal obesity. *Mol Cell Endocrinol* 2016; **435**:20–8.
- Kelly WG. Multigenerational chromatin marks: no enzymes need apply. *Dev Cell* 2014; **31**:142–4.
- Carvan MJ, Kalluvila TA, Klingler RH, Larson JK, Pickens M, Mora-Zamorano FX, Connaughton VP, Sadler-Riggelman I, Beck D, Skinner MK. Mercury-induced epigenetic transgenerational inheritance of abnormal neurobehavior is correlated with sperm epimutations in zebrafish. *PLoS One* 2017; **12**:e0176155.
- Leroux S, Gourichon D, Leterrier C, Labrune Y, Coustham V, Riviere S, Zerjal T, Coville JL, Morisson M, Minvielle F et al. Embryonic environment and transgenerational effects in quail. *Genet Sel Evol* 2017; **49**:14.
- Guerrero-Bosagna C, Morisson M, Liaubet L, Rodenburg TB, de Haas EN, Kostal L, Pitel F. Transgenerational epigenetic inheritance in birds. *Environ Epigenet* 2018; **4**:dvy008.
- Padmanabhan N, Jia D, Geary-Joo C, Wu X, Ferguson-Smith AC, Fung E, Bieda MC, Snyder FF, Gravel RA, Cross JC et al. Mutation in folate metabolism causes epigenetic instability and transgenerational effects on development. *Cell* 2013; **155**:81–93.
- Braunschweig M, Jagannathan V, Gutzwiller A, Bee G. Investigations on transgenerational epigenetic response down the male line in F2 pigs. *PLoS One* 2012; **7**:e30583.
- Northstone K, Golding J, Davey Smith G, Miller LL, Pembrey M. Prepubertal start of father's smoking and increased body fat in his sons: further characterisation of paternal transgenerational responses. *Eur J Hum Genet* 2014; **22**:1382–6.
- Manikkam M, Tracey R, Guerrero-Bosagna C, Skinner M. Plastics derived endocrine disruptors (BPA, DEHP and DBP)

- induce epigenetic transgenerational inheritance of obesity, reproductive disease and sperm epimutations. *PLoS One* 2013; **8**:e55387.
23. Doyle TJ, Bowman JL, Windell VL, McLean DJ, Kim KH. Transgenerational effects of di-(2-ethylhexyl) phthalate on testicular germ cell associations and spermatogonial stem cells in mice. *Biol Reprod* 2013; **88**:112.
 24. Manikkam M, Tracey R, Guerrero-Bosagna C, Skinner MK. Dioxin (TCDD) induces epigenetic transgenerational inheritance of adult onset disease and sperm epimutations. *PLoS One* 2012; **7**:e46249.
 25. Manikkam M, Haque MM, Guerrero-Bosagna C, Nilsson E, Skinner MK. Pesticide methoxychlor promotes the epigenetic transgenerational inheritance of adult onset disease through the female germline. *PLoS One* 2014; **9**:e102091.
 26. Skinner MK, Manikkam M, Tracey R, Guerrero-Bosagna C, Haque MM, Nilsson E. Ancestral dichlorodiphenyltrichloroethane (DDT) exposure promotes epigenetic transgenerational inheritance of obesity. *BMC Med* 2013; **11**:221–16.
 27. Manikkam M, Tracey R, Guerrero-Bosagna C, Skinner M. Pesticide and insect repellent mixture (permethrin and DEET) induces epigenetic transgenerational inheritance of disease and sperm epimutations. *Reprod Toxicol* 2012; **34**:708–19.
 28. Tracey R, Manikkam M, Guerrero-Bosagna C, Skinner M. Hydrocarbons (jet fuel JP-8) induce epigenetic transgenerational inheritance of obesity, reproductive disease and sperm epimutations. *Reprod Toxicol* 2013; **36**:104–16.
 29. Bruner-Tran KL, Ding T, Yeoman KB, Archibong A, Arosh JA, Osteen KG. Developmental exposure of mice to dioxin promotes transgenerational testicular inflammation and an increased risk of preterm birth in unexposed mating partners. *PLoS One* 2014; **9**:e105084.
 30. Bruner-Tran KL, Osteen KG. Developmental exposure to TCDD reduces fertility and negatively affects pregnancy outcomes across multiple generations. *Reprod Toxicol* 2011; **31**:344–50.
 31. McBirney M, King SE, Pappalardo M, Houser E, Unkefer M, Nilsson E, Sadler-Riggleman I, Beck D, Winchester P, Skinner MK. Atrazine induced epigenetic transgenerational inheritance of disease, lean phenotype and sperm epimutation pathology biomarkers. *PLoS One* 2017; **12**:e0184306.
 32. Crews D, Gore AC, Hsu TS, Dangleben NL, Spinetta M, Schallert T, Anway MD, Skinner MK. Transgenerational epigenetic imprints on mate preference. *Proc Natl Acad Sci USA* 2007; **104**:5942–6.
 33. Crews D, Gillette R, Scarpino SV, Manikkam M, Savenkova MI, Skinner MK. Epigenetic transgenerational inheritance of altered stress responses. *Proc Natl Acad Sci USA* 2012; **109**:9143–8.
 34. Skinner MK, Anway MD, Savenkova MI, Gore AC, Crews D. Transgenerational epigenetic programming of the brain transcriptome and anxiety behavior. *PLoS One* 2008; **3**:e3745.
 35. Jawaid A, Roszkowski M, Mansuy IM. Transgenerational epigenetics of traumatic stress. *Prog Mol Biol Transl Sci* 2018; **158**:273–98.
 36. Metz GA, Ng JW, Kovalchuk I, Olson DM. Ancestral experience as a game changer in stress vulnerability and disease outcomes. *Bioessays* 2015; **37**:602–11.
 37. Anway MD, Memon MA, Uzumcu M, Skinner MK. Transgenerational effect of the endocrine disruptor vinclozolin on male spermatogenesis. *J Androl* 2006; **27**:868–79.
 38. Guerrero-Bosagna C, Covert T, Haque MM, Settles M, Nilsson EE, Anway MD, Skinner MK. Epigenetic transgenerational inheritance of vinclozolin induced mouse adult onset disease and associated sperm epigenome biomarkers. *Reprod Toxicol* 2012; **34**:694–707.
 39. Beck D, Sadler-Riggleman I, Skinner MK. Generational comparisons (F1 versus F3) of vinclozolin induced epigenetic transgenerational inheritance of sperm differential DNA methylation regions (epimutations) using MeDIP-Seq. *Environ Epigenet* 2017; **3**:1–12. dx016.
 40. Hao C, Gely-Pernot A, Kervarrec C, Boudjema M, Becker E, Khil P, Tevosian S, Jegou B, Smagulova F. Exposure to the widely used herbicide atrazine results in deregulation of global tissue-specific RNA transcription in the third generation and is associated with a global decrease of histone trimethylation in mice. *Nucleic Acids Res* 2016; **44**:9784–802.
 41. Wolstenholme JT, Edwards M, Shetty SR, Gatewood JD, Taylor JA, Rissman EF, Connelly JJ. Gestational exposure to bisphenol A produces transgenerational changes in behaviors and gene expression. *Endocrinology* 2012; **153**:3828–38.
 42. Mohamed el SA, Song WH, Oh SA, Park YJ, You YA, Lee S, Choi JY, Kim YJ, Jo I, Pang MG. The transgenerational impact of benzo(a)pyrene on murine male fertility. *Hum Reprod* 2010; **25**:2427–33.
 43. Chamorro-Garcia R, Diaz-Castillo C, Shoucri BM, Käch H, Leavitt R, Shioda T, Blumberg B. Ancestral perinatal obesogen exposure results in a transgenerational thrifty phenotype in mice. *Nat Commun* 2017; **8**:2012.
 44. Sanabria M, Cuciolo MS, Guerra MT, Dos Santos Borges C, Banzato TP, Perobelli JE, Leite GA, Anselmo-Franci JA, De Grava Kempinas W. Sperm quality and fertility in rats after prenatal exposure to low doses of TCDD: a three-generation study. *Reprod Toxicol* 2016; **65**:29–38.
 45. Kubsad D, Nilsson EE, King SE, Sadler-Riggleman I, Beck D, Skinner MK. Assessment of glyphosate induced epigenetic transgenerational inheritance of pathologies and sperm epimutations: generational toxicology. *Sci Rep* 2019; **9**:6372.
 46. Dym M, Fawcett DW. The blood-testis barrier in the rat and the physiological compartmentation of the seminiferous epithelium. *Biol Reprod* 1970; **3**:308–26.
 47. Skinner MK, Griswold MD. Sertoli cells synthesize and secrete transferrin-like protein. *J Biol Chem* 1980; **255**:9523–5.
 48. Griswold MD. Interactions between germ cells and Sertoli cells in the testis. *Biol Reprod* 1995; **52**:211–6.
 49. Griswold MD. Protein secretions of Sertoli cells. *Int Rev Cytol* 1988; **110**:133–56.
 50. Skakkebaek NE, Rajpert-De Meyts E, Buck Louis Gm, Toppari J, Andersson A-M, Eisenberg ML, Jensen TK, Jørgensen N, Swan SH, Sapra KJ et al. Male reproductive disorders and fertility trends: influences of environment and genetic susceptibility. *Physiol Rev* 2016; **96**:55–97.
 51. Jensen TK, Jacobsen R, Christensen K, Nielsen NC, Bostofte E. Good semen quality and life expectancy: a cohort study of 43,277 men. *Am J Epidemiol* 2009; **170**:559–65.
 52. Eisenberg ML, Li S, Cullen MR, Baker LC. Increased risk of incident chronic medical conditions in infertile men: analysis of United States claims data. *Fertil Steril* 2016; **105**:629–36.
 53. Levine H, Jørgensen N, Martino-Andrade A, Mendiola J, Weksler-Derri D, Mindlis I, Pinotti R, Swan SH. Temporal trends in sperm count: a systematic review and meta-regression analysis. *Hum Reprod Update* 2017; **23**:646–59.
 54. Anway MD, Rekow SS, Skinner MK. Comparative anti-androgenic actions of vinclozolin and flutamide on transgenerational adult onset disease and spermatogenesis. *Reprod Toxicol* 2008; **26**:100–6.
 55. Skinner MK, Ben Maamar M, Sadler-Riggleman I, Beck D, Nilsson E, McBirney M, Klukovich R, Xie Y, Tang C, Yan W.

- Alterations in sperm DNA methylation, non-coding RNA and histone retention associate with DDT-induced epigenetic transgenerational inheritance of disease. *Epigenet Chromatin* 2018;**11**:1–24.
56. Ben Maamar M, Sadler-Riggleman I, Beck D, McBirney M, Nilsson E, Klukovich R, Xie Y, Tang C, Yan W, Skinner MK. Alterations in sperm DNA methylation, non-coding RNA expression, and histone retention mediate vinclozolin-induced epigenetic transgenerational inheritance of disease. *Environ Epigenet* 2018;**4**:1–19. dvy010.
 57. Kelce WR, Monosson E, Gamcsik MP, Laws SC, Gray L. Environmental hormone disruptors: evidence that vinclozolin developmental toxicity is mediated by antiandrogenic metabolites. *Toxicol Appl Pharmacol* 1994;**126**:276–85.
 58. Mrema EJ, Rubino FM, Brambilla G, Moretto A, Tsatsakis AM, Colosio C. Persistent organochlorinated pesticides and mechanisms of their toxicity. *Toxicology* 2013;**307**:74–88.
 59. Skinner MK. Endocrine disruptor induction of epigenetic transgenerational inheritance of disease. *Mol Cell Endocrinol* 2014;**398**:4–12.
 60. Schuster A, Skinner MK, Yan W. Ancestral vinclozolin exposure alters the epigenetic transgenerational inheritance of sperm small noncoding RNAs. *Environ Epigenet* 2016;**2**:1–10. dvw001.
 61. Yan W. Potential roles of noncoding RNAs in environmental epigenetic transgenerational inheritance. *Mol Cell Endocrinol* 2014;**398**:24–30.
 62. Zhao Y, Sun H, Wang H. Long noncoding RNAs in DNA methylation: new players stepping into the old game. *Cell Biosci* 2016;**6**:45.
 63. Boucheron C, Baxendale V. Isolation and purification of murine male germ cells. *Methods Mol Biol* 2012;**825**:59–66.
 64. Marzowski J, Sylvester SR, Gilmont RR, Griswold MD. Isolation and characterization of Sertoli cell plasma membranes and associated plasminogen activator activity. *Biol Reprod* 1985;**32**:1237–45.
 65. Tung PS, Skinner MK, Fritz IB. Fibronectin synthesis is a marker for peritubular cell contaminants in Sertoli cell-enriched cultures. *Biol Reprod* 1984;**30**:199–211.
 66. Nilsson E, King SE, McBirney M, Kubsad D, Pappalardo M, Beck D, Sadler-Riggleman I, Skinner MK. Vinclozolin induced epigenetic transgenerational inheritance of pathologies and sperm epimutation biomarkers for specific diseases. *PLoS One* 2018;**13**:e0202662.
 67. King SE, McBirney M, Beck D, Sadler-Riggleman I, Nilsson E, Skinner MK. Sperm epimutation biomarkers of obesity and pathologies following DDT induced epigenetic transgenerational inheritance of disease. *Environ Epigenet* 2019;**5**:1–15. dvz008.
 68. Skinner MK, Guerrero-Bosagna C. Role of CpG deserts in the epigenetic transgenerational inheritance of differential DNA methylation regions. *BMC Genomics* 2014;**15**:692.
 69. Kanehisa M, Goto S. KEGG: Kyoto encyclopedia of genes and genomes. *Nucleic Acids Res* 2000;**28**:27–30.
 70. Kanehisa M, Goto S, Sato Y, Kawashima M, Furumichi M, Tanabe M. Data, information, knowledge and principle: back to metabolism in KEGG. *Nucl Acids Res* 2014;**42**:D199–205.
 71. Matzuk MM, Lamb DJ. The biology of infertility: research advances and clinical challenges. *Nat Med* 2008;**14**:1197–213.
 72. Kovac JR, Pastuszak AW, Lamb DJ. The use of genomics, proteomics, and metabolomics in identifying biomarkers of male infertility. *Fertil Steril* 2013;**99**:998–1007.
 73. Jiang XH, Bukhari I, Zheng W, Yin S, Wang Z, Cooke HJ, Shi QH. Blood-testis barrier and spermatogenesis: lessons from genetically-modified mice. *Asian J Androl* 2014;**16**:572–80.
 74. Manku G, Culty M. Mammalian gonocyte and spermatogonia differentiation: recent advances and remaining challenges. *Reproduction* 2015;**149**:R139–157.
 75. Sharpe RM, Skakkebaek NE. Testicular dysgenesis syndrome: mechanistic insights and potential new downstream effects. *Fertil Steril* 2008;**89**:e33–38.
 76. Skinner MK. What is an epigenetic transgenerational phenotype? F3 or F2. *Reprod Toxicol* 2008;**25**:2–6.
 77. Kung JT, Colognori D, Lee JT. Long noncoding RNAs: past, present, and future. *Genetics* 2013;**193**:651–69.
 78. Chen Q, Yan W, Duan E. Epigenetic inheritance of acquired traits through sperm RNAs and sperm RNA modifications. *Nat Rev Genet* 2016;**17**:733–43.
 79. Krawetz SA, Kruger A, Lalancette C, Tagett R, Anton E, Draghici S, Diamond MP. A survey of small RNAs in human sperm. *Hum Reprod* 2011;**26**:3401–12.
 80. Zhang X, Gao F, Fu J, Zhang P, Wang Y, Zeng X. Systematic identification and characterization of long non-coding RNAs in mouse mature sperm. *PLoS One* 2017;**12**:e0173402.
 81. Manikkam M, Guerrero-Bosagna C, Tracey R, Haque MM, Skinner MK. Transgenerational actions of environmental compounds on reproductive disease and identification of epigenetic biomarkers of ancestral exposures. *PLoS One* 2012;**7**:e31901.
 82. Nilsson EE, Anway MD, Stanfield J, Skinner MK. Transgenerational epigenetic effects of the endocrine disruptor vinclozolin on pregnancies and female adult onset disease. *Reproduction* 2008;**135**:713–21.
 83. Guillette LJ Jr, Gross TS, Masson GR, Matter JM, Percival HF, Woodward AR. Developmental abnormalities of the gonad and abnormal sex hormone concentrations in juvenile alligators from contaminated and control lakes in Florida. *Environ Health Perspect* 1994;**102**:680–8.
 84. Guerrero-Bosagna C, Settles M, Lucker B, Skinner M. Epigenetic transgenerational actions of vinclozolin on promoter regions of the sperm epigenome. *PLoS One* 2010;**5**:e13100.
 85. Tung PS, Skinner MK, Fritz IB. Cooperativity between Sertoli cells and peritubular myoid cells in the formation of the basal lamina in the seminiferous tubule. *Ann NY Acad Sci* 1984;**438**:435–46.
 86. Lienhard M, Grasse S, Rolff J, Frese S, Schirmer U, Becker M, Börno S, Timmermann B, Chavez L, Sülthmann H et al. QSEA-modelling of genome-wide DNA methylation from sequencing enrichment experiments. *Nucleic Acids Res* 2017;**45**:e44.
 87. Bolger AM, Lohse M, Usadel B. Trimmomatic: a flexible trimmer for Illumina sequence data. *Bioinformatics* 2014;**30**:2114–20.
 88. Langmead B, Salzberg SL. Fast gapped-read alignment with Bowtie 2. *Nat Methods* 2012;**9**:357–9.
 89. Li H, Handsaker B, Wysoker A, Fennell T, Ruan J, Homer N, Marth G, Abecasis G, Durbin R, 1000 Genome Project Data Processing Group. The sequence alignment/map format and SAMtools. *Bioinformatics* 2009;**25**:2078–9.
 90. Lienhard M, Grimm C, Morkel M, Herwig R, Chavez L. MEDIPS: genome-wide differential coverage analysis of sequencing data derived from DNA enrichment experiments. *Bioinformatics* 2014;**30**:284–6.
 91. Robinson MD, McCarthy DJ, Smyth GK. edgeR: a Bioconductor package for differential expression analysis of digital gene expression data. *Bioinformatics* 2010;**26**:139–40.

92. Durinck S, Spellman PT, Birney E, Huber W. Mapping identifiers for the integration of genomic datasets with the R/Bioconductor package biomaRt. *Nat Protoc* 2009;**4**:1184–91.
93. Cunningham F, Amode MR, Barrell D, Beal K, Billis K, Brent S, Carvalho-Silva D, Clapham P, Coates G, Fitzgerald S et al. Ensembl 2015. *Nucleic Acids Res* 2015;**43**:D662–669.
94. Huang da W, Sherman BT, Lempicki RA. Systematic and integrative analysis of large gene lists using DAVID bioinformatics resources. *Nat Protoc* 2009;**4**:44–57.
95. Mi H, Muruganujan A, Casagrande JT, Thomas PD. Large-scale gene function analysis with the PANTHER classification system. *Nat Protoc* 2013;**8**:1551–66.

RESEARCH

Open Access



Integration of sperm ncRNA-directed DNA methylation and DNA methylation-directed histone retention in epigenetic transgenerational inheritance

Daniel Beck, Millissia Ben Maamar and Michael K. Skinner* 

Abstract

Background: Environmentally induced epigenetic transgenerational inheritance of pathology and phenotypic variation has been demonstrated in all organisms investigated from plants to humans. This non-genetic form of inheritance is mediated through epigenetic alterations in the sperm and/or egg to subsequent generations. Although the combined regulation of differential DNA methylated regions (DMR), non-coding RNA (ncRNA), and differential histone retention (DHR) have been shown to occur, the integration of these different epigenetic processes remains to be elucidated. The current study was designed to examine the integration of the different epigenetic processes.

Results: A rat model of transiently exposed F0 generation gestating females to the agricultural fungicide vinclozolin or pesticide DDT (dichloro-diphenyl-trichloroethane) was used to acquire the sperm from adult males in the subsequent F1 generation offspring, F2 generation grand offspring, and F3 generation great-grand offspring. The F1 generation sperm ncRNA had substantial overlap with the F1, F2 and F3 generation DMRs, suggesting a potential role for RNA-directed DNA methylation. The DMRs also had significant overlap with the DHRs, suggesting potential DNA methylation-directed histone retention. In addition, a high percentage of DMRs induced in the F1 generation sperm were maintained in subsequent generations.

Conclusions: Many of the DMRs, ncRNA, and DHRs were colocalized to the same chromosomal location regions. Observations suggest an integration of DMRs, ncRNA, and DHRs in part involve RNA-directed DNA methylation and DNA methylation-directed histone retention in epigenetic transgenerational inheritance.

Keywords: Epigenetics, ncRNA, DNA methylation, Histone, Transgenerational, Sperm, Non-genetic inheritance, Review

Background

Over the past two decades numerous studies have demonstrated a non-genetic form of inheritance termed epigenetic transgenerational inheritance that is mediated by germline alterations in epigenetic processes [1–3]. One of the first observations involved the environmental

agricultural toxicant vinclozolin, which is one of the most commonly used agricultural fungicides, to induce the epigenetic transgenerational inheritance of testis pathology and DNA methylation alterations [1]. Similar observations with a wide variety of environmental toxicants, from dioxin to DDT (dichloro-diphenyl-trichloroethane), have identified similar epigenetic inheritance impacts on a variety of different disease conditions [3–5]. The transgenerational phenotypic manifestations of vinclozolin and DDT include the induction of testis, prostate,

*Correspondence: skinner@wsu.edu
Center for Reproductive Biology, School of Biological Sciences,
Washington State University, Pullman, WA 99164-4236, USA



kidney, and ovary pathology, as well as obesity [3]. An early observation in mice identified a traumatic stress-induced impact on the epigenetic transgenerational inheritance of behavioral abnormalities [6, 7]. Interestingly, the injection of eggs with the ncRNA from stressed individual male sperm promoted the same transgenerational phenotypes [6]. Subsequent studies have supported a role of either DNA methylation or ncRNA in the germline-mediated epigenetic transgenerational inheritance [3, 8]. This epigenetic transgenerational inheritance phenomenon has been shown to be induced by environmental chemicals, nutrition, stress and trauma abnormalities in rodents and humans [3, 7, 9], as well as a wide variety of environmental stresses in plants [10, 11], insects [12, 13], worms [14], fish [15–17], birds [18, 19], and a variety of mammals such as pigs and humans [20–22]. A number of physiological impacts have been observed including pathologies in the brain, reproductive organs, kidney, immunity, obesity, and infertility [1–3]. The environmentally induced epigenetic transgenerational inheritance phenomenon has been well established, and has significant impacts on disease etiology [2, 3] and other areas of biology such as evolution [23].

Although most previous investigations have focused on an individual epigenetic process such as DNA methylation [3, 4, 10] or ncRNA [6, 8], few have examined multiple processes. Our previous studies demonstrated in both vinclozolin and DDT-induced epigenetic transgenerational inheritance of pathology that the transgenerational F3 generation sperm had coordinately altered differential DNA methylation regions (DMRs), expression of non-coding RNAs (ncRNAs), differential histone retention sites (DHRs), and histone modifications [24, 25]. These observations suggest potential interactions between the different epigenetic processes, but this remains to be elucidated during the epigenetic inheritance phenomenon. Previous studies have demonstrated a role for ncRNA in RNA-directed DNA methylation in a number of different systems [26–28]. The ncRNA can help localize the DNA methylation site and facilitate subsequent chromatin remodeling processes. Therefore, the integration of ncRNA and DNA methylation has been established. Histone modifications can also be modified dramatically by ncRNA and chromatin remodeling in order to transition from euchromatin-active gene expression sites to heterochromatin-inactive sites of DNA [29]. Although information is available on histone retention in sperm and its impacts on the embryo [30, 31], the potential role of different epigenetic processes in histone retention has not been reported. Recently, a role for environmental exposures (e.g., vinclozolin and DDT) to promote transgenerational epigenetic inheritance of sperm histone retention has been observed [24, 25, 32].

The current study investigates the potential integration of DNA methylation, ncRNA, and histone alterations in the epigenetic transgenerational inheritance phenomenon.

Previous analyses of the concurrent expression of the epigenetic processes between the F1, F2, and F3 generations with a stringent statistical threshold have demonstrated negligible overlap between the different generations or between the epigenetic processes [24, 25]. The current study used an extended overlap analysis with a less stringent statistical threshold and found overlaps between the generations and epigenetic marks. The potential integration of the different epigenetic processes and generational conservation was identified.

Results

The experimental design involved F0 generation gestating outbred Sprague Dawley female rats at 120 days of age being exposed during embryonic days 8–14 (E8–E14) transiently to vinclozolin (100 mg/kg body weight/day), or DDT (25 mg/kg body weight/day), or vehicle dimethyl sulfoxide (DMSO) control, as previously described [24, 25]. The F1 generation offspring were obtained and aged to 90 days of age then bred within the lineage (control, vinclozolin, or DDT) in order to generate the F2 generation grand offspring. Afterward, the F2 generation was similarly bred to generate the transgenerational F3 generation great-grand offspring within the lineage. At each generation or lineage no sibling or cousin breeding was used to avoid any inbreeding artifacts [1, 3]. Litter bias was avoided by culling litters to 10 (approximately 5 females and 5 males), and then only one or two males and females from each litter being used for breeding within the lineage, as previously described. All males were aged to 120 days and sacrificed for sperm collection for molecular analysis, as described for previous reported studies [24, 25]. The number of individual animals investigated at each generation for sperm collection and molecular analysis was approximately 10–17 males, so $n = 10–17$ for animals with three different pools of 4–6 animals for each generation and epimutation analysis. The sperm collected were used to isolate RNA, DNA, and chromatin for analysis of ncRNA, DNA methylation, histone retention, and histone modification, as described in previous studies [24, 25], (Fig. 1). The molecular data from these previous studies (GEO # GSE109775, GSE106125, and NCIB SRA: PRJNA430483 largeRNA (control and DTT), PRJNA430740 smallRNA) were analyzed to explore data further bioinformatically.

The sperm DMRs, ncRNA (both small sncRNA and large lncRNA), and DHRs were analyzed in each sample, as previously described [24, 25], for the vinclozolin and DDT F1, F2 and F3 generation sperm samples. The numbers and overlaps of DMRs, ncRNA, and DHRs for

(See figure on next page.)

Fig. 1 Generational epimutation overlap at high stringent statistical threshold. **a** F1 generation vinclozolin lineage DMR ($p < 1e-06$), DHR ($p < 1e-06$), and ncRNA ($p < 1e-04$). **b** F1 generation DDT lineage DMR ($p < 1e-06$), DHR ($p < 1e-06$), and ncRNA ($p < 1e-04$). **c** F2 generation vinclozolin lineage DMR ($p < 1e-06$), DHR ($p < 1e-06$), and ncRNA ($p < 1e-04$). **d** F2 generation DDT lineage DMR ($p < 1e-06$), DHR ($p < 1e-06$), and ncRNA ($p < 1e-04$). **e** F3 generation vinclozolin lineage DMR ($p < 1e-06$), DHR ($p < 1e-06$), and ncRNA ($p < 1e-04$). **f** F3 generation DDT lineage DMR ($p < 1e-06$), DHR ($p < 1e-06$), and ncRNA ($p < 1e-04$)

each generation with a high stringency threshold are presented as previously reported in (Fig. 1). The overlaps with a Venn diagram for the transgenerational F3 generation for the different epigenetic marks is negligible with the high stringency threshold, (Fig. 1e, f), for each exposure, as previously identified [24, 25]. The F1 and F2 generations also were primarily distinct among the epimutations, (Fig. 1a–d). Although the different epigenetic alterations are present at each generation for both exposure lineages, the overlaps with a stringent statistical threshold were negligible, suggesting distinct functions and a lack of integration, as previously suggested [24, 25].

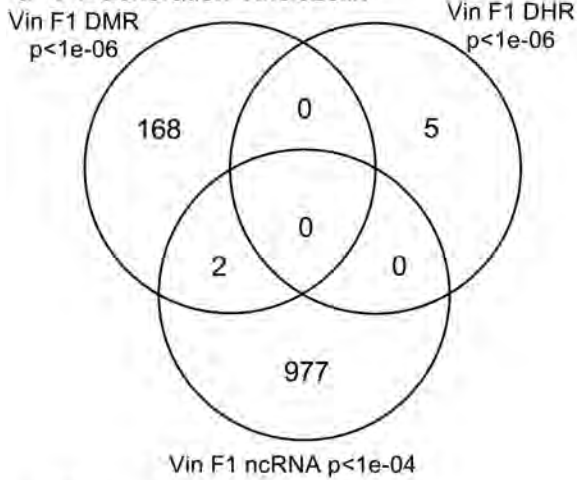
Interestingly, when a comparison of one epimutation at a high stringency was made to the others at $p < 0.05$, a number of genomic locations were identified with the different types of epimutations present. The chromosomal locations of these altered epigenetic marks (i.e., epimutations) are presented in (Fig. 2) and in (Additional file 1: Tables S1–S6) for each generation for both vinclozolin and DDT lineage sperm samples. The color-coded labels identify the DMR, ncRNA, and DHRs throughout the genomes with common chromosomal locations for each generation. Only those sites significant at high stringency (color code index) with one epimutation analysis that overlap with the other epimutations at $p < 0.05$ are shown, (Fig. 2). Specific epimutation chromosomal locations, statistical p-values, and gene associations are presented in (Additional file 1: Tables S1–S6). In the F1 and F2 generations only the alterations in ncRNAs and DMRs were found, as previously described [24, 25]. Therefore, the overlaps were primarily between the ncRNA and DMR in the F1 and F2 generations, (Fig. 2a–d). The DHRs developed in the transgenerational F3 generation, as previously described [24, 25]. In the F1 and F2 generations the ncRNA was predominantly the high statistically significant epimutation and overlap with DMR at the $p < 0.05$, (Fig. 2a–c), with a mix of ncRNA and DMR in the DDT lineage F2 generation, (Fig. 2d). The transgenerational F3 generation also had a mix of ncRNA and DMR at a high statistical significance, as well as a number of DHR, (Fig. 2e, f). Therefore, chromosomal locations with multiple epimutations are identified with ncRNA being predominant in the F1 and F2 generations with the high statistical threshold, and DMRs being more predominant in the F3 generation with a mix of the various epimutations, (Fig. 2 and Additional file 1: Tables S1–S6).

An extended overlap analysis was performed with both the DDT and vinclozolin lineage data using a less stringent statistical threshold for the comparisons, (Fig. 3). The more stringent statistical threshold epigenetic data sets (DMRs $p < 1e-06$, ncRNA $p < 1e-04$, and DHRs $p < 1e-06$) were compared between the generations and the epigenetic marks with a $p < 0.05$ statistical threshold. This optimized the potential to identify overlaps compared to the more stringent thresholds used in (Fig. 1). The rows present the more stringent threshold DMRs, ncRNA, and DHRs for the F1, F2, and F3 generations. The columns present the corresponding $p < 0.05$ threshold overlaps with the higher p-value threshold data sets. Examination of the horizontal rows, as expected, show 100% overlap (i.e., shaded) for the same data set and the number of associated epigenetic marks and percentage (%) overlap with the left margin value. This extended overlap allows the two different threshold stringencies to be compared and to determine additional overlap observations, (Fig. 3). Similar trends in the overlaps are observed for both the DDT and vinclozolin data sets. One of the initial observations was that the F1 generation ncRNA had a high percentage overlap with the F3 generation DMR, (Fig. 3 and Additional file 1: Tables S1 and S2). Similar observations are made with the F1 and F2 generations. For the F1 generation, DDT ncRNA had over a 20% overlap observed with the F1, F2, and F3 generation DMRs, while vinclozolin F1 generation ncRNA had approximately 35% overlap with the F1, F2, and F3 generation DMRs, (Figs. 3 and 4a, b). The lists of overlapping ncRNA and DMR sites are presented in (Additional file 1: Tables S1 and S2). The F2 and F3 generation ncRNA were similar with the overlap with the DDT generation DMRs of approximately 20%, but reduced to 10–15% with the vinclozolin DMRs, (Fig. 3). Therefore, some ncRNAs were common between the generations, and had overlap with the DMRs that ranged between 8–35% overlap for the vinclozolin DMRs and 15–20% overlap for DDT DMRs. The potential that the ncRNA may promote RNA-directed DNA methylation is suggested. The Venn diagrams presented in (Fig. 4a, b) support those overlaps and the epigenetic ncRNA and DMR overlaps are listed in (Additional file 1: Tables S1 and S2).

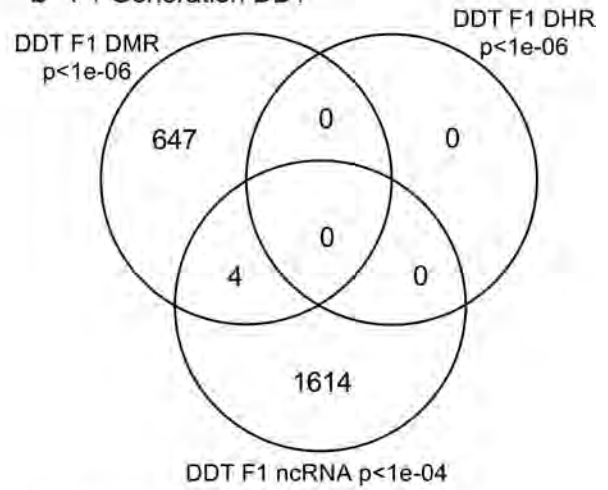
The next observation was that the F1, F2, and F3 generation DMRs had a 20–48% overlap with the F3 generation DHRs for the DDT and vinclozolin lineages, (Fig. 3).

Generational Epimutation Overlap

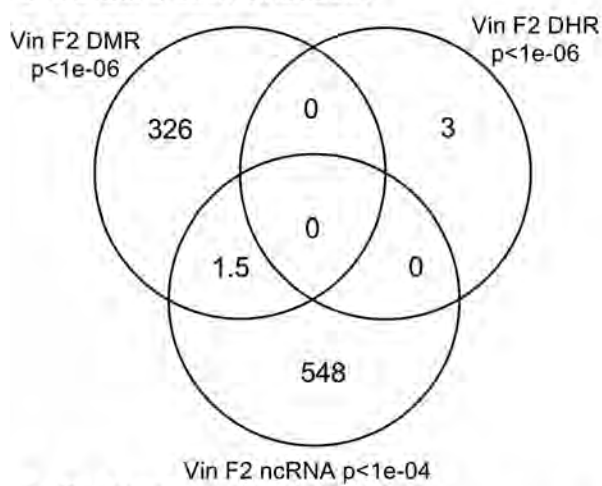
a F1 Generation Vinclozolin



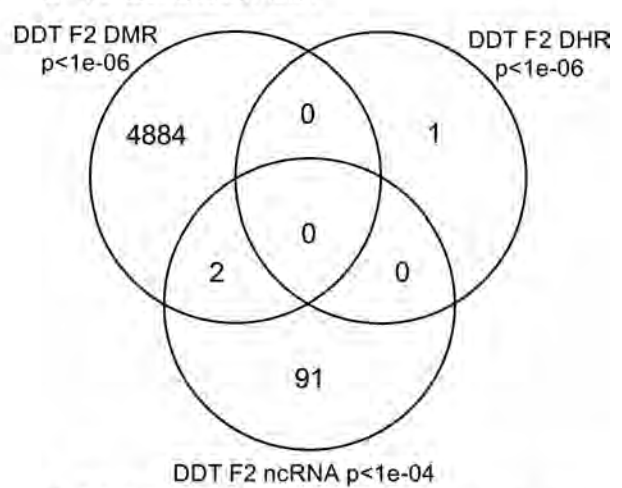
b F1 Generation DDT



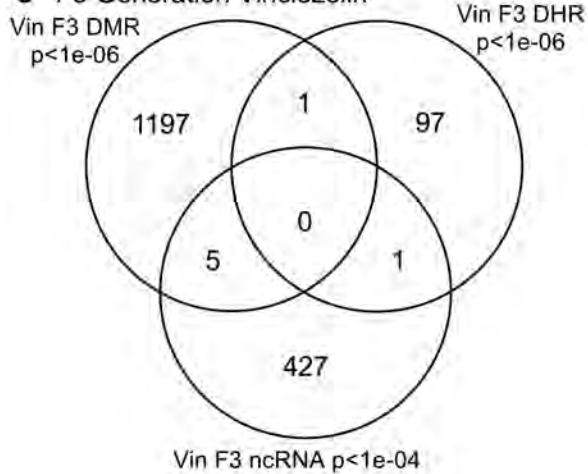
c F2 Generation Vinclozolin



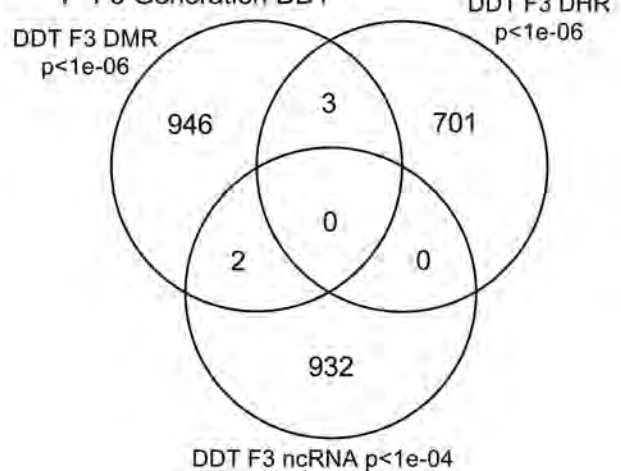
d F2 Generation DDT



e F3 Generation Vinclozolin



f F3 Generation DDT



(See figure on next page.)

Fig. 2 Chromosomal colocalization of overlap epimutations. The overlap of one epimutation at high statistical stringency (DMR $p < 1e-06$, DHR $p < 1e-06$, or ncRNA $p < 1e-04$) overlap with others at $p < 0.05$. The epimutation at high stringency is identified with color and marked as indicated by the inset legend. The chromosomal number and size (megabase) are presented. **a** F1 generation vinclozolin lineage ncRNA and DMR. **b** F1 generation DDT lineage ncRNA and DMR. **c** F2 generation vinclozolin lineage ncRNA and DMR. **d** F2 generation DDT lineage ncRNA and DMR. **e** F3 generation vinclozolin lineage DMR, DHR and ncRNA. **f** F3 generation DDT lineage DMR, DHR and ncRNA

Interestingly, the F3 generation DHRs had a 23–47% overlap with the F1, F2, and F3 generation DMRs for both exposure lineages. The Venn diagram overlaps in (Fig. 4c, d) support these DMR and DHR overlaps and suggests DMRs may help guide DHR formation transgenerationally. The overlapping F3 generation DMRs and DHRs are presented in (Additional file 1: Tables S3 and S4).

An interesting observation was the overlap between the F1, F2, and F3 generation DMRs for both DDT and vinclozolin exposures, (Figs. 3 and 4e, f). The highest overlap for the DDT F1 generation DMRs was the F2 generation DMRs with a 71% overlap, and for the vinclozolin F2 generation DMRs with the F3 generation DMRs with a 73% overlap. The highest for the F3 generation DMRs was 79% overlap with the vinclozolin F2 DMRs. Generally, a 25–50% overlap existed between the F1, F2, and F3 generation DMRs for both exposures, (Fig. 3). A Venn diagram supports this observation and demonstrates approximately 25% overlap for the vinclozolin DMRs and 35% overlap for the DDT DMRs, (Fig. 4e, f). Lists of these overlapping DMRs are presented in (Additional file 1: Tables S5 and S6). Therefore, a percentage (25–35%) of the F1 generation individual DMRs were retained transgenerationally.

Generally, the F3 generation epigenetic alterations had more overlap among each other and with the other generations for both exposures. A Venn diagram analysis was used to identify the epigenetic sites with overlapping DMRs, ncRNA, and DHRs, (Fig. 4). The overlapping F3 generation epigenetic sites were approximately 25% for vinclozolin and DDT lineages. A permutation analysis was performed to demonstrate this is significantly greater than the random overlap observed, with a p value of $p \leq 0.05$ for both 1 kb and 10 kb overlapping sites. Several sites were randomly selected and are mapped to identify the overlapping chromosomal locations of the DMR, ncRNA, and DHR, (Fig. 5). The actual statistical significance of the overlapping epimutations in these examples includes: (Fig. 5a) (ncRNA $p < 1e-04$, DHR $p < 0.03$, and DMR $p < 0.005$); (Fig. 5b) (ncRNA $p < 1e-04$, DHR $p < 0.001$, and DMR $p < 0.0004$); (Fig. 5c) (DHR $p < 1e-08$, ncRNA $p < 0.005$, and DMR $p < 0.04$); and (Fig. 5d) (ncRNA $p < 1e-06$, DMR $p < 1e-04$, and DHR $p < 1e-05$). The potential that RNA-directed DNA methylation and DMR-directed histone retention is involved is reviewed in the “Discussion” section.

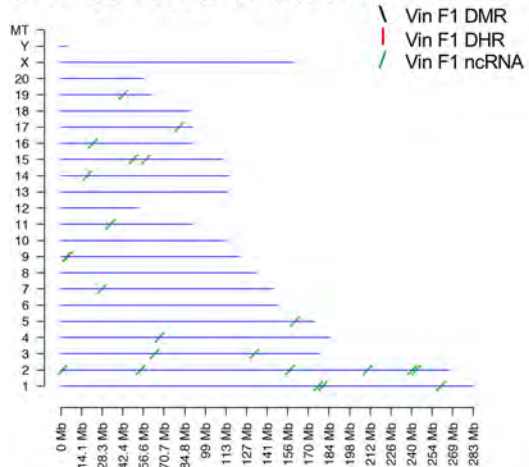
All the previous analyses and overlaps presented were based on a direct overlapping chromosomal location for the ncRNA, DMR and DHR. The question was addressed if a greater number of sites exist with epimutations that were in the same region but not directly overlapped. A 5 kb distance on either side of the epimutations was used to have a 10 kb window for the potential overlapping region. An extended overlap using this 10 kb window was used with the same data that will identify sites that directly overlap and those nearby within the 10 kb window, Fig. 6. The level of overlap with a 10 kb window identified the same overlaps presented and discussed, but the level of overlap was in the 80–99% range, (Fig. 6). Both the vinclozolin and DDT lineage had the same high level of overlap with most being >90% range, with a permutation analysis p value of $p < 0.001$. Using this 10 kb window the majority of ncRNA, DMRs and DHRs overlapped between the generations and epimutations. This supported all the previous observations and demonstrated a significant level of epimutation overlap. Since approximately 90% of the F3 generation DMRs overlapped with the F3 generation DHRs and F1 generation ncRNA, the conserved F3 generation DMRs, (Additional file 1: Table S5 and S6), were used in a Pathway Studio analysis to link DMR associated genes with cellular processes and pathologies, (Additional file 1: S1 and S2). A large number of the DMR and epimutation associated genes linked to various transgenerational pathologies previously observed, including kidney disease, mammary tumors, immune abnormalities, prostate disease, metabolic disease, or behavioral abnormalities [3, 33, 34].

Discussion

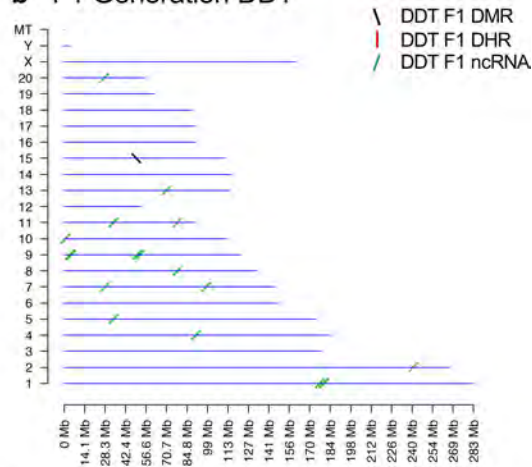
Previous studies have demonstrated the concurrent presence of DMRs, ncRNA, and DHRs in sperm following DDT or vinclozolin exposure of F0 generation gestating females during gonadal sex determination [24, 25]. These data were obtained and reported at a stringent statistical threshold selection and demonstrated negligible overlap at each generation, (Fig. 1) [24, 25]. The current study was designed to further investigate the potential integration of the different epigenetic processes between the F1, F2, and F3 generations. An approach was taken to compare the more stringent statistical threshold values for DMRs, ncRNAs, and DHRs with the less stringent $p < 0.05$ threshold between the different epigenetic processes

Chromosomal Colocalized DMR, ncRNA, and DHRs / F1, F2, F3 generations

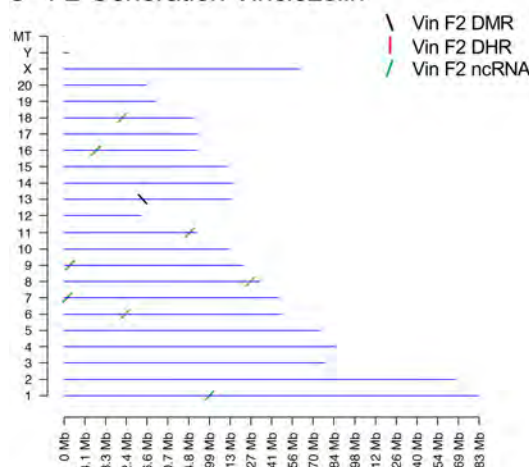
a F1 Generation Vinclozolin



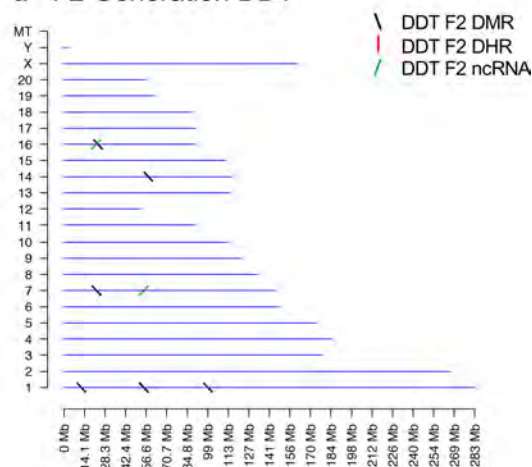
b F1 Generation DDT



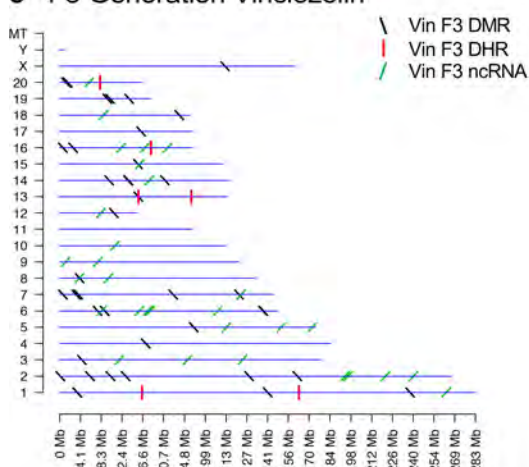
c F2 Generation Vinclozolin



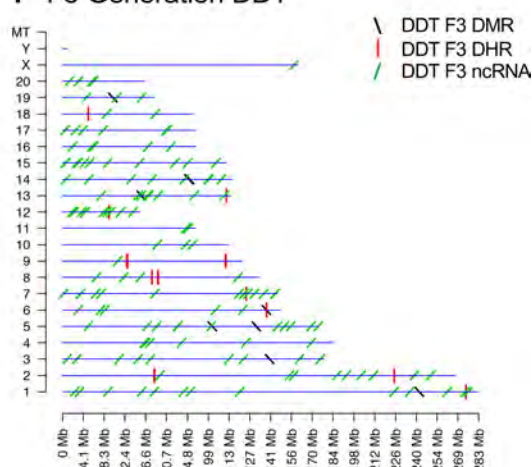
d F2 Generation DDT



e F3 Generation Vinclozolin



f F3 Generation DDT



Extended Epimutation Overlap

a Vinclozolin Epimutations

$p < 1e-5$ \ $p > .05$	F1.DMR	F1.DHR	F1.ncRNA	F2.DMR	F2.DHR	F2.ncRNA	F3.DMR	F3.DHR	F3.ncRNA
F1.DMR	170 (100.00%)	1 (0.59%)	10 (5.88%)	63 (37.06%)	4 (2.35%)	2 (1.18%)	80 (47.06%)	34 (20.00%)	6 (3.53%)
F1.DHR	2 (40.00%)	5 (100.00%)	0 (0.00%)	3 (60.00%)	2 (40.00%)	0 (0.00%)	1 (20.00%)	1 (20.00%)	0 (0.00%)
F1.ncRNA	326 (33.30%)	27 (2.76%)	979 (100.00%)	352 (35.96%)	26 (2.66%)	94 (9.60%)	362 (36.98%)	378 (38.61%)	52 (5.31%)
F2.DMR	155 (47.40%)	31 (9.48%)	14 (4.28%)	327 (100.00%)	21 (6.42%)	7 (2.14%)	241 (73.70%)	118 (36.09%)	15 (4.59%)
F2.DHR	1 (33.33%)	1 (33.33%)	0 (0.00%)	1 (33.33%)	3 (100.00%)	0 (0.00%)	1 (33.33%)	0 (0.00%)	0 (0.00%)
F2.ncRNA	47 (8.55%)	18 (3.27%)	42 (7.64%)	68 (12.36%)	15 (2.73%)	549 (99.82%)	67 (12.18%)	71 (12.91%)	35 (6.36%)
F3.DMR	576 (47.88%)	57 (4.74%)	116 (9.64%)	950 (78.97%)	57 (4.74%)	27 (2.24%)	1203 (100.00%)	359 (29.84%)	64 (5.32%)
F3.DHR	23 (23.23%)	22 (22.22%)	8 (8.08%)	34 (34.34%)	17 (17.17%)	4 (4.04%)	41 (41.41%)	99 (100.00%)	10 (10.10%)
F3.ncRNA	61 (14.06%)	6 (1.38%)	38 (8.76%)	78 (17.97%)	10 (2.30%)	26 (5.99%)	81 (18.66%)	73 (16.82%)	434 (100.00%)

b DDT Epimutations

$p < 1e-5$ \ $p > .05$	F1.DMR	F1.DHR	F1.ncRNA	F2.DMR	F2.DHR	F2.ncRNA	F3.DMR	F3.DHR	F3.ncRNA
F1.DMR	651 (100.0%)	48 (7.4%)	43 (6.6%)	463 (71.1%)	37 (5.7%)	14 (2.2%)	332 (51.0%)	315 (48.4%)	51 (7.8%)
F1.DHR	0 (0.0%)	0 (100.0%)	0 (0.0%)	0 (0.0%)	0 (0.0%)	0 (0.0%)	0 (0.0%)	0 (0.0%)	0 (0.0%)
F1.ncRNA	365 (22.6%)	27 (1.7%)	1614 (99.8%)	432 (26.7%)	22 (1.4%)	76 (4.7%)	344 (21.3%)	608 (37.6%)	97 (6.0%)
F2.DMR	3719 (76.1%)	229 (4.7%)	278 (5.7%)	4886 (100.0%)	208 (4.3%)	91 (1.9%)	2790 (57.1%)	2041 (41.8%)	266 (5.4%)
F2.DHR	0 (0.0%)	0 (0.0%)	0 (0.0%)	0 (0.0%)	1 (100.0%)	0 (0.0%)	0 (0.0%)	0 (0.0%)	0 (0.0%)
F2.ncRNA	22 (23.4%)	4 (4.3%)	14 (14.9%)	26 (27.7%)	2 (2.1%)	94 (100.0%)	19 (20.2%)	39 (41.5%)	17 (18.1%)
F3.DMR	256 (26.9%)	25 (2.6%)	37 (3.9%)	351 (36.9%)	27 (2.8%)	18 (1.9%)	951 (100.0%)	213 (22.4%)	30 (3.2%)
F3.DHR	334 (47.4%)	22 (3.1%)	38 (5.4%)	319 (45.3%)	17 (2.4%)	11 (1.6%)	240 (34.1%)	704 (100.0%)	36 (5.1%)
F3.ncRNA	243 (26.0%)	28 (3.0%)	135 (14.5%)	335 (35.9%)	18 (1.9%)	127 (13.6%)	199 (21.3%)	338 (36.2%)	928 (99.4%)

Fig. 3 Extended epimutation overlap. The epimutations at high stringency (DMR $p < 1e-06$, DHR $p < 1e-06$, and ncRNA $p < 1e-04$) in rows were compared to epimutations at $p < 0.05$ in columns. The number of overlap epimutations and percentage of the total are presented for each overlap. As anticipated, 100% overlap was observed for the same generation and epimutation indicated by shaded box. **a** Vinclozolin lineage epimutation and **b** DDT lineage epimutation overlap

(See figure on next page.)

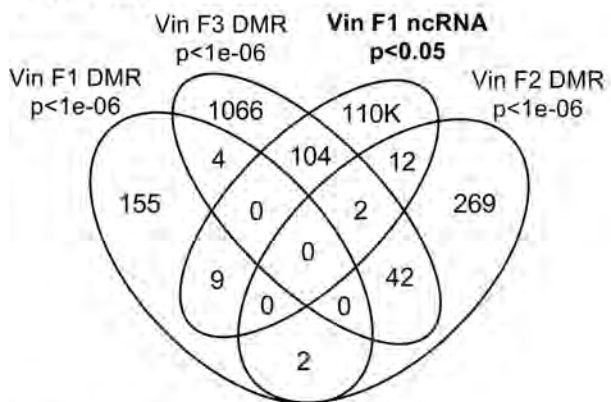
Fig. 4 Epimutation overlaps. Generational DMR overlap with F1 generation ncRNA $p < 0.05$. A Venn diagram overlap of F1, F2, and F3 generation DMR ($p < 1e-06$) with F1 generation ncRNA ($p < 0.05$). **a** Vinclozolin lineage DMR and ncRNA overlap. **b** DDT lineage DMR and ncRNA overlap. Generational DMR overlap with F3 generation DHR $p < 0.05$. A Venn diagram overlap of F1, F2, and F3 generation DMR ($p < 1e-06$) with F3 generation DHR ($p < 0.05$). **c** Vinclozolin lineage DMR and DHR overlap. **d** DDT lineage DMR and DHR overlap. Generational DMR overlap. A Venn diagram overlap of F1 generation DMR ($p < 1e-06$) with F2 and F3 generation DMR ($p < 0.05$). **e** Vinclozolin lineage DMR overlap. **f** DDT lineage DMR overlap

and generations. This extended overlap approach generated a number of observations to suggest an integration between generations for the epigenetic transgenerational inheritance phenomenon.

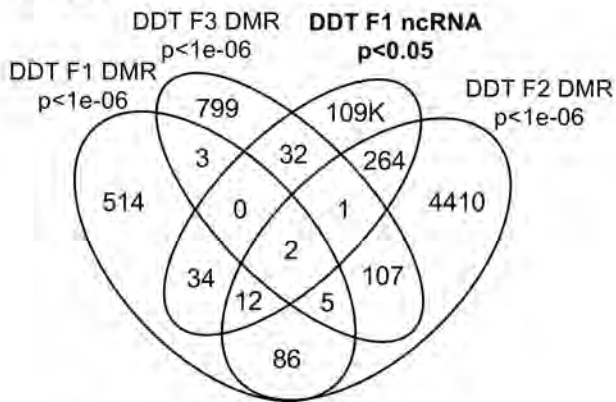
An interesting observation from the extended overlap of DMRs demonstrated that approximately 40–50% of the F1 generation sperm DMRs were retained and also present in the F2 and transgenerational F3 generations,

Generational DMR Overlap with F1 Generation ncRNA or DHR at $p < 0.05$

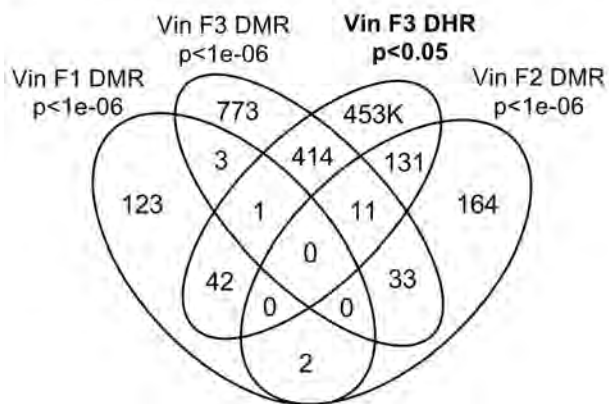
a Vinclozolin



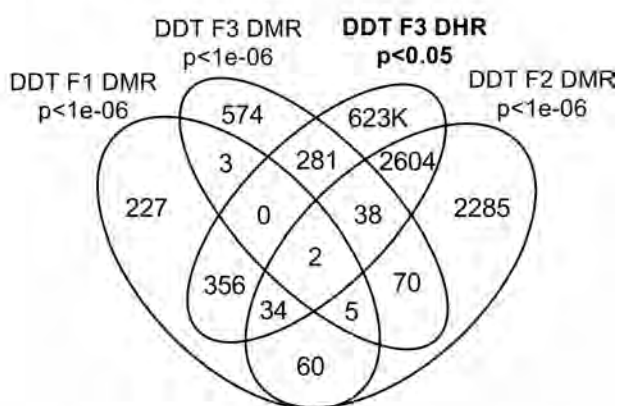
b DDT



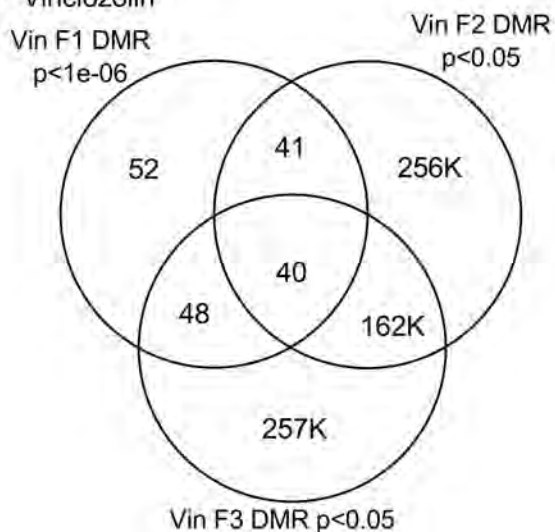
c Vinclozolin



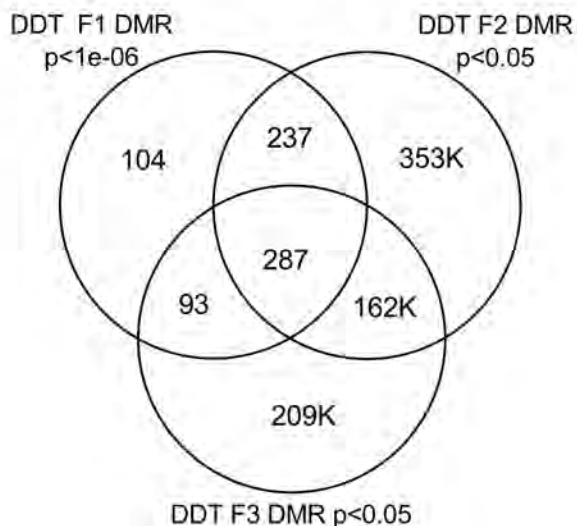
d DDT

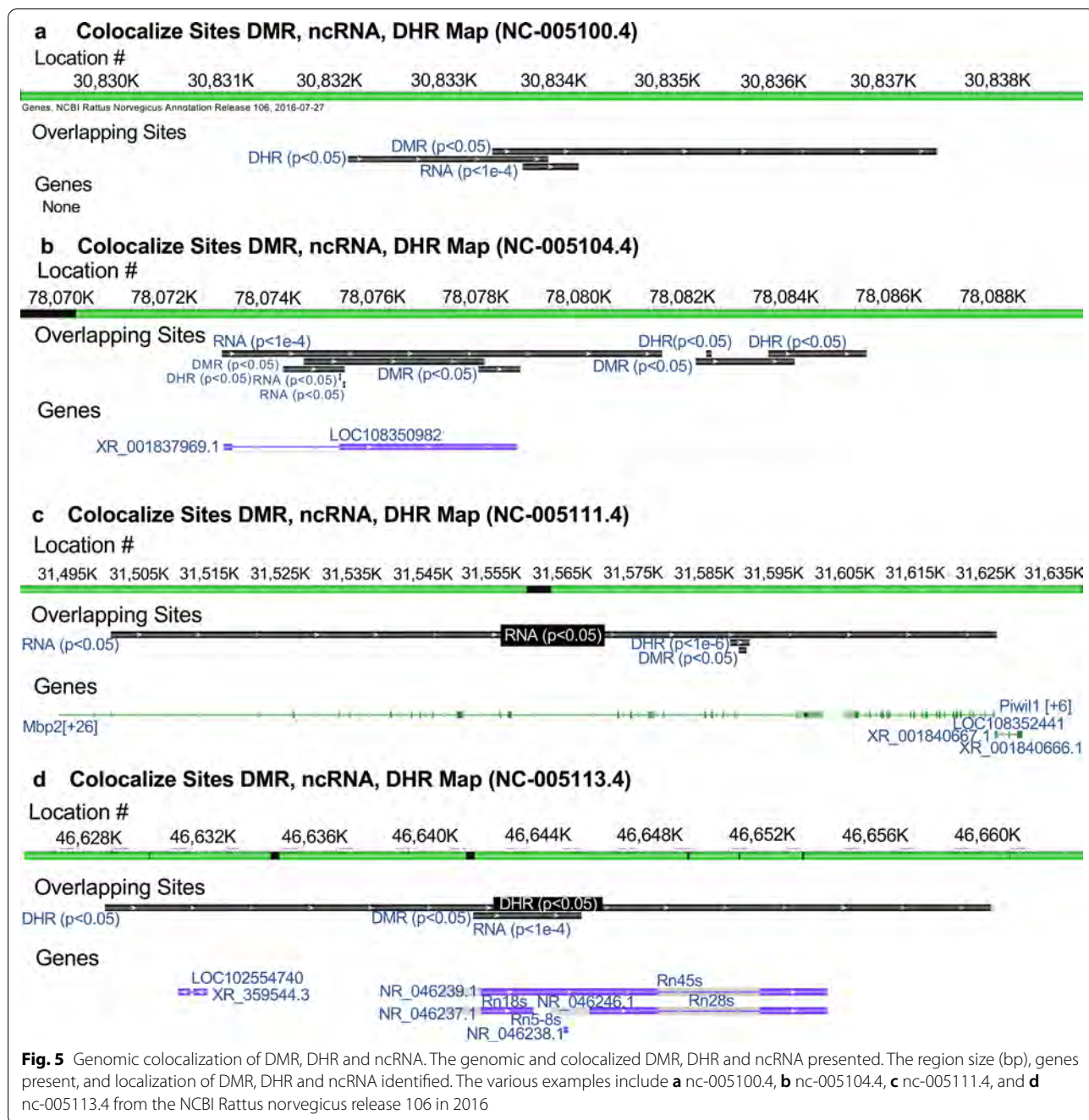


e Vinclozolin



f DDT





(Figs. 3 and 4e, f). This was 88–97% of the DMRs when 10 kb windows were used, (Fig. 6). A permutation analysis demonstrated this was significant ($p < 0.001$) and not due to random associations. The list of conserved F1 generation DMRs in subsequent generations is presented in (Additional file 1: Tables S5 and S6, and those DMRs with gene associations suggest approximately 50% of these conserved DMRs were associated with genes. Many of these genes had associations with a variety of pathologies,

Additional file 1: Figures S1 and S2). Therefore, a percentage of the F1 generation sperm DMRs were programmed and then conserved in subsequent generations. Although a majority of the F1 generation sperm DMRs were conserved generationally, there were minimal similarities between the different generations for ncRNAs, (Figs. 3 and 6). The DHRs were primarily present in the F3 generation sperm, so not conservation between generations, (Fig. 3.) In contrast, when a 10 kb region is considered

Extended 10 kb Window Epimutation Overlap

a Vinclozolin Epimutations (10 kb)

$p < 1e-5$ \ $p > .05$	F1.DMR	F1.DHR	F1.ncRNA	F2.DMR	F2.DHR	F2.ncRNA	F3.DMR	F3.DHR	F3.ncRNA
F1.DMR	170 (100.0%)	25 (14.7%)	17 (10.0%)	150 (88.2%)	21 (12.4%)	8 (4.7%)	155 (91.2%)	151 (88.8%)	7 (4.1%)
F1.DHR	5 (100.0%)	5 (100.0%)	0 (0.0%)	4 (80.0%)	4 (80.0%)	0 (0.0%)	5 (100.0%)	5 (100.0%)	0 (0.0%)
F1.ncRNA	831 (84.9%)	89 (9.1%)	979 (100.0%)	892 (91.1%)	73 (7.5%)	308 (31.5%)	891 (91.0%)	879 (89.8%)	74 (7.6%)
F2.DMR	283 (86.5%)	68 (20.8%)	23 (7.0%)	327 (100.0%)	54 (16.5%)	12 (3.7%)	312 (95.4%)	294 (89.9%)	15 (4.6%)
F2.DHR	2 (66.7%)	3 (100.0%)	0 (0.0%)	3 (100.0%)	3 (100.0%)	0 (0.0%)	3 (100.0%)	3 (100.0%)	0 (0.0%)
F2.ncRNA	403 (73.3%)	74 (13.5%)	119 (21.6%)	471 (85.6%)	68 (12.4%)	549 (99.8%)	456 (82.9%)	487 (88.5%)	55 (10.0%)
F3.DMR	1092 (90.8%)	129 (10.7%)	155 (12.9%)	1171 (97.3%)	104 (8.6%)	47 (3.9%)	1203 (100.0%)	1060 (88.1%)	74 (6.2%)
F3.DHR	84 (84.8%)	45 (45.5%)	11 (11.1%)	86 (86.9%)	37 (37.4%)	8 (8.1%)	87 (87.9%)	99 (100.0%)	11 (11.1%)
F3.ncRNA	352 (81.1%)	75 (17.3%)	89 (20.5%)	370 (85.3%)	59 (13.6%)	91 (21.0%)	372 (85.7%)	378 (87.1%)	434 (100.0%)

b DDT Epimutations (10 kb)

$p < 1e-5$ \ $p > .05$	F1.DMR	F1.DHR	F1.ncRNA	F2.DMR	F2.DHR	F2.ncRNA	F3.DMR	F3.DHR	F3.ncRNA
F1.DMR	651 (100.0%)	102 (15.7%)	56 (8.6%)	637 (97.8%)	93 (14.3%)	24 (3.7%)	599 (92.0%)	643 (98.8%)	59 (9.1%)
F1.DHR	0 (0.0%)	0 (100.0%)	0 (0.0%)	0 (0.0%)	0 (0.0%)	0 (0.0%)	0 (0.0%)	0 (0.0%)	0 (0.0%)
F1.ncRNA	1438 (88.9%)	155 (9.6%)	1614 (99.8%)	1529 (94.5%)	128 (7.9%)	178 (11.0%)	1349 (83.4%)	1577 (97.5%)	193 (11.9%)
F2.DMR	4735 (96.9%)	590 (12.1%)	440 (9.0%)	4886 (100.0%)	520 (10.6%)	139 (2.8%)	4471 (91.5%)	4764 (97.5%)	327 (6.7%)
F2.DHR	1 (100.0%)	1 (100.0%)	0 (0.0%)	1 (100.0%)	1 (100.0%)	0 (0.0%)	1 (100.0%)	0 (0.0%)	0 (0.0%)
F2.ncRNA	88 (93.6%)	14 (14.9%)	28 (29.8%)	89 (94.7%)	9 (9.6%)	94 (100.0%)	79 (84.0%)	92 (97.9%)	30 (31.9%)
F3.DMR	801 (84.2%)	121 (12.7%)	64 (6.7%)	859 (90.3%)	119 (12.5%)	26 (2.7%)	951 (100.0%)	872 (91.7%)	37 (3.9%)
F3.DHR	638 (90.6%)	72 (10.2%)	58 (8.2%)	660 (93.8%)	55 (7.8%)	17 (2.4%)	596 (84.7%)	704 (100.0%)	40 (5.7%)
F3.ncRNA	822 (88.0%)	134 (14.3%)	257 (27.5%)	871 (93.3%)	106 (11.3%)	202 (21.6%)	790 (84.6%)	894 (95.7%)	928 (99.4%)

Fig. 6 Extended epimutation overlap within a 10-kb region. The epimutations at high stringency (DMR $p < 1e-06$, DHR $p < 1e-06$, and ncRNA $p < 1e-04$) in rows were compared to epimutations at $p < 0.05$ in columns. The number of overlap epimutations and percentage of the total are presented for each overlap. As anticipated, 100% overlap was observed for the same generation and epimutation indicated by shaded box. **a** Vinclozolin lineage epimutation and **b** DDT lineage epimutation overlap

approximately 40% of the F3 generation DHRs are present in the F1 and F2 generations, (Fig. 6). The potential role of these DMRs for guided transgenerational histone retention is discussed below.

The second interesting observation was the overlap of the F1 generation sperm ncRNA with the F1, F2, and F3 generation DMRs. Over 20% in DDT and 35% in vinclozolin F1 generation ncRNA overlapped with the F1, F2, and F3 generation DMRs, (Figs. 3 and 4 and Additional file 1: Tables S1 and S2). Observations suggest

the potential role of ncRNA-directed DNA methylation in the direct exposure F1 generation and transgenerational F3 generation. Previous literature has established a role for RNA-directed DNA methylation in a number of biological and cellular systems [26–28]. This involves the ability of the ncRNA to recruit or direct chromatin remodeling proteins and proteins such as DNA methyltransferase to guide the DNA methylation at a chromosomal site, which has been established in a variety of different organisms and developmental processes

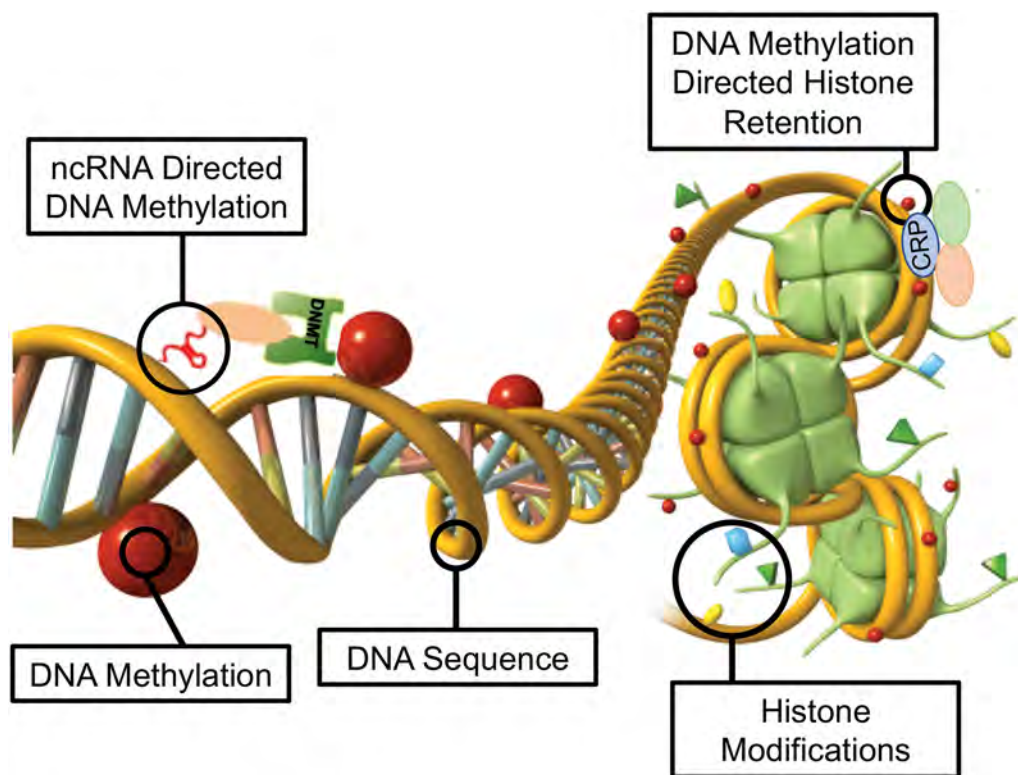


Fig. 7 Diagram of ncRNA-directed DNA methylation and DNA methylation-directed histone retention. The red dot identifies DNA methylation, green histone the nucleosome with modifications in histone tails indicated. The ncRNA association with cofactors and DNA methyltransferase (DNMT) promoting DNA methylation (red dot) for RNA-directed DNA methylation. The DNA methylation (red dot) association with chromatin remodeling proteins (CRP) to promote histone retention is indicated

[26–28]. Observations suggest ncRNA-directed DNA methylation may have a role in the epigenetic transgenerational inheritance phenomenon. Although the F1 generation ncRNA have the highest overlap with the F3 generation DMRs, overlaps are also observed with the F1 and F2 generation ncRNA with the various generation DMRs, (Fig. 3). When a 10 kb region overlap is considered, the F1 generation ncRNAs have a 91% overlap with the F2 and F3 generation DMRs, (Fig. 6). The overlaps of the ncRNA and DMRs suggest ncRNA-directed DNA methylation has a potential role in the epigenetic transgenerational inheritance process, (Fig. 7). A combination of F1 generation direct exposure alterations in ncRNA and subsequent transgenerational F3 generation actions on DNA methylation appears to be involved. The colocalized epigenetic sites with ncRNA and DNA methylation support this proposal, (Fig. 5). Although the molecular process of RNA-directed DNA methylation has been established [26–28], and suggested in generational impacts in plants and humans [35, 36], the current study only demonstrates the strong correlations of the ncRNA and DMRs. Future studies are needed to provide more molecular insights and

validation of the ncRNA-directed DNA methylation in the epigenetic transgenerational phenomenon.

Another interesting observation was the overlap of the transgenerational F3 generation DMRs with the DHRs. Although negligible DHRs are present in the F1 or F2 generations, the F3 generation has DHRs that overlap with F1 and F2 generation DMRs, (Fig. 3). For the DDT DMRs there was a range of 35–50% overlap and for vinclozolin DMRs, a 23–41% overlap. Considering a 10 kb region overlap, the F3 generation DHRs had an 85–95% overlap with the DMRs at all the generations, (Fig. 6). The permutation analysis demonstrated this number of 10 kb region overlaps is not due to random associations ($p < 0.001$). The literature for spermatid exchange of histones for protamines to condense the DNA into the head of the sperm is well established in most organisms investigated [37–39]. Although the vast majority of the sperm DNA has associated protamines, a percentage of the histones are retained, which varies between 5–10% of the DNA in different mammalian species [40]. Previously, we found histone retention was significantly increased in the transgenerational F3 generation sperm with the presence of new retention sites [24, 25, 32]. Therefore,

an additional epigenetic mechanism influenced during the epigenetic transgenerational inheritance process involves altered histone retention [32]. Previous literature has described the transition proteins and processes of the replacement of histones for protamines [41, 42], but the role of epigenetic processes such as DNA methylation have not been considered. Our previous observations suggest a role for this process in epigenetic inheritance [24, 25]. The current study indicates a potential role for DNA methylation in guiding or directing histone retention (Figs. 3 and 6). Previous studies have demonstrated a critical role for DNA methylation in the actions of chromatin remodeling proteins [41–43]. So, DNA methylation could alter the associated proteins and secondary structure of DNA that is an aspect of the process of histone retention. Although further investigation of the molecular processes is required in future studies, the observations from the current study suggest a potential role of DNA methylation-directed differential histone retention, (Fig. 7). The DMRs are proposed to assist in the guiding or directing of histone retention sites such that an increased number of sites appear transgenerationally. Therefore, the existence of DNA methylation-directed histone retention is proposed, and the observations support an integration of DMRs and DHRs transgenerationally. An interesting additional observation is the F1 and F2 generation DMRs that develop following direct exposure to toxicants are similar to the F3 generation DMRs, but that the DHRs did not form until the transgenerational F3 generation, (Figs. 3 and 6).

The current study findings help integrate the previous data obtained with ncRNA, DMRs, and DHRs [24, 25]. Potential roles of ncRNA-directed DMRs and DMR-directed DHRs are suggested. A percentage of the F1 generation DMRs are retained and conserved for subsequent F2 and F3 generations. The F1 generation ncRNA overlapped with the F2 and F3 generation DMRs, supporting the role for ncRNA-directed DNA methylation and formation of DMRs, (Fig. 7). The specific subtypes of sncRNA and lncRNA in this process will require further investigation. The potential for DMR-directed DHRs is suggested, but further information is required to elucidate the specific processes involved. Approximately half of the overlapping epimutations had associated known genes. Many of these genes are associated with previously identified pathologies, (Additional file 1: Figures S1 and S2), so support a mechanism for transgenerational pathology. The proposed model and integration of the transgenerational ncRNAs, DMRs and DHRs are presented in (Fig. 7). The current study observations suggest the integration of epigenetic processes in the epigenetic transgenerational phenomenon. Insights are provided into the development and generational transmission of

these environmentally induced sperm epimutations that have previously been shown to associate with disease development and etiology. The potential use of these integrated epigenetic chromosomal sites as biomarkers to identify exposure and/or disease susceptibility suggests they could be used as diagnostics to facilitate preventative medicine in the future. Further investigation is needed to more thoroughly establish these mechanisms in the epigenetic transgenerational inheritance phenomenon, but the current study provides support and a framework for the integration of the various epigenetic processes.

Conclusions

The observations with the two different exposures of DDT or vinclozolin suggest the generational impacts and transgenerational integration of the ncRNA, DMRs, and DHRs are similar. Variation in the percent overlaps is observed, but the same trends and conclusions of integration of the various epimutations are similar for both DDT and vinclozolin exposure lineages. The colocalized epimutation sites for the different exposures demonstrate the same phenomenon, but independent sites are observed for each exposure. The two different models of environmentally induced epigenetic transgenerational inheritance support the general mechanism proposed for ncRNA-directed DNA methylation and DMR-directed DHR development. Although the current study identifies such colocalized and interacting epimutation sites, many of the specific ncRNAs, DMRs and DHRs are not colocalized [24, 25]. Therefore, independent actions of ncRNAs, DMRs and DHRs will also be important in the mechanism involved in environmentally induced epigenetic transgenerational inheritance. A combination of ncRNA, DMR, and DHR epimutations developed during gametogenesis allows for post fertilization embryonic impacts and suggests integration of ncRNA and DMR will be involved in the epigenetic inheritance. The proposed mechanism in (Fig. 7) helps elucidate the molecular mechanisms involved in the epigenetic transgenerational inheritance phenomenon.

Materials and methods summary

Animal studies and breeding

As previously described [24, 25] and expanded in the (Additional file 1: Supplemental Methods), outbred Sprague Dawley SD male and female rats were fed a standard diet with water ad lib and mated. Gestating female rats were exposed to DDT or vinclozolin, and offspring were bred within each lineage for three generations in the absence of exposure. The F3 generation was aged to 120 days for sperm isolation and molecular analysis, as described in the (Additional file 1: Supplemental

Methods). Sperm were isolated and used for epigenetic analysis, as described in the (Additional file 1: Supplemental Methods). All experimental protocols for the procedures with rats were pre-approved by the Washington State University Animal Care and Use Committee (protocol IACUC # 6252), and all methods were performed in accordance with the relevant guidelines and regulations.

Epigenetic analysis, statistics and bioinformatics

As previously described [44], DNA was isolated from sperm collected at the time of dissection. The DNA isolation protocol has been previously described [33, 34], (Additional file 1: Supplemental Methods). Methylated DNA immunoprecipitation (MeDIP), followed by next generation sequencing (MeDIP-Seq) was performed on the isolated DNA. MeDIP-Seq, sequencing libraries, next generation sequencing, and bioinformatics analysis were performed, as described previously [33, 34] and in the (Additional file 1: Supplemental Methods). All molecular data has been deposited into the public database at NCBI (GEO # GSE109775 and GSE106125), and R code computational tools are available at GitHub (<https://github.com/skinnerlab/MeDIP-seq>) and <https://skinner.wsu.edu/genomic-data-and-r-code-files/>.

Supplementary Information

The online version contains supplementary material available at <https://doi.org/10.1186/s13072-020-00378-0>.

Additional file 1: Figure S1. Vinclozolin lineage F3 generation conserved DMR in common with DHR and F1 generation ncRNA. **Figure S2.** DDT lineage F3 generation conserved DMR in common with DHR and F1 generation ncRNA. **Table S1.** Vinclozolin lineage F1 generation ncRNA & F1, F2 and F3 generation DMR overlap list. **Table S2.** DDT lineage F1 generation ncRNA & F1, F2 and F3 generation DMR overlap list. **Table S3.** F3 generation vinclozolin DMR & F3 generation DHR overlap list. **Table S4.** F3 generation DDT DMR & F3 generation DHR overlap list. **Table S5.** Vinclozolin lineage F1, F2, F3 generation DMR overlap list. **Table S6.** DDT lineage F1, F2, F3 generation DMR overlap list.

Acknowledgements

We thank Drs. Eric Nilsson and Jennifer L.M. Thorsen for critical review of the manuscript. We acknowledge Ms. Amanda Quilty for editing and Ms. Heather Johnson for assistance in preparation of the manuscript. We thank the Genomics Core laboratory at WSU Spokane for sequencing data. This study was supported by John Templeton Foundation (50183and61174) (<https://templeton.org/>) grants to MKS and NIH (ES012974) (<https://www.nih.gov/>) grant to MKS. The funders had no role in study design, data collection and analysis, decision to publish, or preparation of the manuscript.

Authors' contributions

DB: bioinformatic analysis, data analysis, wrote and edited manuscript. MBM: molecular analysis, data analysis, edited manuscript. MKS: conceived, oversight, obtained funding, data analysis, wrote and edited manuscript. All authors read and approved the final manuscript.

Funding

This study was supported by John Templeton Foundation (50183and61174) (<https://templeton.org/>) grants to MKS and NIH (ES012974) (<https://www.nih.gov/>).

[gov/](https://www.nih.gov/)) grant to MKS. The funders had no role in study design, data collection and analysis, decision to publish, or preparation of the manuscript.

Availability of data and materials

All molecular data have been deposited into the public database at NCBI (GEO # GSE109775 and GSE106125, NCIB SRA accession numbers: PRJNA430483 largeRNA (control and DTT), PRJNA430740 smallRNA (control, vinclozolin and DTT)). The specific scripts used to perform the analysis can be accessed at github.com/skinnerlab and at www.skinner.wsu.edu/genomic-data-and-r-code-files.

Ethics approval and consent to participate

All experimental protocols for the procedures with rats were pre-approved by the Washington State University Animal Care and Use Committee (IACUC approval # 02568-39).

Consent for publication

Not applicable.

Competing interests

The authors declare that they have no competing interests.

Received: 30 September 2020 Accepted: 12 December 2020

Published online: 12 January 2021

References

- Anway MD, Cupp AS, Uzumcu M, Skinner MK. Epigenetic transgenerational actions of endocrine disruptors and male fertility. *Science*. 2005;308(5727):1466–9.
- Jirtle RL, Skinner MK. Environmental epigenomics and disease susceptibility. *Nat Rev Genet*. 2007;8(4):253–62.
- Nilsson E, Sadler-Riggleman I, Skinner MK. Environmentally induced epigenetic transgenerational inheritance of disease. *Environ Epigenetics*. 2018;4(2):1–13.
- Manikkam M, Guerrero-Bosagna C, Tracey R, Haque MM, Skinner MK. Transgenerational actions of environmental compounds on reproductive disease and identification of epigenetic biomarkers of ancestral exposures. *PLoS ONE*. 2012;7(2):1–12.
- Chamorro-Garcia R, Sahu M, Abbey RJ, Laude J, Pham N, Blumberg B. Transgenerational inheritance of increased fat depot size, stem cell reprogramming, and hepatic steatosis elicited by prenatal exposure to the obesogen tributyltin in mice. *Environ Health Perspect*. 2013;121(3):359–66.
- Gapp K, Jawaid A, Sarkies P, Bohacek J, Pelczar P, Prados J, et al. Implication of sperm RNAs in transgenerational inheritance of the effects of early trauma in mice. *Nat Neurosci*. 2014;17(5):667–9.
- Jawaid A, Roszkowski M, Mansuy IM. Transgenerational Epigenetics of Traumatic Stress. *Prog Mol Biol Transl Sci*. 2018;158:273–98.
- Yan W. Potential roles of noncoding RNAs in environmental epigenetic transgenerational inheritance. *Mol Cell Endocrinol*. 2014;398(1–2):24–30.
- Burdge GC, Lillycrop KA, Jackson AA. Nutrition in early life, and risk of cancer and metabolic disease: alternative endings in an epigenetic tale? *Br J Nutr*. 2009;101(5):619–30.
- Zheng X, Chen L, Li M, Lou Q, Xia H, Wang P, et al. Transgenerational variations in DNA methylation induced by drought stress in two rice varieties with distinguished difference to drought resistance. *PLoS ONE*. 2013;8(11):e80253.
- Suter L, Widmer A. Environmental heat and salt stress induce transgenerational phenotypic changes in *Arabidopsis thaliana*. *PLoS ONE*. 2013;8(4):e60364.
- Norouzitallab P, Baruah K, Vandegehuchte M, Van Stappen G, Catania F, Vanden Bussche J, et al. Environmental heat stress induces epigenetic transgenerational inheritance of robustness in parthenogenetic *Artemia* model. *FASEB J*. 2014;28(8):3552–63.
- Waddington CH. Gene assimilation of an acquired character. *Evolution*. 1953;7:118–26.
- Greer EL, Maures TJ, Ucar D, Hauswirth AG, Mancini E, Lim JP, et al. Transgenerational epigenetic inheritance of longevity in *Caenorhabditis elegans*. *Nature*. 2011;479(7373):365–71.

15. Carvan M, Kalluvila TA, Klingler RH, Larson JK, Pickens M, Mora-Zamorano FX, et al. Mercury-induced epigenetic transgenerational inheritance of abnormal neurobehavior is correlated with sperm epimutations in zebrafish. *PLoS ONE*. 2017;12(5):1–26.
16. Knecht AL, Truong L, Marvel SW, Reif DM, Garcia A, Lu C, et al. Transgenerational inheritance of neurobehavioral and physiological deficits from developmental exposure to benzo[a]pyrene in zebrafish. *Toxicol Appl Pharmacol*. 2017;329:148–57.
17. Bhandari RK, vom Saal FS, Tillitt DE. Transgenerational effects from early developmental exposures to bisphenol A or 17 α -ethinylestradiol in medaka *Oryzias latipes*. *Sci Rep*. 2015;5:9303.
18. Leroux S, Gourichon D, Letterier C, Labrune Y, Coustham V, Riviere S, et al. Embryonic environment and transgenerational effects in quail. *Genet Sel Evol*. 2017;49(1):14.
19. Brun JM, Bernadet MD, Cornuez A, Leroux S, Bodin L, Basso B, et al. Influence of grand-mother diet on offspring performances through the male line in Muscovy duck. *BMC Genet*. 2015;16(1):145.
20. Braunschweig M, Jagannathan V, Gutzwiller A, Bee G. Investigations on transgenerational epigenetic response down the male line in F2 pigs. *PLoS ONE*. 2012;7(2):e30583.
21. Bygren LO, Tinghog P, Carstensen J, Edvinsson S, Kaati G, Pembrey ME, et al. Change in paternal grandmothers' early food supply influenced cardiovascular mortality of the female grandchildren. *BMC Genet*. 2014;15:12.
22. Veenendaal MV, Painter RC, de Rooij SR, Bossuyt PM, van der Post JA, Gluckman PD, et al. Transgenerational effects of prenatal exposure to the 1944–45 Dutch famine. *BJOG*. 2013;120(5):548–53.
23. Skinner MK. Environmental epigenetics and a unified theory of the molecular aspects of evolution: a Neo-Lamarckian concept that facilitates Neo-Darwinian evolution. *Genome Biol Evol*. 2015;7(5):1296–302.
24. Ben Maamar M, Sadler-Riggelman I, Beck D, McBirney M, Nilsson E, Klukovich R, et al. Alterations in sperm DNA methylation, non-coding RNA expression, and histone retention mediate vinclozolin-induced epigenetic transgenerational inheritance of disease. *Environ Epigenetics*. 2018;4(2):1–19.
25. Skinner MK, Ben Maamar M, Sadler-Riggelman I, Beck D, Nilsson E, McBirney M, et al. Alterations in sperm DNA methylation, non-coding RNA and histone retention associate with DDT-induced epigenetic transgenerational inheritance of disease. *Epigenetics Chromatin*. 2018;11(1):8.
26. Cuerda-Gil D, Slotkin RK. Non-canonical RNA-directed DNA methylation. *Nat Plants*. 2016;2(11):16163.
27. Chow HT, Chakraborty T, Mosher RA. RNA-directed DNA Methylation and sexual reproduction: expanding beyond the seed. *Curr Opin Plant Biol*. 2019;54:11–7.
28. Matzke MA, Mosher RA. RNA-directed DNA methylation: an epigenetic pathway of increasing complexity. *Nat Rev Genet*. 2014;15(6):394–408.
29. Kouzarides T. Chromatin modifications and their function. *Cell*. 2007;128(4):693–705.
30. Jenkins TG, Carrell DT. The sperm epigenome and potential implications for the developing embryo. *Reproduction*. 2012;143(6):727–34.
31. Jenkins TG, Carrell DT. The paternal epigenome and embryogenesis: poisoning mechanisms for development. *Asian J Androl*. 2011;13(1):76–80.
32. Ben Maamar M, Sadler-Riggelman I, Beck D, Skinner MK. Epigenetic transgenerational inheritance of altered sperm histone retention sites. *Sci Rep*. 2018;8:5308.
33. King SE, McBirney M, Beck D, Sadler-Riggelman I, Nilsson E, Skinner MK. Sperm epimutation biomarkers of obesity and pathologies following DDT induced epigenetic transgenerational inheritance of disease. *Environ Epigenetics*. 2019;5(2):1–15.
34. Nilsson E, King SE, McBirney M, Kubsad D, Pappalardo M, Beck D, et al. Vinclozolin induced epigenetic transgenerational inheritance of pathologies and sperm epimutation biomarkers for specific diseases. *PLoS ONE*. 2018;13(8):1–29.
35. Saenen ND, Martens DS, Neven KY, Alfano R, Bove H, Janssen BG, et al. Air pollution-induced placental alterations: an interplay of oxidative stress, epigenetics, and the aging phenotype? *Clinical epigenetics*. 2019;11(1):124.
36. Kumar S, Kumari R, Sharma V, Sharma V. Roles, and establishment, maintenance and erasing of the epigenetic cytosine methylation marks in plants. *J Genet*. 2013;92(3):629–66.
37. Ooi SL, Henikoff S. Germline histone dynamics and epigenetics. *Curr Opin Cell Biol*. 2007;19(3):257–65.
38. van der Heijden GW, Derijck AA, Ramos L, Giele M, van der Vlag J, de Boer P. Transmission of modified nucleosomes from the mouse male germline to the zygote and subsequent remodeling of paternal chromatin. *Developmental biology*. 2006;298(2):458–69.
39. Meyer-Ficca ML, Lonchar JD, Ihara M, Meistrich ML, Austin CA, Meyer RG. Poly(ADP-ribose) polymerases PARP1 and PARP2 modulate topoisomerase II beta (TOP2B) function during chromatin condensation in mouse spermiogenesis. *Biol Reprod*. 2011;84(5):900–9.
40. Hammoud S, Liu L, Carrell DT. Protamine ratio and the level of histone retention in sperm selected from a density gradient preparation. *Andrologia*. 2009;41(2):88–94.
41. Berson A, Nativio R, Berger SL, Bonini NM. Epigenetic regulation in neurodegenerative diseases. *Trends Neurosci*. 2018;41(9):587–98.
42. Zhao M, Shirley CR, Yu YE, Mohapatra B, Zhang Y, Unni E, et al. Targeted disruption of the transition protein 2 gene affects sperm chromatin structure and reduces fertility in mice. *Mol Cell Biol*. 2001;21(21):7243–55.
43. Vymetalkova V, Vodicka P, Vodenkova S, Alonso S, Schneider-Stock R. DNA methylation and chromatin modifiers in colorectal cancer. *Mol Aspects Med*. 2019;69:73–92.
44. McBirney M, King SE, Pappalardo M, Houser E, Unkefer M, Nilsson E, et al. Atrazine induced epigenetic transgenerational inheritance of disease, lean phenotype and sperm epimutation pathology biomarkers. *PLoS ONE*. 2017;12(9):1–37.

Publisher's Note

Springer Nature remains neutral with regard to jurisdictional claims in published maps and institutional affiliations.

Ready to submit your research? Choose BMC and benefit from:

- fast, convenient online submission
- thorough peer review by experienced researchers in your field
- rapid publication on acceptance
- support for research data, including large and complex data types
- gold Open Access which fosters wider collaboration and increased citations
- maximum visibility for your research: over 100M website views per year

At BMC, research is always in progress.

Learn more biomedcentral.com/submissions

